Quantum Chaos, Information Scrambling and Eigenstate Thermalization in Coupled Harmonic Oscillators

by

Yusrat Sadia Nailat
22311003

A thesis submitted to the Department of Mathematics and Physical Sciences
in partial fulfillment of the requirements for the degree of
Bachelors of Science in Physics

Department of Mathematics and Physical Sciences
BRAC University
May 2026

Declaration

It is hereby declared that

1. The thesis submitted is my own original work while completing degree at BRAC University.
2. The thesis does not contain material previously published or written by a third party, except where this is appropriately cited through full and accurate referencing.
3. The thesis does not contain material which has been accepted, or submitted, for any other degree or diploma at a university or other institution.
4. I have acknowledged all main sources of help.

Student's Full Name & Signature:

_____

Yusrat Sadia Nailat

22311003

Approval

The thesis titled "Quantum Chaos, Information Scrambling and Eigenstate Thermalisation in Couple Harmonic Oscillators" submitted by

Yusrat Sadia Nailat (22311003)

Of Spring 2026 has been accepted as satisfactory in partial fulfillment of the requirement for the degree of Bachelors of Science in Physics on May 3, 2026

Examining Committee:

Supervisor:
(Member)

Prof. Tibra Ali, PhD

Professor
Department of Mathematics and Physical Sciences
BRAC University

Program Coordinator:
(Member)

Mohammed Lutfur Rahman

Associate Professor
Department of Mathematics and Physical Sciences
BRAC University

Head of Department:
(Chair)

Md. Firoze H. Haque, PhD

Associate Professor
Department of Mathematics and Physical Sciences
BRAC University

Abstract

This thesis investigates the connection between quantum chaos and the Eigenstate Thermalization Hypothesis (ETH) in a system of two and three coupled harmonic oscillators with non-linear coupling. First, we numerically calculate thermal out-of-time-ordered correlators (OTOCs) for systems of two and three coupled harmonic oscillators. Next, we identify an early-time exponential growth regime, from which we extract temperature-dependent quantum Lyapunov exponent. We analyze the diagonal and off-diagonal matrix elements of the local position operator acting on first degree of freedom e.g. the first oscillator, x_1^2, in the energy eigenbasis and examine their consistency with the ETH ansatz.

We also probe a possible connection between early time exponential growth of OTOC and eigenstate thermalisation. By inserting the ETH ansatz into the four-point correlation function underlying the OTOC, we show that the smooth and gaussian random structure of chaotic eigenstates and observables within the ETH framework can consistently account for signatures of coarse-grained picture of information scrambling. This supports the connection between information scrambling and eigenstate thermalization.

Keywords: *eigenstate thermalization hypothesis, out-of-time-ordered correlators, quantum chaos, information scrambling, quantum thermalization, open quantum systems*

Dedication

The author dedicates this thesis to her parents, Syeda Saliha Saliheen Sultana and Mohammed Nazrul Hoque, her grandfather, Khondoker Abdul Hafiz, and finally to her high school physics teacher, Abdullah Al Hasan Kawshik.

Acknowledgement

I consider myself extremely lucky to have crossed paths with the most amazing and the smartest people I have ever known—my seniors, peers, friends, and teachers—during my undergraduate degree at BRAC University.

Firstly, I would like to extend my deepest gratitude to my thesis supervisor, Prof. Tibra Ali, for his endless care, support, and guidance from my very first day at BRAC University. His mentorship has profoundly shaped my life, and I believe it will continue to do so for many years to come. I know his door will always be open to me.

I am indebted to the faculty members from the Physics, Computer Science, and Mathematics programs for their careful teaching. I am especially grateful to our former physics lecturer, Tushar Mitra, whose exceptional teaching helped me develop a strong foundation in physics. I am thankful to him not only for his patient teaching but also for the trust he placed in me when I could not even find a reason to trust myself. Without his continuous encouragement, I would not have come this far. I am also grateful to Rafsanjay Jim, our former mathematics lecturer. I had the pleasure of engaging in many valuable discussions with him on different topics in mathematics and physics, although I was never officially enrolled in any of his courses. Most importantly, both he and Tushar Mitra taught me that the only path to achieving greatness and excellence in life is to remain humble. Next, I extend my gratitude to Sayeda Tashnuba Jahan for her unwavering support. Being one of the few female students in our program, I draw a lot of inspiration from her to excel in physics. I am also grateful to Reaz Shafqat for the valuable discussions that helped me clarify my concepts, thoughts and ideas relating to my thesis and beyond.

I am extremely grateful to Shadman Shahriar for his passionate lectures on quantum computing and the many discussions I had the pleasure of having with him, which helped me develop a strong foundation in linear algebra and topics of quantum information theory. Finally, I sincerely thank Avinandan Banerjee for always taking the time to answer my many computer science questions with patience and enthusiasm. I draw a lot of inspiration from him in the most unexpected ways.

I am thankful to my amazing friends—Noor-E-Tasnim Hiya, Kazi Fahim Reza Arko, M. Fahim Hoque, Sheikh Saleh Ahmed Pushan, Walid Hasan, Tahmid Shahriar, and Uddipto Syed—for their continual kindness, care, and support, which helped ensure my mental well-being and a smooth academic journey. I have learned so much from them beyond academics. I have made so many amazing memories with these people that I will cherish for the rest of my life. I am incredibly thankful to Ahmed Rakin Kamal for always being there for me whenever I needed any kind of help, especially during the times I needed it the most, to Mishaal Hai for helping me edit the thesis at the last minute, to Prof. Mahbub Alam Majumdar for providing the necessary logistic supports whenever I needed that, and finally to Saif Ar Rasul, my former student tutor, for his enthusiastic and passionate teaching and guidance. Lastly, I thank Rakib Muhammed Saki for sharing his codes from his thesis.

Table of Contents

List of Figures

Chapter 1

Introduction

One of the most interesting aspects of quantum information is that it can never be entirely lost, but it can be exceedingly well hidden. In interacting systems of many particles, information encoded in a given particle can quickly spread across all the degrees of freedom. Understanding how quantum information spreads have wide-ranging implications, from understanding the information paradox in black holes to imposing fundamental limits on transport properties of strongly correlated materials [21]. Therefore, information scrambling, the process by which quantum information spreads and become inaccessible, is a central problem of quantum information and quantum statistical mechanics. Another interesting and central problem of quantum statistical mechanics is the concept of thermalisation. Due to the lack of concrete phase space representation, there is no direct analogue of classical ergodic hypothesis in quantum mechanics. Therefore, our classical understanding of thermalisation is not directly transferrable to quantum mechanical context.

The unitarity of the quantum evolution also presents a problem to our understanding of quantum thermalization. Recall that information is preserved under unitary transformations and therefore systems never truly forget its initial conditions, unlike how the observables behave in thermal equilibrium. At equilibrium, the expectation value of the quantum observations are independent of its initial states. Nevertheless, experimental evidences show that quantum systems thermalise. Moreover, in classical systems, thermalisation is strongly related to the chaotic dynamics of systems with many degrees of freedom and a proper coarse-graining in phase space. However, writing down the Hamiltonian for many body quantum systems is tedious job. It was Eugene Wigner who formulated that the Hamiltonian of many body systems like heavy nuclei can be modeled by a matrix whose elements are drawn from a random distribution. This idea laid the foundation for random matrix theory and our modern understanding of quantum many body dynamics. Later, Bohigas, Giannoni, and Schmit formulated that level repulsion of quantum chaotic systems whose classical analogue is chaotic can be described by RMT. This is known by the BGS conjecture. In the case of isolated quantum many-body systems, there is a growing consensus that the foundations of their thermalization lay the so-called eigenstate thermalization hypothesis (ETH), which has also been considered as the quantum analogue of ergodic hypothesis [20]. ETH states that in quantum chaotic systems, the eigenstates correspond to superpositions of random waves, and the level statistics follow Gaussian random matrix distributions, inspired by the idea

of "quantum chaology" introduced by Michael Berry in 1970s [5]. Understanding the correlation between quantum chaos and thermalisation has been explored extensively in recent researches. In particular, understanding the fine structures of eigenstates and its influence on information scrambling can help us address many foundational problems of quantum mechanics.

1.1 Motivation

Understanding quantum chaos and its connection with quantum thermalisation is one of the most elusive problems of modern physics. However, there are not many good measure of quantum chaos. One of such a widely accepted methods of quantifying and analysing quantum chaos is the out-of-time-order correlators. [19][25]. In their paper, Hashimoto et al. [19] explores whether OTOCs can be used to indicate quantum chaos in different billard systems. In a different paper, Akutagawa et al. [25] discusses that for a system of two coupled harmonic oscillators with non-linear coupling, OTOCs are a better indicator of quantum chaos than level statistics. Therefore, instead of sketching level statistics for a system of two and three coupled harmonic oscillators with non-linear coupling, we extract the quantum Lyapunov exponent to confirm that these systems are indeed quantum chaotic. We then probe the consistency of the structure of the operator x_1^2 acting on these systems in terms of Eigenstate Thermalisation Hypothesis. We then ask the question: since for a quantum chaotic system, information is likely to scramble after the Ehrenfest time, can we find any different perspective in our understanding on information scrambling using ETH? To answer this question, we decided to find a possible connection of four point correlation function and ETH analytically in this thesis.

1.2 Organization of the paper

This paper is divided into two main parts. The first four chapters cover basic concepts to make the later concepts accessible to the readers. We start our paper by discussing the general concepts of classical and quantum statistical mechanics in chapter 2. Then, on chapter 3, we move on to discuss classical limit of quantum dynamics and basic ideas of classically integrable and non-integrable systems. We briefly illustrate the basics of random matrix theory in chapter 4. In chapter 5, we introduce out-of-time-order correlators and develop methodology to extract quantum Lyapunov exponent to test whether our system of interest is chaotic. At the same time, we numerically calculate quantum Lyapunov exponents for these systems. Eigenstate thermalisation hypothesis has been extensively discussed in chapter 6. Our original work has been presented in chapter 7, where we demonstrate that the structure of chaotic eigenstates and operators within the ETH framework can consistently account for signatures of information scrambling. Finally, we give a brief summary of our work and conclusion drawn from our calculation in chapter 8.

Chapter 2

Review on Statistical Mechanics

> Statistical mechanics is the art of turning the microscopic laws of physics into a description of Nature on a macroscopic scale. - David Tong

Most of the physical systems are too complex to analyze directly since the number of equation of motions of the system increases with the number of degrees of freedom. Solving for the motion of all the atoms in a complex system is simply infeasible. Despite this, such systems often show simple, striking behavior. To reduce the most tedious job of solving equation of motions directly, we try to interpret the behavior of the system statistically. The trick of statistical mechanics is not to study a single system, but a large collection or ensemble of systems. Where understanding a single system is often impossible, calculating the behavior of an enormous collection of similarly prepared systems often allows one to answer most questions that physics can be expected to address. Historically, the techniques of statistical mechanics proved to be a crucial tool for understanding the deeper laws of physics. This is interesting because the development of this amazing branch of physics is related to the first evidence for the existence of atoms as well as the discovery of quantum mechanics! We will start our discussion with a short review on the equilibrium behavior of matter: the historical origin of statistical mechanics. An isolated system is said to approach the *equilibrium* if and when it settles down at long times to a state which is independent of the initial conditions (except for conserved quantities like the total energy). Equilibrium statistical mechanics describes the equilibrium state as an average over all states consistent with the conservation laws. On the other hand, non-equilibrium statistical mechanics describes how systems outside of thermodynamic equilibrium, with a central goal of explaining phenomena such as thermalization —the process by which such systems relax toward equilibrium.

2.1 Review on Classical Statistical Mechanics

We consider the box to have perfectly smooth walls such that the total energy of the N - particle system remains conserved when they bounce off the wall. Ignoring quantum mechanics, we can in principle exactly determine the position $\mathbf{q} = (x_1, y_1, z_1, x_2, ..., x_N, y_N, z_N)$ and momenta $\mathbf{p} = (p_1, p_2, ...p_3N)$ [1]. The hamil-

[1] The $3N$ dimensional space of positions $\mathbf{q}$ is called the configuration space. The $3N$ dimensional space of momenta $\mathbf{p}$ is called momentum space. Togather, the $6N$ dimensional space $\mathbf{p}, \mathbf{q}$ is called Phase Space

ton's equations are,

$$\dot{\mathbf{p}} = \frac{\partial \mathcal{H}}{\partial q}, \tag{2.1}$$

$$\dot{\mathbf{q}} = -\frac{\partial \mathcal{H}}{\partial p}. \tag{2.2}$$

Here, $\mathcal{H}$ is the Hamiltonian of the system. In general, solving these equations is plainly not feasible. First, many systems of interest involve far too many particles to allow one to solve for their trajectories. Moreover, the complex and chaotic motion of atoms quickly erases any specific information about their starting positions and velocities. This process of "scrambling" is how the system reaches equilibrium [11]. Consequently, the only certain knowledge we are left with is the system's total energy, E (and angular momentum if the container were spherical). Instead of tracking precise initial conditions, we can propose that energy alone is sufficient to define the system's equilibrium state. This assumption forms the basis of the microcanonical ensemble in statistical mechanics, which describes equilibrium by considering all possible atomic configurations that possess the same energy E. The approach is simple: we calculate the properties of our ensemble by averaging over states with energies in a shell $(E, E + \delta E)$ taking the limit $\delta E \to \infty$. Let's define the function $\Omega(E)$ to be the phase-space volume of this thin shell:

$$\Omega(E)\,\delta E = \int\limits_{E<H(P,Q)<E+\delta E} \mathrm{d}P\,\mathrm{d}Q. \tag{2.3}$$

Here, $H(P, Q)$ is the Hamiltonian for our system. The Hamiltonian H is the function of P and Q that gives the energy. For our purposes, this will always be $P^2/2m + V(Q) = \sum_{\alpha=1}^{3N} p_\alpha^2/2m + V(q_1, \ldots, q_{3N})$. The average of a property A in the microcanonical ensemble is done by averaging $A(P, Q)$ over this same energy shell,

$$\langle A \rangle_E = \frac{1}{\Omega(E)\delta E} \int\limits_{E<H(P,Q)<E+\delta E} A(P,Q)\mathrm{d}P\mathrm{d}Q. \tag{2.4}$$

By averaging equally over all states in phase space, we have made a hidden assumption that all points in phase space (with a given energy) are a priori equally likely, so the average should treat them all with equal weight. The long-time equilibrium behavior of a system is precisely the typical behavior of all systems with the same value of the conserved quantities [11].

In context of quantum mechaincs, the dynamics of systems are defined by a Hamiltonian $\hat{H}$, and the goal is typically to solve the time-independent Schrödinger equation:

$$\hat{H}|\psi\rangle = E|\psi\rangle.$$

The energy eigenstates $|\psi\rangle$ become extremely complex objects since they contain information about the behavior of each individual particle. These states are referred to as *microstates*. It would be impossibly tedious to keep track of the dynamics which leads to transitions between the different states. Instead we will resort to statistical methods. We will describe the system in terms of a probability distribution over the quantum states. In other words, the system is in a mixed state rather than a pure

state. Since we have fixed the energy, there will only be a non-zero probability for states which have the specified energy E. We will denote a basis of these states as $|n\rangle$ and the probability that the systems sits in a given state as $p(n)$. Within this probability distribution, the expectation value of any operator $\hat{O}$ is

$$\langle \hat{O} \rangle = \sum_n p(n) \langle n|\hat{O}|n\rangle.$$

Our immediate goal is to understand what probability distribution $p(n)$ is appropriate for large systems [15].

2.1.1 The Microcanocial Ensemble

Now we state the fundamental assumption of statistical mechanics - we treat all states the same. Or, more precisely:

Microcanonical ensemble

For an isolated system in equilibrium, all accessible microstates are equally likely.

For the seek of clarity, we restate the definiation to the microstates.

$$\Omega(E) = \text{The number of state with energy } E,$$

$$p(n) = \frac{1}{\Omega(E)}. \tag{2.5}$$

This probability distribution, relevant for systems with fixed energy, is known as the *microcanonical ensemble* [15]. It is important to note that $\Omega(E)$ is an extremely large number. We define the entropy of the system to be

$$S(E) = k_B \log \Omega(E). \tag{2.6}$$

Here, k_B is a fundamental constant, known as Boltzmann's constant. It has units of Joules per Kelvin

$$k_B \approx 1.381 \times 10^{-23}\,\mathrm{J\,K^{-1}}. \tag{2.7}$$

While the number of states is of order $\Omega \sim e^N$, the entropy is proportional to the number of particles in the system, $S \sim N$. One of the consequences of this is that entropy is an additive quantity. To see this, consider two non-interacting systems with energies E_1 and E_2 respectively. Then the total number of states of both systems is

$$\Omega(E_1, E_2) = \Omega_1(E_1)\Omega(E_2).$$

While the entropy for both systems is

$$S(E_1, E_2) = S_1(E_1) + S_2(E_2).$$

From here, we can carry on and establish four laws of classical thermodynamics.

2.1.2 Laws of Thermodynamics

The Zeroth Law

The zeroth law establishes temperature as a fundamental quantity and defines thermal equilibrium. From statistical mechanics, temperature emerges from the fundamental definition of entropy:

$$\frac{1}{T} = \frac{\partial S}{\partial E}.$$

Two systems in thermal contact will exchange energy until $\frac{\partial S_1}{\partial E_1} = \frac{\partial S_2}{\partial E_2}$, establishing equal temperatures and thermal equilibrium.

The First Law

The first law states energy conservation:

$$dU = dQ - dW.$$

In statistical mechanics, the internal energy U is the ensemble average:

$$U = \langle E \rangle = \sum_n p(n) E_n.$$

Heat transfer dQ corresponds to changes in probability distribution $p(n)$, while work dW involves changes in energy levels E_n.

The Second Law

The second law of thermodynamics can be formulated as a statement about the direction of heat flow that occurs as a system approaches equilibrium. Hence there is a connection with the direction of the arrow of time. Heat is always observed to flow from a hot body to a cold body and and the reverse process in isolation never occurs. The second law dictates that entropy never decreases in isolated systems. Therefore, following **Clausius**, we can state the second law of thermodynamics as follows:

Second Law of Thermodynamics (Clausius Statement)

No process is possible whose sole result is the transfer of heat from a colder to a hotter body.

An equivalent statement was given by **Kelvin**. Which is as follows:

Second Law of Thermodynamics (Kelvin–Planck Statement)

No process is possible whose sole result is the complete conversion of heat into work.

Now suppose there are two paths I and II connecting an initial state A to a final state B. Path I is assumed to be irreversible and path II is reversible. Then Clausius' identity implies:

$$\int_A^B \frac{dQ}{T}\bigg|_{\mathrm{I}} \leq \int_A^B \frac{dQ}{T}\bigg|_{\mathrm{II}} = S(B) - S(A)$$

$$\Rightarrow \int_A^B \frac{dQ}{T}\bigg|_{\mathrm{I}} \leq S(B) - S(A)$$

It is important to note that for an irreversible process, T cannot be interpreted as the temperature of the body but rather that of the reservoir that is supplying the heat, and so one cannot use $dS = dQ/T$ for irreversible paths. Now if the irreversible path is adiabatic, i.e., $dQ = 0$, then we get:

$$S(B) - S(A) \geq 0.$$

This means that for an isolated system, entropy can never decrease. Statistically, we can write:

$$\Omega_{\mathrm{B}} \geq \Omega_{\mathrm{A}}$$

Since $S = k_B \log \Omega(E)$, it can be inferred that the logarithmically increasing number of accessible states drives the system toward maximum entropy configurations.

The Third Law

From the Gibbs free energy definition $G = H - TS$, we expect that

$$\Delta G = \Delta H - T\Delta S, \tag{2.8}$$

so that as $T \to 0$, $\Delta G \to \Delta H$. Experimental data showed that this was true, but ΔG and ΔH not only came closer together on cooling, but they approached each other asymptotically. On the basis of the data, Nernst postulated that as we approach temperature to zero kelvin, the entropy of the system also goes to zero. His statement of the third law, dating from 1906, can be written as:

Nernest's statement for the third law

Near absolute zero, all reactions in a system in internal equilibrium take place with no change in entropy.

Max Planck added more meat to the bones of the statement by making a further hypothesis in 1911. [12] The final point can almost be elevated to the status of another statement of the third law:

Plack's statement for the third law

The entropy of all systems in internal equilibrium is the same at absolute zero, and may be taken to be zero.

The main point of this law is that it is impossible to cool to $T = 0$ in a finite number of steps. Statistical mechanics thus provides microscopic foundations for thermodynamics, deriving macroscopic laws from the statistical behavior of numerous microscopic constituents.

2.1.3 The canonical ensemble and Partition function

The microcanocial ensemble is not general enough to cover all interacting physcial processes. For example. the microcanocial ensemble requires that the system to be

isolated and its energy to be fixed. Most of the physical systems, however, interact with the environment thus the total energy of the system fluctuates. We can consdier a System $\mathcal{S}$ interacting with a large reservoir $\mathcal{R}$. We assue that the reservoir $\mathcal{S}$ at the temperature T, is connected to $\mathcal{S}$ through an impermeablebut diathermal wall. Let use assume that P_α is the probability that the system is in the unique state α. Let the energy of the state be E_α. So P_α is the probability that the system has energy E_α, which is proportional to the number of microstates that are accesible to the reservoir multipled by the number of microstates accessible to the system e.g. $\Omega_{\mathcal{S}}(E_\alpha) = 1$. Then the probability that the system is in the state α is given by

$$P_\alpha = C \times \Omega_R(E - E_\alpha)$$

Here, E is the total energy. Since S is small compared to R, E_α is going to be small compared to E. We then expand P_α as a Taylor series around E_α:

$$\log P_\alpha = \log C + \log \Omega_2(E - E_\alpha) \approx \log C + \log \Omega_2(E) - \frac{\partial \log \Omega_2}{\partial E} E_\alpha + \frac{1}{2} \frac{\partial^2 \log \Omega_2}{\partial E^2} E_\alpha^2 + \cdots$$

Now the temperature of the reservoir $T = \left(k_B \frac{\partial \log \Omega_2}{\partial E}\right)^{-1}$. We ignore the higher-order terms because E_α is small compared to E, and so we get:

$$P_\alpha \propto e^{-\beta E_\alpha}$$

The equation below is the Boltzmann distribution, also known as the canonical ensemble.

$$P_\alpha = \frac{1}{Z} e^{-\beta E_\alpha} \tag{2.9}$$

where Z is a normalization constant. From the requirement

$$\sum_x P_\alpha = 1,$$

Z can be determined to be

$$Z = \sum_\alpha e^{-\beta E_\alpha} \tag{2.10}$$

Z is called the partition function and it is of central importance in statistical mechanics. All thermodynamic quantities of interest can be derived from the partition function. Notice that the details of the reservoir have dropped out. We don't need to know $S_{\mathcal{R}}(E)$ for the reservoir; all that remains of its influence is the temperature T. The exponential suppression in the Boltzmann distribution means that it is very unlikely that any of the states with $E_n \gg k_B T$ are populated. However, all states with energy $E_n \leq k_B T$ have a decent chance of being occupied. Note that as $T \to 0$, the Boltzmann distribution forces the system into its ground state (i.e., the state with lowest energy); all higher energy states have vanishing probability at zero temperature.

Average energy and its flactuation

The energy of the system is not fixed and is allowed to fluctuate. What is the value of the average energy and how large are the fluctuations? Here we use the

partition function to obtain these answers. Let $\langle E \rangle = \frac{1}{Z}\sum_\alpha E_\alpha e^{-\beta E_\alpha} = -\frac{\partial \log Z}{\partial \beta}$. On the other hand, we can compute the variance by:

$$(\Delta E)^2 = \langle E^2 \rangle - \langle E \rangle^2 = \frac{1}{Z}\sum_x E_\alpha^2 e^{-\beta E_\alpha} - \left(\frac{1}{Z}\sum_\alpha E_\alpha x e^{-\beta E_\alpha}\right)^2 = \frac{\partial^2 \log Z}{\partial \beta^2}.$$

This allows us to compute C_v:

$$(\Delta E)^2 = k_B T^2 \frac{\partial \langle E \rangle}{\partial T} = k_B T^2 C_v.$$

Let us compute ΔE for a cup of coffee at room temperature: $C_v \approx 10^3\,\mathrm{J/K}$, $\rho = 1.381 \times 10^{-23}\,\mathrm{J\ K^{-1}}$. At room temperature $T = 300\,\mathrm{K}$:

$$\Delta E \approx 10^{-10}, \quad \Delta E \approx 10^{-8}\,\text{Joules}.$$

Thus for large enough C_v, ΔE can be quite significant. This plays an important role in the fluctuation-dissipation theorem, which says that for a system which has a way of dissipating energy (say through friction), there is a reverse process involving fluctuation of energy.

Thermodynamic Limit!

It is conventional to denote the average energy $\langle E \rangle$ as E. For classical systems with N degrees of freedom, one has $C_v \sim N$. Then $\Delta E \sim \sqrt{N}T$ and $E \sim N$. Thus we have $\frac{\Delta E}{E} \sim \frac{1}{\sqrt{N}}$. In the thermodynamic limit $N \to \infty$, $\frac{\Delta E}{E} \to 0$ and the energy is sharply peaked around the average E. Thus in the thermodynamic limit, the canonical ensemble reduces to the microcanonical ensemble.

2.1.4 A Density Matrix for the Canonical Ensemble

In statistical mechanics, the inherent probabilities of the quantum world are joined with probabilities that arise from our ignorance of the underlying state. The correct way to describe this is in terms of a density matrix, $\hat{\rho}$. The canonical ensemble is really a choice of density matrix:

$$\hat{\rho} = \frac{e^{-\beta \hat{H}}}{Z} = \frac{e^{-\beta E_n} |n\rangle \langle n|}{Z}. \tag{2.11}$$

Here, $|n\rangle$ is the energy eigenstate with energy eigenvalue E_n. If we make a measurement described by an operator $\hat{O}$, then the probability that we find ourselves in the eigenstate $|\phi\rangle$ is given by

$$p(\phi) = \langle \phi | \hat{\rho} | \phi \rangle.$$

For energy eigenstates, this coincides with our earlier result [15].

Entropy

In this section, we will explore the concept of entropy from a different point of view. We take a large number - say W in number - of identical copies of our system of interest $\mathcal{S}$ where each system is in the state $|n\rangle$. If W is large enough, the number

of systems that sit in state $|n\rangle$ must be simply $p(n)W$. To determine the entropy we can treat the whole collection of W systems as sitting in the microcanonical ensemble to which we can apply the familiar Boltzmann definition of entropy. The multiplicity of states is given by:

$$\Omega = \frac{W!}{\prod_n (p(n)W)!}. \tag{2.12}$$

Using Stirling's formula, the entropy for all W copies is:

$$S = k_B \log \Omega = -k_B W \sum_n p(n) \log p(n). \tag{2.13}$$

For a single system, the entropy is additive, leading to the Gibbs entropy:

$$S = -k_B \sum_n p(n) \log p(n) \tag{2.14}$$

Substituting the Boltzmann distribution $p(n) = e^{-\beta E_n}/Z$:

$$S = -\frac{k_B}{Z} \sum_n e^{-\beta E_n} \log \left(\frac{e^{-\beta E_n}}{Z} \right) = k_B \beta \langle E \rangle + k_B \log Z. \tag{2.15}$$

This can be elegantly expressed in terms of the partition function as:

$$S = k_B \frac{\partial}{\partial T} (T \log Z). \tag{2.16}$$

It is important to note that here we have viewed S as a function of a probability distribution unlike the case in microcanonical ensemble. Here the probability distribution is itself determined by the choice of energy E. If we take a special case where $p(n) = \frac{1}{\Omega(E)}$, the Gibbs entropy reverts to Boltzmann entropy for all states $|n\rangle$ with energy E.

The expression of entropy in (2.14) was rediscovered some decades later in the context of information theory where it goes by the name of Shannon entropy for classical systems or Von Neumann entropy for quantum systems. In quantum mechanics, using the density matrix $\hat{\rho}$, this becomes:

$$S = -k_B \operatorname{Tr}(\hat{\rho} \log \hat{\rho}) \tag{2.17}$$

2.1.5 The grand canonical ensemble

Now we are in the position to consider the case particles are free to move between the system and the reservoir, then N e.g the number of particle is no longer fixed. In such a situation, we will require that the reservoir sits at fixed chemical potential μ as well as fixed temperature T. The probability distribution that we need to use in this case is called the grand canonical ensemble. We introduce the grand canonical partition function

$$\mathcal{Z}(T, \mu, V) = \Sigma_n \exp(-\beta(E_n - \mu N_n)) \tag{2.18}$$

The probability that we find a particle in $|n\rangle$ is given by,

$$p(n) = \frac{e^{-\beta(E_n - \mu N_n)}}{\mathcal{Z}} \tag{2.19}$$

In the canonical ensemble, all the information that we need is contained within the partition function Z. In the grand canonical ensemble it is contained within $\mathcal{Z}$. The entropy (2.14) is once again given by

$$S = k_B \frac{\partial}{\partial T}(T \log \mathcal{Z}) \tag{2.20}$$

while differentiating with respect to β gives us

$$\langle E \rangle - \mu \langle N \rangle = -\frac{\partial}{\partial \beta} \log \mathcal{Z} \tag{2.21}$$

The average particle number $\langle N \rangle$ in the system can then be separately extracted by

$$\langle N \rangle = \frac{1}{\beta} \frac{\partial}{\partial \mu} \log \mathcal{Z} \tag{1.42}$$

and its fluctuations,

$$\Delta N^2 = \frac{1}{\beta^2} \frac{\partial^2}{\partial \mu^2} \log \mathcal{Z} = \frac{1}{\beta} \frac{\partial \langle N \rangle}{\partial \mu} \tag{2.22}$$

Just as the average energy is determined by the temperature in the canonical ensemble, here the average particle number is determined by the chemical potential. The relative size of these fluctuations scales in the same way as the energy fluctuations, $\Delta N / \langle N \rangle \sim 1/\sqrt{\langle N \rangle}$, and in the thermodynamic limit $N \to \infty$ results from all three ensembles coincide.

2.1.6 The BBGKY Hierarchy

We now briefly review the BBGKY hierarchy. This discussion serves as motivation for our subsequent treatment of the Eigenstate Thermalization Hypothesis. Although the two frameworks arise in different contexts, both aim to explain how thermodynamic behavior emerges from the microscopic dynamics of many-body systems. The conceptual role played by the BBGKY hierarchy in classical statistical mechanics is similar to the role played by the Eigenstate Thermalization Hypothesis in quantum many-body systems. While the BBGKY hierarchy describes the time evolution of reduced distribution of N - particles in an integrable many body system in absence of quantum fluctuations, eigenstate thermalisation hypothesis offers stationary solution which describes the final state of a quantum chaotic system in terms of the properties of the energy eigenstates.

Our starting point is simply the Hamiltonian dynamics for N identical point particles. The hamiltonian takes the form,

$$H = \frac{1}{2m} \sum_{i=1}^{N} \vec{p_i}^2 + \sum_{i=1}^{N} V(\vec{r_i}) + \sum_{i<j} U(\vec{r_i} - \vec{r_j}) \tag{2.23}$$

Let $f(\vec{r}_i, \vec{p}_i; t)$ be a probability distribution over the $6N$-dimensional phase space. This function tells us the probability that the system will be found in the vicinity of the point $(\vec{r}_i, \vec{p}_i)$. As with all probabilities, the function is normalized as

$$\int dV\, f(\vec{r}_i, \vec{p}_i; t) = 1, \qquad \text{with} \qquad dV = \prod_{i=1}^{N} d^3r_i\, d^3p_i. \tag{2.24}$$

Instead of working with a probablity distribution of N identical particles, we deal with one-particle distribution function. This captures the expected number of particles lying at some point $(\vec{r}, \vec{p})$. It is defined by

$$f_1(\vec{r}, \vec{p}; t) = N \int \prod_{i=2}^{N} d^3r_i\, d^3p_i\, f(\vec{r}, \vec{r}_2, \ldots, \vec{r}_N, \vec{p}, \vec{p}_2, \ldots, \vec{p}_N; t). \tag{2.25}$$

where f_1 remains normalised,

$$\int d^3p\, d^3r\, f_1(\vec{r}, \vec{p}; t) = N \tag{2.26}$$

We now derive a equation governing the time evolution of f_1. For that we calculate the time evolution of f_1

$$\frac{\partial f_1}{\partial t} = N \int \prod_{i=2}^{N} d^3r_i\, d^3p_i \frac{\partial f}{\partial t} = N \int \prod_{i=2}^{N} d^3r_i\, d^3p_i \{H, f\}. \tag{2.27}$$

Using the Hamiltonian given above, this becomes

$$\frac{\partial f_1}{\partial t} = N \int \prod_{i=2}^{N} d^3r_i\, d^3p_i \left[-\sum_{j=1}^{N} \frac{\vec{p}_j}{m} \cdot \frac{\partial f}{\partial \vec{r}_j} + \sum_{j=1}^{N} \frac{\partial V}{\partial \vec{r}_j} \cdot \frac{\partial f}{\partial \vec{p}_j} + \sum_{j=1}^{N} \sum_{k<l} \frac{\partial U(\vec{r}_k - \vec{r}_l)}{\partial \vec{r}_j} \cdot \frac{\partial f}{\partial \vec{p}_j} \right] \tag{2.28}$$

After integrating by parts we are only left with $\vec{r_1}$ and $\vec{p_1}$. Relabeling $\vec{r_1} = \vec{r}$ and $\vec{p_1} = \vec{p}$

$$\frac{\partial f_1}{\partial t} = N \int \prod_{i=2}^{N} d^3r_i\, d^3p_i \left[-\frac{\vec{p}}{m} \cdot \frac{\partial f}{\partial \vec{r}} + \frac{\partial V}{\partial \vec{r}} \cdot \frac{\partial f}{\partial \vec{p}} + \sum_{k=1}^{N} \frac{\partial U(\vec{r}_k - \vec{r}_l)}{\partial \vec{r}} \cdot \frac{\partial f}{\partial \vec{p}} \right] \tag{2.29}$$

$$\frac{\partial f_1}{\partial t} = \{H_1, f_1\} + N \int \prod_{i=2}^{N} d^3r_i\, d^3p_i \left[\sum_{k=1}^{N} \frac{\partial U(\vec{r}_k - \vec{r}_l)}{\partial \vec{r}} \cdot \frac{\partial f}{\partial \vec{p}} \right] \tag{2.30}$$

Here, H_1 is a one particle hamiltonian which includes only the external force V acting on the particle. Notice that this hamiltonian does not include any interaction potential. Eqn (2.30) can be expressed as a Liouville-like equation with an extra term,

$$\frac{\partial f_1}{\partial t} = \{H_1, f_1\} + \left(\frac{\partial f_1}{\partial t} \right)_{coll} \tag{2.31}$$

Since all particles are identical, we have

$$\left(\frac{\partial f_1}{\partial t} \right)_{coll} = N(N-1) \int d^3r_2\, d^3p_2 \frac{\partial U(\vec{r} - \vec{r_2})}{\partial \vec{r}} \cdot \frac{\partial}{\partial \vec{p}} \int \prod_{i=3}^{N} d^3r_i\, d^3p_i\, f(\vec{r}, \vec{r}_2, \ldots, \vec{p}, \vec{p}_2, \ldots; t). \tag{2.32}$$

However, the collision integral cannot be expressed in terms of the one-particle distribution function since f_1 contains no information about where any of the other particles are in relation to the first. So we take two particle distribution in consideration.

$$f_2(\vec{r}_1, \vec{r}_2, \vec{p}_1, \vec{p}_2; t) \equiv N(N-1) \int \prod_{i=3}^{N} d^3 r_i \, d^3 p_i \, f(\vec{r}_1, \vec{r}_2, \ldots, \vec{p}_1, \vec{p}_2, \ldots; t) \tag{2.33}$$

With this definition, the collision integral is written simply as

$$\left(\frac{\partial f_1}{\partial t} \right)_{\text{coll}} = \int d^3 r_2 \, d^3 p_2 \, \frac{\partial U(\vec{r} - \vec{r}_2)}{\partial \vec{r}'} \cdot \frac{\partial f_2}{\partial \vec{p}} \tag{2.34}$$

We see that in order to evolve single particle distribution f_1, we need some information regarding two particle probability distribution f_2. Again, the evolution of f_2 is given by the Liouville-like equation we discussed earlier. In general, the $n-$particle distribution function

$$f_n(\vec{r}_1, \ldots, \vec{r}_n, \vec{p}_1, \ldots, \vec{p}_n; t) = \frac{N!}{(N-n)!} \int \prod_{i=n+1}^{N} d^3 r_i \, d^3 p_i \, f(\vec{r}_1, \ldots, \vec{r}_N, \vec{p}_1, \ldots, \vec{p}_N; t) \tag{2.35}$$

obeys the equation,

$$\frac{\partial f_n}{\partial t} = \{H_n, f_n\} + \sum_{i=1}^{n} \int d^3 r_{n+1} \, d^3 p_{n+1} \, \frac{\partial U(\vec{r}_i - \vec{r}_{n+1})}{\partial \vec{r}_i} \cdot \frac{\partial f_{n+1}}{\partial \vec{p}_i} \tag{2.36}$$

This equations are known as the BBGKY hierarchy [14].

2.2 Review on Quantum Statistical Mechanics

Let us consider a gas of non-interacting quantum particles in a box of volume V. The wavefunction of each particle is given by:

$$\psi(\mathbf{r}) = e^{i\mathbf{k}\cdot\mathbf{r}}$$

These wavefunctions satisfy periodic boundary conditions. If the size of the box is L on each side, then $\mathbf{k} = \frac{2\pi}{L}\mathbf{n}$, where $\mathbf{n} = (n_x, n_y, n_z)$ with $n_i \in Z$. The allowed energy eigenvalues are:

$$E_{\mathbf{n}} = \frac{\hbar^2 k^2}{2m} = \frac{\hbar^2}{2m} \left(\frac{2\pi}{L} \right)^2 (n_x^2 + n_y^2 + n_z^2) = \frac{2\pi^2 \hbar^2}{mL^2} (n_x^2 + n_y^2 + n_z^2)$$

Partition function:

$$Z = \sum_{\mathbf{n}} e^{-\beta E_{\mathbf{n}}}$$

For temperatures that are not too low, we can approximate this sum by an integral. The argument in the exponent has $\lambda_{\text{th}} = \frac{h}{\sqrt{2\pi m k_B T}}$, and for $\lambda_{\text{th}} \ll L$ we can write:

$$\sum_{\mathbf{n}} \approx \int d^3 n = \left(\frac{L}{2\pi} \right)^3 \int d^3 k$$

Thus:

$$Z \approx \left(\frac{L}{2\pi}\right)^3 \int d^3k e^{-\beta\hbar^2k^2/2m} = V \int \frac{d^3k}{(2\pi)^3} e^{-\beta\hbar^2k^2/2m}$$

Using $d^3k = 4\pi k^2 dk$, we get:

$$Z = V \int_0^\infty g(E) dE$$

where $g(E) = \frac{(2m)^{3/2}V}{4\pi^2\hbar^3}\sqrt{E}$ is the density of states for a non-relativistic gas. According to classical statistical mechanics, the radiation energy density emitted by a hot body is finite. However, in reality when heated up, a blackbody radiates in a very well-defined spectrum that can be thought of as an idealisation of the way a generic body radiates. Clearly, the radiation of a blackbody is temperature-dependent and classical statistical mechanics fails to describe it. Historically, Max Planck addressed this issue by assuming that the surface of the blackbody is made up of quantum harmonic oscillators. Here, we consider a photon-gas and apply the canonical ensemble and the density of states formula derived in the previous section to derive the total radiant energy density. Since in quantum mechanics, photons are non-interacting particles thus for photons of different frequencies, the partition function will be the product of the individual partition function e.g. $Z = Z(\omega_1) \times Z(\omega_2) \times Z(\omega_3) .... \times Z(\omega_N)$, where ω is a continuous variable. The total partition function is then given by:

$$\log Z = \int_0^\infty g(\omega) \log Z_\omega = -\int_0^\infty d\omega \frac{v\omega^2}{\pi^2 c^3} \log(1 - e^{-\beta\hbar\omega}) \tag{2.37}$$

Since the energy is given by $E = -\frac{\partial \log Z}{\partial \beta}$, The Plankcs distribution comes,

$$E(\omega)d\omega = \frac{v\hbar}{\pi^2 c^3} \frac{\omega^3}{e^{\hbar\beta\omega} - 1} \tag{2.38}$$

2.2.1 Symmetries of Wavefunctions

There are two types of non-interacting gases based on whether they are consists of bosons or fermions. Imagine a scenario where a certain type of particles are housed in a box of length L. If the thermal de Brogile wavelength, λ_{th} of the particles is compatible with the size of the box, L, then the quantum nature of the particles become dominant. Consider the hamiltonian of two particle system

$$H = \frac{\hat{P}_1}{2m_1} + \frac{\hat{P}_2}{2m_2} + V(r_1, r_2). \tag{2.39}$$

For non-interacting gasses, we have $V(r_1, r_2) = 0$. Define a parity operator that exchanges the position of two particles - the eigenvalue of this operator is either $+1$ or -1

1. for eigenvalue $+1$, we conclude the wavefunction is symmetric, naming the corresponding particle as Boson

$$\psi(x_1, x_2) = \psi(x_2, x_1) \tag{2.40}$$

Bosons have natural affinity to each other

2. Similarly for eigenvalue -1, we conclude the wavefunction is symmetric, naming the corresponding particle as Fermions

$$\psi(x_1, x_2) = -\psi(x_2, x_1) \tag{2.41}$$

Fermions have natural repulsion to each other

Quantum particles are are indistinguishable, meaning if two particles come in the same place such that their wavefunction overlap, then there is no way to tell which particle is which after they move away from that particular position in space. So, for bosons, the allowed possible states are $|0\rangle_1 |0\rangle_2$, $|1\rangle_1 |1\rangle_2$, $\frac{|0\rangle_1|1\rangle_2+|1\rangle_1|0\rangle_2}{\sqrt{2}}$, where all states are eigenstates of the permutation operator with eigenvalue 1. On the other hand, the only possible fermionic state is $\frac{|0\rangle_1|1\rangle_2-|1\rangle_1|0\rangle_2}{\sqrt{2}}$, which is an eigenstate of the permutation operator with eigenvalue -1. Note that because of the anti symmetry of the fermionic wavefunctions, no state is allowed in which the two particles have the same state because the total wavefuncion would be zero. This is precisely the Pauli exclusion principle.

2.2.2 The Postulates

Now we define the postulates for quantum statistical mechanics that are equivalent to the classical ones in appropriate limit

Postulate 1

The first postulate for classical statistical mechanics states that [28]

Classical Postulate 1

The expectation values of the classical observables O equals to the temporal average,

$$O_{avg} \equiv \bar{O} = \lim_{\tau\to\infty} \int_0^\tau O(t)dt \tag{2.42}$$

Quantum Postulate 1

The quantum expectation value of an observable equals the temporal average of the observable,

$$\bar{O}_{obs} = \bar{O}(t) \tag{2.43}$$

Postulate 2

In classical statistical mechanics, the second postulate is called the ergodic hypothesis which states

Classical Postulate 2

The average over the ensemble of a classical observable equals the time average of observables

$$\langle O\rangle_{cls} = \bar{O} \tag{2.44}$$

In quantum statistics, the classical observables are replaced by the quantum mechanical observables which are hermitian operators with real eigenvalues. Also, the statistical average is different in this case [28].

Quantum Postulate 2

The expectation value of the quantum observables are equal to the quantum statistical ensemble average of those observables

$$\langle O_{obs} \rangle = \langle O \rangle_{ensemble} = \mathrm{Tr}(\hat{\rho}\hat{O}) \tag{2.45}$$

Postulate 3

The third postulate, of a priori equal probabilities, known as the Tollman postulate, says that for an isolated system, the probability density in phase space is constant for all the accessible states (i.e., those consistent with the external boundary conditions). [28] Mathematically, we write

$$\rho = \begin{cases} C, & x \in D, \\ 0, & x \notin D. \end{cases} \tag{2.46}$$

In quantum statistics, the postulate is

Quantum Postulate 3

For a quantum state, the amplitudes of $c_\alpha^{(j)}$, for an expansion in the basis $|\psi_\alpha\rangle$ are a prior equal, and the phases of the same are a prior random

$$c_\alpha^{(j)} = r^{(j)} e^{i\phi_\alpha^j}$$

where $r(j)$ is independent of α and the ϕ_α are random as a function of α. Defining the classical ensemble average (denoted by an overbar) as an average over the states j, the conditions are

$$\overline{r_\alpha^2} = \rho_0, \qquad \overline{\cos(\phi_\alpha - \phi_\beta)} = 0, \qquad \overline{\sin(\phi_\alpha - \phi_\beta)} = 0.$$

Then the density matrix in the basis $|\psi_\alpha\rangle$ is constant and diagonal,

$$\rho_{\alpha\beta} = \begin{cases} \rho_0\, \delta_{\alpha\beta}, & (\alpha, \beta) \in D, \\ 0, & (\alpha, \beta) \notin D. \end{cases}$$

The properties of the statistical operator $\hat{\rho}$, known as the density matrix as well, are as follows.

1. It is a hermitian operator
2. It is normalized by
$$\mathrm{Tr}\ \hat{\rho} = 1.$$
3. The eigenvalues of $\hat{\rho}$ are semi-positive-definite, i.e., ≥ 0. This must be so, since they represent probabilities.

4. $\hat{\rho}$ is bounded, meaning that

$$|\rho_{\alpha\beta}| \leq 1.$$

Further, to determine $\hat{\rho}$ for an isolated system and in general, we have the Liouville–von Neumann equation,

$$i\frac{\partial\hat{\rho}}{\partial t} = [\hat{H}, \hat{\rho}].$$

From this discussion, we interpret what it means for a quantum observable to reach thermal equilibrium: a statistical ensemble at equilibrium gives observables that are time independent. Therefore

$$A_{\text{obs}} = \langle A \rangle = \text{Tr}(\hat{\rho}\hat{A})$$

But, by the Liouville - von Neumann equation, we have

$$\frac{\partial\hat{\rho}}{\partial t} = 0 \;\Rightarrow\; [\hat{\rho}, \hat{H}] = 0.$$

Since these two Hermitian operators commute, it means that we can measure them simultaneously. But then, classically, ergodicity would mean that the distribution depends on the energy only,

$$\rho(p, q) = \rho\big(H(p, q)\big).$$

The same statement in quantum mechanics is that now the statistical operator is a function of the Hamiltonian,

$$\hat{\rho} = \rho(\hat{H}).$$

We can now define the quantum version of ensembles and their associated distributions. We define the ensemble by saying that it is composed of isolated systems, each with energy in a very small region $E' \in (E, E + \Delta E)$. Since the statistical operator is a function of the Hamiltonian,

$$\hat{\rho} = \rho(\hat{H}), \tag{2.47}$$

for the energy eigenvalues we have

$$\rho_{nm} = \rho(E_n)\,\delta_{nm}. \tag{2.48}$$

Defining a domain

$$D = \{\, n \mid E < E_n < E + \Delta E \,\}, \tag{2.49}$$

and a function

$$\Delta_D(x) = \begin{cases} 1, & x \in D, \\ 0, & x \notin D, \end{cases} \tag{2.50}$$

the quasi-microcanonical distribution is

$$\rho(E_n) = \begin{cases} \text{constant}, & n \in D, \\ 0, & \text{otherwise.} \end{cases} \tag{2.51}$$

This can be rewritten as

$$\rho_{nm} = \frac{\Delta_{\Delta E}(E_n - E)}{\Omega(E, \Delta E)}\,\delta_{nm}, \tag{2.52}$$

With the appropriate normalization for the matrix so that we have $\sum_n \rho_{nn} = 1$. This can be extended in the quantum case to the formula

$$\hat{\rho} = \frac{\Delta_{\Delta E}(\hat{H} - E\mathbf{1})}{\Omega(E, \Delta E)}, \tag{2.53}$$

where $\Delta_{\Delta E}(\hat{H} - E\mathbf{1})$ is a projector onto the domain D. Then the expectation value for an observable A is given by

$$\langle A \rangle = \frac{1}{\Omega(E, \Delta E)} \sum_{n \in D} \langle n | \hat{A} | n \rangle. \tag{2.54}$$

Postulate 4

We define the entropy of an isolated system in terms of the number of states in the domain D (of energy in $(E, E + \Delta E)$), Ω, as

$$S = k_B \ln \Omega. \tag{2.55}$$

The formula for the entropy S should satisfy the condition that, if the system is made of two subsystems, $S = S_a \cup S_b$, then the density of states at energy E

$$\omega(E) \simeq \omega^{(a)}\big(E^{(a)}\big)\, \omega^{(b)}\big(E^{(b)}\big)\, \Delta E. \tag{2.56}$$

In the thermodynamic limit, of an infinite number of particles, volume, and energy, with fixed ratios,

$$N \to \infty, \qquad V \to \infty, \qquad E \to \infty, \qquad \frac{E}{N} = \text{fixed}, \qquad \frac{V}{N} = \text{fixed}, \tag{2.57}$$

We define the distribution function of the statistical ensemble as

$$\rho = \frac{dN}{N\, d\Gamma}, \tag{2.58}$$

where N denotes the number of systems in the ensemble and $d\Gamma$ is the differential of the total number of states with energy $\leq E$, given by

$$\Gamma(E) = \int_{H \leq E} d\Gamma. \tag{2.59}$$

We also define the number of states in the energy interval between E and $E + \Delta E$ as

$$\Omega(E, \Delta E) = \int_{E \leq H \leq E + \Delta E} d\Gamma. \tag{2.60}$$

The energy density of states is defined as

$$\omega(E) = \frac{\partial \Gamma(E)}{\partial E}, \tag{2.61}$$

so that for small ΔE, we have

$$\Omega(E, \Delta E) \simeq \omega(E)\, \Delta E. \tag{2.62}$$

we have other formulas for the entropy that are equivalent to the above,

$$S = k_B \ln \omega, \qquad S = k_B \ln \Gamma, \qquad S = -k_B \langle \ln \rho \rangle. \tag{2.63}$$

These formulas are based on the fact that, for a very large dimension of the phase space, $N \to \infty$,

$$\omega \, \Delta E \simeq \Gamma \simeq \Omega. \tag{2.64}$$

Moreover, the last relation, based on the distribution ρ, becomes in quantum mechanics, using the standard averaging with $\hat{\rho}$

$$S = -k_B \, \mathrm{Tr}(\hat{\rho} \ln \hat{\rho}) \,, \tag{2.65}$$

which is the von Neumann entropy, generalizing the Gibbs entropy, or also known by the name Gibbs state. We also note that the entropy is only additive in the thermodynamic limit.

2.2.3 Canonical and Grand Canonical Ensembles in Quantum Statistics

In this section, we discuss the quantum analogue of statistical ensembles which will be useful for our discussion in quantum statistical distributions: Bose-Einstein and Fermi Dirac Distribution

Canonical Ensemble

The simplest and most standard one is the canonical distribution, in which case the system is connected to a reservoir, $\mathcal{S} \cup \mathcal{R}$, at temperature T as we discussed earlier. Since the variatthe entropy is related to heat (energy variation) divided by temperature, we obtain

$$\delta S = \frac{\delta Q}{T}. \tag{2.66}$$

Using the statistical expression for entropy,

$$S = -k_B \langle \ln \rho \rangle. \tag{2.67}$$

This relation is satisfied by a Maxwell–type distribution in the thermodynamic limit,

$$\rho \propto e^{-H/(k_B T)}. \tag{2.68}$$

Including normalization, the formula becomes

$$\rho = \frac{1}{Z} e^{-H/(k_B T)}. \tag{2.69}$$

Defining

$$\beta = \frac{1}{k_B T}, \tag{2.70}$$

the partition function Z is the sum over the exponential factors,

$$Z = \sum_n e^{-\beta E_n}. \tag{2.71}$$

Where the sum is over all possible ways of partitioning N particles. Unfortunately, the need to impose this constraint makes the sums tricky. Here we do not allow the number of particles to fluctuate, although it is awkward to use since quantum particles are indistinguishable. However, in quantum mechanics, this formula becomes more useful, since the statistical operator

$$\hat{\rho} = \rho(\hat{H}) = \frac{1}{Z(\beta, V, N)} e^{-\beta \hat{H}}, \tag{2.72}$$

becomes discrete for energy eigenstates,

$$\rho_n(E_n) = \frac{e^{-\beta E_n}}{Z(\beta, V, N)}. \tag{2.73}$$

The partition function also becomes discrete,

$$Z(\beta, V, N) = \sum_n g_n e^{-\beta E_n}, \tag{2.74}$$

such that ρ_n is normalized to one,

$$\sum_n g_n \rho_n = 1. \tag{2.75}$$

In this ensemble, we define the internal energy as the average of the energies

$$U \equiv \langle E \rangle = \sum_n g_n \rho_n E_n = \frac{\sum_n g_n E_n e^{-\beta E_n}}{Z} = -\frac{\partial}{\partial \beta} \ln Z. \tag{2.76}$$

But since in thermodynamics

$$U = \frac{\partial}{\partial \beta}[\beta F(T, V, N)] = F + \beta \frac{\partial F}{\partial \beta}, \tag{2.77}$$

we can identify the free energy F (the thermodynamic potential in this case) as

$$F(T, V, N) = -k_B T \ln Z. \tag{2.78}$$

Grand Canonical Ensemble

Another relevant ensemble is the grand canonical one, in which case there is a reservoir of heat and particles in contact with our system, keeping fixed the system's temperature T and chemical potential μ, $S \cup R_{T,\mu}$. Then the classical distribution is

$$\rho = \frac{1}{Z(\beta, \beta\mu)} e^{-\beta(H - \mu N)}, \tag{2.79}$$

which at the quantum level leads to the operator

$$\hat{\rho} = \rho(\hat{H}, \hat{N}) = \frac{1}{Z(\beta, \beta\mu)} e^{-\beta(\hat{H} - \mu \hat{N})}, \tag{2.80}$$

with eigenvalues

$$\rho_n = \frac{1}{Z(\beta, \beta\mu)} e^{-\beta(E_n - \mu N_n)} \tag{2.81}$$

Then the partition function is

$$Z(\beta, \beta\mu) = \sum_n g_n e^{-\beta(E_n - \mu N_n)}. \tag{2.82}$$

and the thermodynamic potential is now

$$\Omega(T, V, \mu) = -k_B T \ln Z(\beta, \beta\mu). \tag{2.83}$$

The total average energy and number of particles can be calculated from the thermodynamic potential (or equivalently from Z) as

$$U = \langle H \rangle = -\left(\frac{\partial \ln Z}{\partial \beta}\right)_{\beta\mu}, \tag{2.84}$$

$$\langle N \rangle = \left(\frac{\partial \ln Z}{\partial(\beta\mu)}\right)_{\beta}. \tag{2.85}$$

2.2.4 Bose-Einstein and Fermi-Dirac Statistics

Many-body quantum statistical mechanics is hard. We consider systems consisting of identical quantum particles, bosons or fermions, which are identical and indistinguishable and must therefore satisfy either Bose–Einstein or Fermi–Dirac statistics. In the case of Bose–Einstein statistics, in each state we can have an arbitrary number of particles

$$n_\alpha = 0, 1, 2, \ldots, \infty.$$

In the case of Fermi–Dirac statistics, because of the Pauli exclusion principle we can only have

$$n_\alpha = 0 \text{ or } 1$$

implying that the state is either occupied or not. Then in both cases, the energy splits over the energy states, so does the total number of particles,

$$E = \sum_\alpha \epsilon_\alpha n_\alpha, \qquad N = \sum_\alpha n_\alpha. \tag{2.86}$$

Moreover, the partition function also factorizes,

$$Z = \prod_\alpha Z_\alpha, \tag{2.87}$$

where

$$Z_\alpha = \sum_{n_\alpha} e^{-\beta n_\alpha(\epsilon_\alpha - \mu)}. \tag{2.88}$$

(1) Bose–Einstein statistics Summing over $n_\alpha = 0, 1, \ldots, \infty$, we get

$$Z_\alpha = \frac{1}{1 - e^{-\beta(\epsilon_\alpha - \mu)}}. \tag{2.89}$$

So the grand canonical potential is

$$\Omega = -k_B T \ln Z = -\sum_\alpha k_B T \ln Z_\alpha. \tag{2.90}$$

Then we obtain the average number of particles

$$\langle N \rangle = -\frac{\partial \Omega}{\partial \mu} = \sum_\alpha \langle n_\alpha \rangle, \tag{2.91}$$

where the Bose–Einstein distribution function is

$$\langle n_\alpha \rangle = \frac{1}{e^{\beta(\epsilon_\alpha - \mu)} - 1} \equiv f_{BE}(\epsilon_\alpha). \tag{2.92}$$

The Bose–Einstein distribution describes the filling of single–particle eigenstates by non–interacting bosons. The average occupation number is

$$\langle n(\epsilon) \rangle_{BE} = \frac{1}{e^{\beta(\epsilon - \mu)} - 1}. \tag{2.93}$$

For states with low occupancies, where $\langle n \rangle \ll 1$, we have

$$\langle n \rangle_{BE} \approx e^{-\beta(\epsilon - \mu)}, \tag{2.94}$$

So, the boson populations reduce to the classical Maxwell–Boltzmann form [28]. The condition for low occupancy is

$$\epsilon - \mu \gg k_B T, \tag{2.95}$$

which often occurs at high temperatures, where the chemical potential becomes large and negative. Notice also that

$$\langle n \rangle_{BE} \to \infty \quad \text{as} \quad \mu \to \epsilon_k, \tag{2.96}$$

since the denominator vanishes. In fact, for a system of non–interacting bosons the chemical potential always satisfies

$$\mu \leq \epsilon_0, \tag{2.97}$$

where ϵ_0 is the lowest single–particle energy eigenvalue.

(2) Fermi–Dirac statistics In the case of Fermi–Dirac statistics, summing over $n_\alpha = 0, 1$, we have

$$Z_\alpha = 1 + e^{-\beta(\epsilon_\alpha - \mu)}, \tag{2.98}$$

from which we similarly obtain the Fermi–Dirac distribution function,

$$\langle n_\alpha \rangle = \frac{1}{e^{\beta(\epsilon_\alpha - \mu)} + 1} \equiv f_{FD}(\epsilon_\alpha). \tag{2.99}$$

Therefore, we find two quantum statistical distribution

$$\boxed{f(\epsilon) = \frac{1}{e^{\beta(\epsilon - \mu)} \mp 1}} \quad \begin{cases} - & \text{bosons (Bose–Einstein)} \\ + & \text{fermions (Fermi–Dirac)} \end{cases}$$

where $f(\epsilon)$ is also known as the Fermi function. Again, when the occupancy of a state is low, it is approximately given by the Boltzmann probability distribution,

$$f(\epsilon) \approx e^{-\beta(\epsilon-\mu)}. \tag{2.100}$$

Here the chemical potential can be either greater than or less than any given eigenenergy ϵ_α. Indeed, at low temperatures the chemical potential μ separates filled states from empty ones:

$$\epsilon_\alpha < \mu \;\Rightarrow\; \text{state mostly filled}, \qquad \epsilon_\alpha > \mu \;\Rightarrow\; \text{state mostly empty}. \tag{2.101}$$

Only states within roughly $k_B T$ of μ are partially filled.

Chapter 3

Review on Classical and Quantum Dynamics

In this section, we briefly discuss the classical limit of quantum mechanics and the phenomena this limit gives rise to. In particular, we are interested in understanding how a quantum system exchanges energy (and thus information) with its surroundings, leading to the loss of its quantum coherence and the emergence of classical behavior. For a non-isolated system, this is described by the reduced density operator calculated by discarding the environmental degrees of freedom. The evolution of the reduced density operator shows that off-diagonal elements in a given basis decay over time, indicating a loss of coherence between different states. This process, known as decoherence, explains how classical properties arise from an underlying quantum description. However, the classical limit of the dynamics of a quantum system is a subtle problem, since there is no direct notion of phase space in quantum mechanics. Therefore, the probabilistic interpretation, as given by Liouville's theorem in classical phase space, cannot be directly translated to quantum mechanical Hilbert space. To address this problem, we will briefly introduce the Wigner distribution and examine how it satisfies the master equation. We will start this section with a brief discuss on weyl transformation to appreciate the beauty of wigner distribution.

3.1 Weyl Quantization

Wigner-Weyl transform is the invertible map between functions in phase space $f(q,p)$ and the operators on Hilbert space, $\hat{f}$. Sometimes, this is called the **Weyl Transform** or, **Weyl Quantisation**, while the inverse map is called the **Wigner Transform** [1]. Regardless, the Weyl–Wigner transform is a well-defined integral transform between the phase-space and operator representations, and yields insight into the workings of quantum mechanics. Most importantly, the Wigner quasi-probability distribution is the Wigner transform of the quantum density matrix, and, conversely, the density matrix is the Weyl transform of the Wigner function. In this section we explain the Weyl quantisation on $\mathbf{E^2}$. Let a coordinate on the phase space be (q,p) and a function which is well-defined on the entire phase space is given by f. Two operators of hilbert spacegiven by Q and P satisfying the canonical commutation relation $[Q,P] = i\hbar$. However, it's not always clear on which vectors in the Hilbert space Q and P operators are defined. To bypass these

problems, we don't work with Q and P directly and work with their exponential versions, e^{iaQ} and e^{ibP}, where a and b are real numbers. These are called Weyl operators. These exponentiated operators are unitary, bounded, and defined on the entire Hilbert space. Using the Baker-Campbell-Hausdorff formula and the original CCR ($[Q, P] = i\hbar$), one can derive the combination of these unitary operators. The result is the Weyl form of the canonical commutation relations:

$$e^{iaQ}e^{ibP} = e^{-i\hbar ab}e^{ibP}e^{iaQ}. \tag{3.1}$$

This relation guarantees that Q and P are bounded. The explicit form of the tranformation is the following:

$$\Phi[\hat{f}] = \frac{1}{(2\pi)^2}\iiint f(q,p)\left(e^{i(a(Q-q)+b(P-p))}\right)dq\,dp\,da\,db. \tag{3.2}$$

Performing the integral over q and p first, we get the following form the transformation, we get a simpler form of the transformation. Note that computing the integral of q and p has the same effect of computing the Fourier transform $\tilde{f}$ of f

$$\Phi[\hat{f}] = \frac{1}{(2\pi)^2}\iint f(q,p)e^{iaQ+ibP}da\,db. \tag{3.3}$$

We think of Weyl transformation as the ordinary Fourier transform of the function $f(p,q)$, but then when applying the Fourier inversion formula, we substitute the quantum operators P and Q for the original classical variables p and q, thus obtaining a "quantum version of f"

3.1.1 Wigner Function

Wigner Function, often called Wigner Quasi-probability distribution is a distribution in phase space first introduced by Eugene Wigner in 1932 to study quantum corrections to classical statistical mechanics. His aim was to correlate the wavefunction (which are solutions to the Schrodinger Equation) belonging to the Hilbert space with a probability distribution in phase space. In classical mechanics, since a particle has a definite position and momentum, the state of that particle can be represented by a point (x, p) in phase space. Therefore, given an ensemble of particle, the probability of finding a particle at a certain point (x, p) is specified by the Liouville Density, which is a probability distribution. However, a quasi-probability distribution like Wigner Function satisfies a set of properties. The Wigner Distribution $W(x, p)$ for a pure state is defined as

$$W(x,p) \equiv \frac{1}{\pi\hbar}\int_{-\infty}^{\infty}\psi^*(x+y)\psi(x-y)e^{2ipy/\hbar}dy. \tag{3.4}$$

Here, y simply parametrize the relative displacement around the neighborhood of the phase space point (x, p) thus it parameterized off-diagonal structure. This off-diagonal terms of the density matrix encodes interference and coherence information of a quantum state. In momentum space, the Wigner function is expressed as

$$W(x,p) = \frac{1}{\pi\hbar}\int_{-\infty}^{\infty}\varphi^*(p+q)\,\varphi(p-q)\,e^{-2ixq/\hbar}\,dq, \tag{3.5}$$

where $\varphi(p)$ is the normalized momentum-space wavefunction, proportional to the Fourier transform of $\psi(x)$. In three dimensions this generalizes to

$$W(\vec{r},\vec{p}) = \frac{1}{(2\pi)^3}\int \psi^*\left(\vec{r}+\tfrac{\hbar\vec{s}}{2}\right)\,\psi\left(\vec{r}-\tfrac{\hbar\vec{s}}{2}\right)\,e^{i\vec{p}\cdot\vec{s}}\,d^3s. \tag{3.6}$$

For a mixed state described by the density matrix $\hat{\rho}$, the Wigner function is defined as the Wigner transform of $\hat{\rho}$:

$$W(x,p) = \frac{1}{\pi\hbar}\int_{-\infty}^{\infty}\langle x-y|\hat{\rho}|x+y\rangle\,e^{2ipy/\hbar}\,dy, \tag{3.7}$$

where $\langle x|\psi\rangle = \psi(x)$. This mapping is the inverse of the Weyl transform, which assigns phase-space functions to Hilbert-space operators in Weyl quantization. Thus, the Wigner function forms a cornerstone of quantum mechanics in phase space. In 1949, J.E.Moyal demonstrated that the Wigner function serves as the integration measure in phase space, in analogy with a probability density. For a classical function $g(x,p)$ corresponding (via the Weyl transform) to an operator $\hat{G}$, the expectation value is

$$\langle\hat{G}\rangle = \int dx\,dp\,W(x,p)\,g(x,p). \tag{3.8}$$

This parallels classical probability theory, with the important distinction that $W(x,p)$ is a quasiprobability distribution [2].

3.1.2 Mathematical Properties of the Wigner Function

The Wigner function $W(x,p)$ satisfies the following properties:

1. **Reality:** Wigner functions are real-valued functions.

$$W(x,p) \in R.$$

2. **Marginals:** The position and momentum probability distributions are obtained as

$$\int_{-\infty}^{\infty} dp\,W(x,p) = \begin{cases}|\psi(x)|^2, & \text{pure state,}\\ \langle x|\hat{\rho}|x\rangle, & \text{mixed state}\end{cases}$$

$$\int_{-\infty}^{\infty} dx\,W(x,p) = \begin{cases}|\psi(p)|^2, & \text{pure state,}\\ \langle p|\hat{\rho}|p\rangle, & \text{mixed state}\end{cases}$$

The normalization condition follows:

$$\int_{-\infty}^{\infty}dx\int_{-\infty}^{\infty}dp\,W(x,p) = \mathrm{Tr}(\hat{\rho}) = 1.$$

3. **Reflection Symmetries:**

$$\begin{aligned}\psi(x)\to\psi(x)^* \quad &\Rightarrow \quad W(x,p)\to W(x,-p),\\ \psi(x)\to\psi(-x) \quad &\Rightarrow \quad W(x,p)\to W(-x,-p).\end{aligned}$$

4. **Galilean Covariance:** A spatial translation of the wavefunction shifts the Wigner function:

$$\psi(x) \to \psi(x+a) \quad \Rightarrow \quad W(x,p) \to W(x+a,p).$$

However, Wigner function it is not Lorentz-covariant.

5. **Equation of Motion:** In the absence of external forces, the Wigner function evolves classically:

$$\frac{\partial W(x,p)}{\partial t} = -\frac{p}{m}\frac{\partial W(x,p)}{\partial x}.$$

This remains true in the presence of harmonic forces. Furthermore, this equation is first-order in both x and t. So, the temporal evolution of the Wigner function reminds unaffected by the diffusion affects, unlike the Schrodinger equation. Thus, the Wigner function of a wave-packet with a fixed momentum maintains its shape, even if the wavefunction does not.

6. **State Overlap:** The overlap of two pure states ψ and θ is

$$|\langle\psi|\theta\rangle|^2 = 2\pi\hbar \int_{-\infty}^{\infty} dx \int_{-\infty}^{\infty} dp\, W_\psi(x,p)\, W_\theta(x,p).$$

This is a measurement of how one is similar to another state, just like Fidelity.

7. **Expectation Values:** The Wigner transform of an operator $\hat{G}$ is

$$g(x,p) \equiv \int_{-\infty}^{\infty} dy \left\langle x - \tfrac{y}{2}\middle|\hat{G}\middle| x + \tfrac{y}{2}\right\rangle e^{ipy/\hbar},$$

and the expectation value is computed as

$$\langle\psi|\hat{G}|\psi\rangle = \mathrm{Tr}(\hat{\rho}\hat{G}) = \int_{-\infty}^{\infty} dx \int_{-\infty}^{\infty} dp\, W(x,p)\, g(x,p).$$

8. **Positivity Condition:** For all pure states $|\theta\rangle$,

$$\int_{-\infty}^{\infty} dx \int_{-\infty}^{\infty} dp\, W(x,p)\, W_\theta(x,p) \geq 0.$$

9. **Boundedness:** For a pure state,

$$-\frac{2}{h} \;\leq\; W(x,p) \;\leq\; \frac{2}{h}.$$

This bound disappears in the classical limit, $\hbar \to 0$. In this limit, $W(x,p)$ reduces to the probability density in coordinate space $\rho(x)$, usually highly localized, multiplied by δ-functions in momentum. Thus, this bound forbids a Wigner function from being perfectly localized as a δ-function in phase space to respect the uncertainty principle.

The Wigner transform is basically the Fourier transform of the density matrix along the anti diagonal direction — and that makes it a natural tool to study decoherence.

3.2 Review on Quantum Decoherence

In quantum mechanics, physical systems are expressed as Quantum states. Quantum states can be classified as pure state and mixed. For quantum systems, the probabilities associated with the outcomes upon measurement are calculated by apply Born's rule. For a state, if there exists a measurement for which the one of the possible outcomes will occur the probability 1, then the state is called pure state. In absence of environmental interaction, the state evolves unitarily. Therefore, a pure state remains over unitary time evolution.

$$|\psi(t)\rangle = U(t)\,|\psi(0)\rangle$$

For an isolated system evolving under the Schrodinger equation,

$$\rho(t) = U(t)\,\rho(0)\,U^{\dagger}(t), \tag{3.9}$$

where $\rho(0) = |\psi(0)\rangle\,\langle\psi(0)|$ is the density matrix of the initial state. Also the norm is persevered under the unitary time translation. The diagonal terms of the density matrix corresponds to the classical probability of measurement outcomes, while the off-diagonal terms contains the measurement of phase relationship between different quantum states. Therefore, they go by the name coherence term. Consequently, the off-diagonal elements of $\rho(t)$ do not decay: they may acquire time-dependent phases and thus oscillate, but their norm remain invariant. In other words, coherence is preserved under unitary dynamics. Thus, interference effects remain possible indefinitely in an isolated system. However, if the system is not isolated, interactions with the environment cause the off-diagonal elements of the density matrix to diminish. As a result, the density matrix becomes approximately diagonal, with the diagonal elements corresponding to the classical probabilities of the measurement outcomes. This process, known as decoherence, effectively suppresses interference effects and makes the system appear classical. Decoherence is strictly irreversible, meaning that once coherence is lost, it cannot be recovered by simple time reversal of the system alone.

3.2.1 Example: Two-level system

Let the Hilber space $\mathcal{H}_s$, the Hilbert space of the system, be spanned by the orthonormal set $\{|0\rangle, |1\rangle\}$ and the Hilbert space of the environment be spanned by the orthonormal set $\{|\uparrow\rangle_i, |\downarrow\rangle_i\}$ where $i = 1, 2, 3...N$. We are allowing our spin-$\frac{1}{2}$ system to interact with a large number of qubits which represents the environment. The composite 2^{N+1} dimensional hilbert space is given by [30]

$$\mathcal{H} = \mathcal{H}_s \otimes \mathcal{H}_{\epsilon_{i\in\mathcal{N}}}^{\otimes N}. \tag{3.10}$$

We assume that the dynamics of the combine system is driven by the interaction Hamiltonian only, therefore the hamiltonian is diagonal in computational basis. The interaction Hamiltonian is

$$H_I = \frac{1}{2}\,\sigma_z \otimes \sum_{i=1}^{N} g_i\,\sigma_z^{(i)} = \frac{1}{2}\sigma_z \otimes \hat{E}, \tag{3.11}$$

where:

- σ_z acts on the system (a single qubit). $\sigma_z = |0\rangle\langle 0| - |1\rangle\langle 1|$ is called the interaction operator or the spin operator.
- $\sigma_z^{(i)}$ acts on the i-th environment qubit,
- g_i is the coupling constant between the system and the i-th environment qubit, and
- N is the total number of environmental qubits,
- $\hat{E} = \sum_{i=1}^{N} g_i \sigma_z^{(i)}$.

The time-evolution operator generated by the interaction Hamiltonian is given by

$$U(t) = e^{-iH_I t}. \tag{3.12}$$

Suppose the system is initially in the state $|0\rangle$ and the environment is in some initial state $|E_{\text{initial}}\rangle$. Then, the total initial state is

$$|\Psi(0)\rangle = |0\rangle\,|E_{\text{initial}}\rangle\,. \tag{3.13}$$

Acting with the unitary evolution operator, we obtain

$$\begin{aligned} U(t)\,|0\rangle\,|E_{\text{initial}}\rangle &= e^{-\frac{i}{2}\sigma_z t\sum_i g_i\sigma_z^{(i)}}\,|0\rangle\,|E_{\text{initial}}\rangle \\ &= |0\rangle\; e^{-\frac{i}{2}t\sum_i g_i\sigma_z^{(i)}}\,|E_{\text{initial}}\rangle \\ &= |0\rangle\,|E(t)\rangle\,. \end{aligned}$$

Here, the state of the environment can start off as complicated as we wish, with each qubit in a superposition:

$$|E_{\text{initial}}\rangle = \bigotimes_{i=1}^{N}(a_i\,|\uparrow\rangle_i + b_i\,|\downarrow\rangle_i) = (a_1\,|\uparrow\rangle_1 + b_1\,|\downarrow\rangle_1)\otimes\cdots\otimes(a_N\,|\uparrow\rangle_N + b_N\,|\downarrow\rangle_N)\,. \tag{3.14}$$

we have used the fact that $\sigma_z\,|0\rangle = +\,|0\rangle$, which allows us to factor out the system state. The environment state $|E(t)\rangle$ evolves according to

$$|E(t)\rangle = e^{-\frac{i}{2}t\sum_i g_i\sigma_z^{(i)}}\,|E_{\text{initial}}\rangle\,. \tag{3.15}$$

The system and environment remain *unentangled* during this evolution. The system state $|0\rangle$ is unchanged, while only the environment undergoes a phase evolution. Thus, $|0\rangle$ is a *pointer state* – an eigenstate of the interaction Hamiltonian that remains dynamically stable under decoherence [30] [10]. We can similarly show that $|1\rangle$ is also an eigenstate of the interaction Hamiltonian, thus a pointer state. Note that a state is dynamically stable or a pointer state if under the unitary time evolution generated by the interaction hamiltonian, the state remains untangled with the envirnoment thus preserves its purity. Mathematically,

$$U(t)\,|E(0)\rangle\,|\psi\rangle_s = |\psi\rangle_s\,|E'(t)\rangle \tag{3.16}$$

So, under the unitary only the quantum state of the environment evolves, while the state of the system remains invariant. However, if the system were to start off in

some superposition of $|0\rangle$ and $|1\rangle$, then the environment will become entangled with it and cause decoherence. Also the interaction hamiltonian commutes with the spin operator. Thus the state of the system is an energy eigenstate where the energy remains conversed. This implies that the system does not exchange any energy with the environment. Even if we start off in an initial state with which is a superposition of pointer state and get entangled with the environment and decoherence, the energy still remains conversed. Let us now examine the state of the environment. Recall that if the system starts off in a superposition then,

$$e^{-i\hat{H}_I t}\big(a\,|0\rangle + b\,|1\rangle\,\big)\,|E_{\text{initial}}\rangle \;\longrightarrow\; a\,|0\rangle\,|E_0(t)\rangle + b\,|1\rangle\,|E_1(t)\rangle$$

Tracing out the envirnoment, we get the reduced density operator for the environment

$$\rho_S(t) = \begin{pmatrix} |a|^2 & ab^*\langle E_1(t) \mid E_0(t)\rangle \\ a^*b\langle E_0(t) \mid E_1(t)\rangle & |b|^2 \end{pmatrix} \tag{3.17}$$

The off-diagonal terms encodes the measure of decohorence. Thus at the limit $\langle E_1(t)|E_2(t)\rangle \to 0$ and $\langle E_0(t)|E_1(t)\rangle \to 0$, decohorence is suppressed. Thus that the rate of decoherence depends on the overlap of the environment states that are entangled with each of the system states and the degree to which they are orthogonal (distinguishable).

$$r(t) = \langle E_1(t)|E_0(t)\rangle \tag{3.18}$$

Simplifying, we get

$$\langle E_0(t)| = \sum_{j=1}^{2^N} e^{-i\epsilon_j t/2} c_j\,|n\rangle_j \tag{3.19}$$

$$\langle E_1(t)| = \sum_{j=1}^{2^N} e^{+i\epsilon_j t/2} c_j\,|n\rangle_j \tag{3.20}$$

we define $r(t)$ as the following:

$$r(t) = \langle E_1(t) \mid E_0(t)\rangle = \sum_{i,j}^{2^N} e^{-i\epsilon_i t/2} e^{ie_j t/2} c_i^* c_j \delta_{ij} = \sum_{i=1}^{2^N} e^{-ie_i t}|c_i|^2 \tag{3.21}$$

In his classic paper [6], [10], Zurek showed that the evolution of $r(t)$ reduces to a *random walk problem* in the 2-dimensional complex plane. The time-averaged modulus squared of the complex vector $r(t)$ scales as

$$\langle |r(t)|^2\rangle \sim 2^{-N} \quad\longrightarrow\quad 0 \quad \text{as } N \to \infty \tag{3.22}$$

That is, the rate of decoherence scales *exponentially* with the size of the environment. For very large N, the decoherence rate is roughly a Gaussian decay:

$$r(t) \sim e^{-\Gamma^2 t^2} \tag{3.23}$$

The decay constant Γ^2 depends on the distribution of the coupling strengths g_i between the system and each of the qubits in the environment. It is important to note that the loss of coherence is irreversible. Irreversibility can also arise from more familiar, statistical causes: due to large number of interacting degrees of freedom, extracting information becomes as difficult as reversing trajectories in a Boltzmann gas [30].

3.2.2 Relating Dissipation and Decoherence

Although our physical intuition tells us that for a quantum system, there can decohere even if there is no energy dissipation at all – the environment can gain information about the system without any exchange of energy — in real physical systems, one is accompanied by the other. We define τ_r as the relaxation time and τ_d as the time taken by a system to achieve decoherence. Decoherence and dissipation have different timescales,

$$\tau_d \ll \tau_r \tag{3.24}$$

We start with a very specific model - a particle with position x and a scalar field $\phi(q,t)$ propagating in direction q, interacting through the $H_I = \varepsilon x \frac{d\phi}{dt}$. The density matrix $\rho(x,x')$ of the particle in position representation evolves according to the *master equation* [6]

$$\frac{d\rho}{dt} = -\frac{i}{\hbar}[H,\rho] - \gamma(x-x')\Big(\frac{\partial\rho}{\partial x} - \frac{\partial\rho}{\partial x'}\Big) - \frac{2m\gamma k_B T}{\hbar^2}(x-x')^2\rho \tag{3.25}$$

where

- H is the particle's hamiltonian with potential $V(x)$
- γ is the relaxation rate
- T is the temperature of the field, and k_B is the Boltzmann constant

We can break down each term on the right hand side as the following

- the first term comes from Von Neumann equation, can be derived from Schrodinger equation. Classically, it generates Newton's equations of motion for the average of the observable (Ehrenfest's theorem)
- the second tem causes dissipation, causing the loss of energy and a decrease of average momentum. the relaxation rate is $\gamma = \eta/2m$, where the viscosity $\eta = \varepsilon^2/2$ is caused by the interaction
- the last term is responsible for the fluctuations or random kicks that lead to Brownian Motion. The effect of this term on quantum superposition is very important: this destroys the quantum coherence. Therefore, it is also responsible for the classical structure of phase space as it converts superpositions into mixtures of localized wavepackets that, in the classical limit, turn into the familiar points in phase space.

The effect of last term on the diagonal peaks $x \approx x'$ is negligible, while for the off-diagonal peaks, $(x-x')^2 \approx \Delta x^2$. Therefore the decay rate of the off-diagonal term is

$$\tau_d = \tau_r\Big(\frac{\hbar^2}{2mk_BT(\Delta x)^2}\Big) = \gamma^{-1}\Big(\frac{\lambda_{th}}{\Delta x}\Big)^2 \tag{3.26}$$

Here, λ_{th} is the thermal De Brogile wavelength and τ_d has the dimension of time. For a macroscopic object with mass $m = 1$ g at room temperature ($T = 300$ K), the thermal de Broglie wavelength is extremely small:

$$\lambda_{\text{th}} \sim 10^{-23}\ \text{m},$$

which is expected, since classical objects have negligibly small quantum wavelengths. If we consider a superposition over a spatial separation $\Delta x = 1$ cm, the ratio of the relaxation time to the decoherence time becomes astronomically large:

$$\frac{\tau_r}{\tau_d} \sim 10^{42}$$

Therefore, decoherence occurs extremely quickly for classical objects (like cats!) and thus macroscopic bodies follow essentially *perfectly Newtonian trajectories*.

3.2.3 Classical Limit of Quantum Dynamics

The Schrödinger equation can be derived from classical mechanics in the Hamilton–Jacobi formulation. Consequently, it is unsurprising that it reproduces classical equations of motion in the limit where $\hbar \to 0$, alternatively, the action $\mathcal{S} \gg \mathcal{O}(\hbar)$. This connection is formalized in Ehrenfest's theorem and Bohr's correspondence principle, and is reflected in the close relationship between quantum commutators and classical Poisson brackets. Nevertheless, establishing the full quantum–classical correspondence requires considering not only the equations of motion but also the quantum states themselves. Quantum Mechanics is formulated in Hilbert space where position and momentum operators are not simultaneously measurable. Whereas in classical mechanics, the position and momentum coordinates of a particle in the phase space is precisely defined. The transition from quantum to classical remains an unsolved problem.

To facilitate the study of the problem, it is convenient to introduce the Wigner transform of a wavefunction $\psi(x)$:

$$W(x,p) = \frac{1}{\hbar}\int dy\, \psi^*\Big(x + \frac{y}{2}\Big)\psi\Big(x - \frac{y}{2}\Big)e^{-ipy/\hbar}, \tag{3.27}$$

which expresses quantum states as functions of position and momentum. The Wigner distribution $W(x,p)$ is real, but it can be negative. Hence, it cannot be regarded as a probability distribution. It is called a quasi-probability distribution. Nevertheless, when integrated over either variable, it yields the probability distribution for the other; for example,

$$\int W(x,p)\, dp = |\psi(x)|^2. \tag{3.28}$$

For a minimum-uncertainty wavepacket (e.g. the ground state gaussian state for simple harmonic oscillator)

$$\psi(x) \sim \exp\Big[-\frac{(x-x_0)^2}{2\sigma^2} + ip_0x/\hbar\Big] \tag{3.29}$$

The Wigner distribution is a Gaussian in x and p:

$$W(x,p) \sim \exp\Big[-\frac{(x-x_0)^2}{2\sigma^2} - \frac{(p-p_0)^2\sigma^2}{\hbar^2}\Big].$$

A system described by this type of Wigner distribution is localized in both x and p e.g. a classical point in phase space. The Wigner distribution is easily generalized to the case of a general density matrix ρ:

$$W(x,p) = \frac{1}{\hbar}\int dy\, \rho\Big(x+\frac{y}{2}, x-\frac{y}{2}\Big)e^{-ipy/\hbar}.$$

We will be using the evolving (initially pure but eventually mixed) density matrix of the particle discussed above. The Wigner transform suggests a strategy for exhibiting classical behavior: whenever $W(x,p)$ is a mixture of localized wavepackets (as in the Gaussian above), it can be regarded as a classical probability distribution in phase space. See below (3.1)

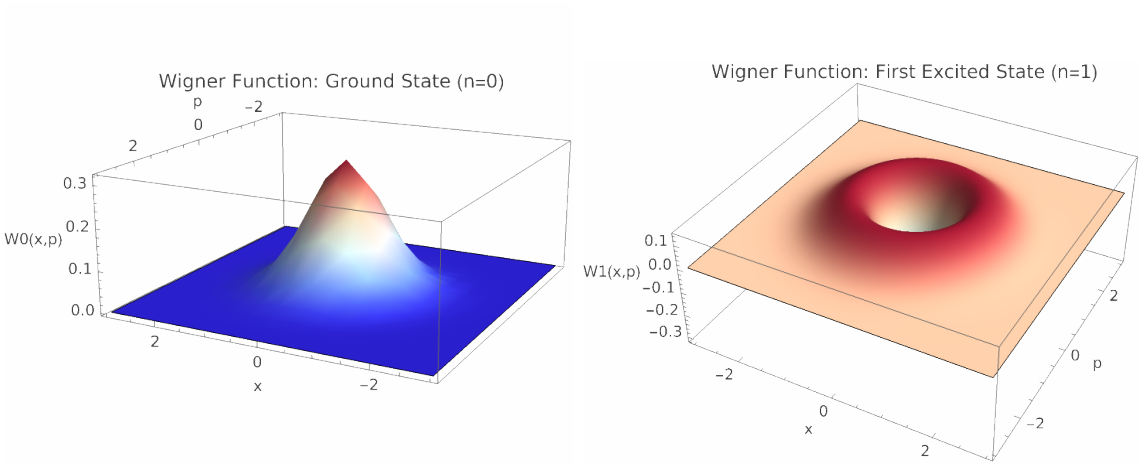

Figure 3.1: Wigner distribution of the ground state of the simple harmonic oscillator (left), which is a minimum uncertainty state, and the first excited state (right). The Wigner function of the first excited state has negative contributions and therefore is not a true probability distribution in phase space. The Mathematica code used for computing the Wigner function and plotting them is given in Appendix (A.1).

However, when the underlying state is truly quantum, its Wigner distribution function will have alternating sign. This implies if we plot wigner function for a purely quantum states, there will be several positive peaks as long well oscillating interference term with negative contribution. Thus $W(x,p)$ cannot be regarded as the classical probability distribution in phase space.

We are interested in the equation of motion for $W(x,p)$. For harmonic oscillator ($V \approx x^2$), it does not depend on $\hbar$!

$$\frac{dW}{dt} = \Big(-\frac{p}{m}\frac{\partial W}{\partial x} + \frac{\partial V}{\partial x}\frac{\partial W}{\partial p}\Big) + 2\gamma\frac{\partial(pW)}{\partial p} + D^2\frac{\partial^2 W}{\partial^2 p^2} \tag{3.30}$$

Where V is the renormalised potential and $D = 2m\gamma k_B T = \eta k_B t$. Each term of this equations can be interpreted as the following [6]

- the term term is identified as a classical Poissson bracket H, W. Consequently, for a particle interacting with a classical scalar field, the classical Liouville equation, which governs the evolution of a phase-space probability distribution, emerges naturally from the underlying quantum dynamics. For a more general

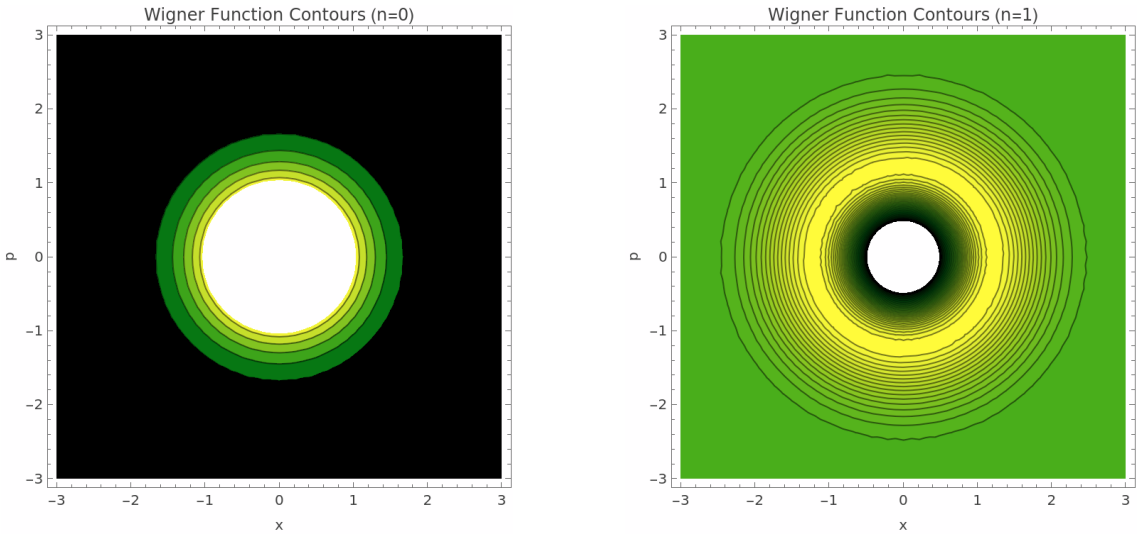

(a) Ground state (b) First excited state

Figure 3.2: Contour plot for Wigner distribution of simple harmonic oscillator.

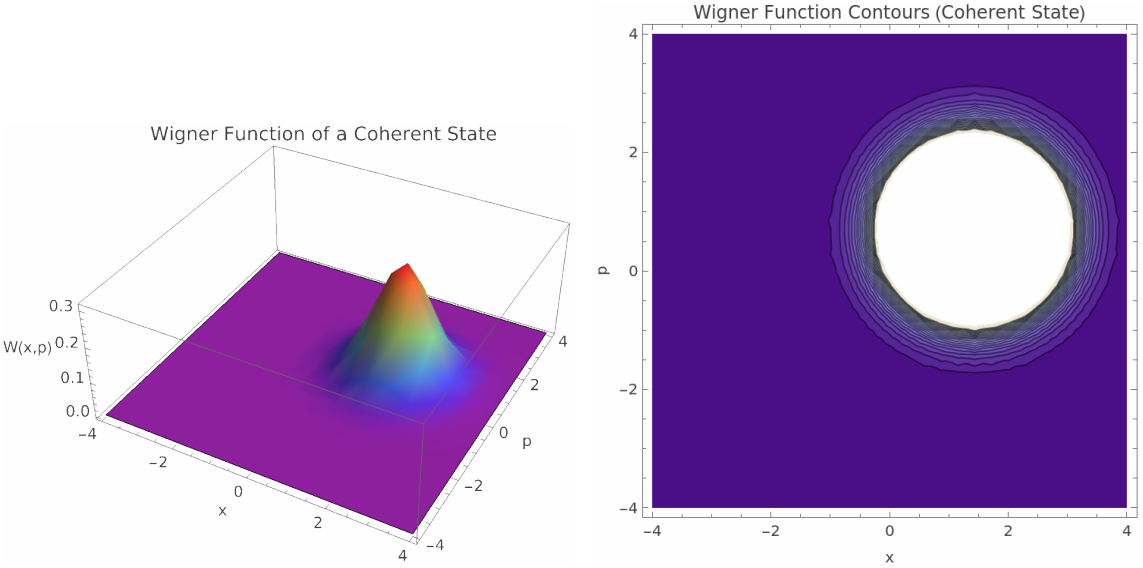

Figure 3.3: Wigner distribution of coherent state (left) and the contour plot for the wigner distribution (right)

potential $V(x)$, however, the Poisson bracket is no longer sufficient on its own; additional terms of order $\hbar$ must be included, reflecting the presence of inherently quantum corrections beyond the classical limit.

- the second term is friction
- The last term leads to the diffusion of $W(x,p)$ in momentum space at a rate D. This term, along with the friction term, washes out quantum features of the Wigner function and thus make the function appear classical. Especially the diffusion term is crucial for decoherence.

To see this, suppose we have a particle whose wavefunction is a superposition of two

spatially separated localised wavepackets centred at $x = \pm\frac{\Delta x}{2}$

$$\psi(x) = \frac{1}{\sqrt{2}}\Big[\psi_1(x) + \psi_2(x)\Big]$$

If we insert this into the definitaion of wigner function, we shall get three terms.

$$W(x,p) \sim W_1(x) + W_2(x) + W_{int}(x)$$

where, W_1 and W_2 contributed from $\psi_1\psi_1^*$ and $\psi_2\psi_2^*$, and interference term W_{int} is contributed by $\psi_1\psi_2^*$ and $\psi_2\psi_1^*$. We assume the interference term to be oscillatory; therefore,

$$W_{int} \propto cos\Big(\frac{p\Delta x}{\hbar}\Big) f(x,p) \tag{3.31}$$

Solving the diffusion term for this Wigner function, we get

$$W_{int}(t) = W_{int}(0)e^{-Dt(\frac{\Delta x}{\hbar})^2} \tag{3.32}$$

The interference term decays exponentially with a characteristic decoherence time:

$$\tau_D^{-1} = D\Big(\frac{\Delta x}{\hbar}\Big)^2 \tag{3.33}$$

We see that the larger the spatial separation of two wave packets, the faster the decoherence (the loss of quantum characteristics). This explains why the macroscopic objects decohere extremely fast[10].

3.3 Integrable Systems

The definition of integrability is the following: let N be the number of degrees of freedom and let s be the number of constants of motion. If $s = N$, the system is called integrable. The constants of motion $c_i(q,p)$ must be independent and in involution. Here, "in involution" means that they satisfy the relations

$$\{c_i, c_j\} = 0 \qquad \text{for all } i,j \tag{3.34}$$

The second condition states that the differential one-forms $dc_i(q,p)$ are linearly independent at each point of the set

$$M_C = \{(q,p) \,:\, c_i(q,p) = C_i \text{ for } i = 1,\ldots,N\}. \tag{3.35}$$

The independence of the constants of motion ensures that they actually characterise the dynamics throughout the entire accessible phase space. If N constants of motion exist, the canonical transformation defined by

$$(q,p) \;\longrightarrow\; (\theta, I), \tag{3.36}$$

with

$$I_i = C_i, \tag{3.37}$$

This transformation gives a solution of the Hamilton–Jacobi equation. Therefore, another equivalent definition of integrability is that a solution of the Hamilton–Jacobi equation can be found in terms of the action–angle variables (θ, I). Let θ_i, $i = 1, \ldots, N$, be the angle variables. We assume they are scaled such that

$$\theta_i \in [0, 2\pi).$$

Taking a basis of cycles on the invariant torus γ_i, $i = 1, \ldots, N$, one can define the action variables by

$$I_i = \frac{1}{2\pi} \oint_{\gamma_i} p(I, \theta)\, dq(I, \theta). \tag{3.38}$$

A basis of cycles is defined such that the increase of the coordinate θ_i along the cycle γ_j is equal to 2π if $i = j$ and 0 if $i \neq j$; that is,

$$\Delta_{\gamma_j} \theta_i = 2\pi\, \delta_{ij}. \tag{3.39}$$

This means that the invariant surface of motion is topologically an N-dimensional torus T^N, and the cycles γ_i form a basis of its fundamental loops, each winding once around one angle direction. Here, a torus is defined as,

$$T \equiv \Big\{ (p, q) \in \text{phase space} \ : \ p = p(I, \theta),\ q = q(I, \theta),\ \theta_i \in [0, 2\pi),\ I = \text{fixed} \Big\}$$

with periodicity in the angle variables,

$$q\big(I; \ldots, \theta_i + 2\pi, \ldots\big) = q\big(I; \ldots, \theta_i, \ldots\big), \tag{3.40}$$

$$p\big(I; \ldots, \theta_i + 2\pi, \ldots\big) = p\big(I; \ldots, \theta_i, \ldots\big) \tag{3.41}$$

The solution of the equations of motion for an integrable system is then given in the possibly high–dimensional phase space parametrized by the action–angle variables (I, θ):

$$\theta(t) = \theta_0 + \omega(I)\, t, \qquad \omega(I) = \frac{\partial H}{\partial I} = \text{const.} \tag{3.42}$$

Here, the action variables I_i are constants of motion. The fact that the components of θ are angle–like, and therefore called cyclic variables in the Lagrangian formalism, does not necessarily mean that the actual motion in phase space is periodic. This is only true for a system with one spatial degree of freedom, where the motion is along a simple circle. The following table summarizes the dimensionality of the important objects in phase space for integrable systems where a torus structure exists:

Phase space	:	$2N$
Energy surface	:	$2N - 1$
Invariant torus	:	N

(3.43)

3.4 Non Integrable Systems

A system is said to be non-integrable if the number of independent constants of motion is smaller than the number of degrees of freedom. A well-known example is

the three-body Kepler problem, whose Hamiltonian (assuming equal masses m for simplicity) is given by

$$H = \frac{1}{2m}(p_1^2 + p_2^2 + p_3^2) - \frac{\gamma m^2}{|r_1 - r_2|} - \frac{\gamma m^2}{|r_2 - r_3|} - \frac{\gamma m^2}{|r_3 - r_1|}. \tag{3.44}$$

Here, γ denotes the gravitational constant. The system consists of three particles, each with three spatial coordinates, resulting in a total of nine degrees of freedom. However, the number of independent conserved quantities is only six. Therefore the system is non integrable. In 1899, Poincaré showed that for the N-body Kepler problem with $N \geq 3$, it is impossible to obtain general solutions valid for long times. However, in a series of works, Kolmogorov, Arnold, and Moser demonstrated that certain non-integrable systems can still exhibit a form of stability. The Kolmogorov–Arnold–Moser (KAM) theorem states that, under appropriate conditions, many of the invariant structures of the integrable system survive, and the resulting dynamics remain close to those of the unperturbed system. This result provides a justification for the use of perturbation theory and shows that predictability can persist even in weakly non-integrable systems [16]. In this thesis, we will not go into the details of these sophisticated ways of looking into classically non integrable systems. Here we are particularly interested in the dynamics of non integrable systems. Classically non integrable systems exhibit chaotic dynamics characterized by the sensitivity to the initial conditions of the systems, contrary to the dynamics of regular systems which move along invariant tori.

3.4.1 Lyapunov Exponent

Here, we quantify the sensitive dependence to the initial condition in phase space using lyapunov exponent. We start with a a system in one dimensional phase space x. Let's consider two different states starting from two initial points x_0 and $x_0 + \delta x(0)$. Here, $\delta x(0)$ is the infinitesimal separation between two initial conditions at time $t = 0$. If the system is chaotic, the time evolution of these two trajectories would lead to an exponential increase in their separation. We will quantify the separation at some late time t as

$$\delta x(t) \approx e^{\lambda t}\, \delta x(0) \tag{3.45}$$

λ is the lyapunov characteric exponent. Solving the above equation for λ and taking long time limit, we have

$$\lambda = \lim_{t\to\infty} \frac{1}{t} \ln\left(\frac{\delta x(t)}{\delta x(0)}\right) \tag{3.46}$$

A positive lyapunov exponent is a signature of classical chaos. For multi - dimensional systems, we will have to calculate the lyapunov exponent for each dimension in phase space separately. In that case, the system will exhibit chaos if one or more than one of these exponents are positive. For dissipative systems, the phase space volume decreases over time. Therefore, the sum of the lyapunov exponent will be negative [9].

Now, it is useful define the time evolution of the systems using a function called *mapping*. This method involves discretising the evolution and denoting each pieces

with index n. We express the time evolution of the system using a recurrence relation e.g. expressing the evolution of $(n+1)$th state in terms of nth state. In general

$$x_{n+1} = g(x_n) \tag{3.47}$$

We call g a map of the system and $(n+1)$th state the iterator. Here, g can be both a function of x_n and a constant α which may contain additional information of the system. We can use a mapping to derive an expression for the Lyapunov exponent, as illustrated in [9], [29]. Let an observable x evolve under the map given above. Consider two nearby initial conditions x_0 and $x_0 + \delta x$, where δx is infinitesimally small. After one iteration, the separation between the two trajectories becomes

$$\Delta_1 = g(x_0 + \delta x) - g(x_0) \approx \delta x \left.\frac{dg}{dx}\right|_{x_0}. \tag{3.48}$$

After n iterations, the separation is

$$\Delta_n = g^n(x_0 + \delta x) - g^n(x_0), \tag{3.49}$$

where g^n denotes the n-fold composition of the map. Since δx represents the initial separation, we can write

$$\Delta_n \approx \delta x\, e^{n\lambda}, \tag{3.50}$$

where λ is the Lyapunov exponent. Dividing both sides by δx and taking the logarithm, we obtain

$$\ln\left(\frac{g^n(x_0 + \delta x) - g^n(x_0)}{\delta x}\right) = n\lambda. \tag{3.51}$$

Thus,

$$\lambda = \frac{1}{n}\ln\left(\frac{g^n(x_0 + \delta x) - g^n(x_0)}{\delta x}\right). \tag{3.52}$$

Taking the limit $\delta x \to 0$, this becomes

$$\lambda = \frac{1}{n}\ln\left|\left.\frac{dg^n(x)}{dx}\right|_{x_0}\right|. \tag{3.53}$$

The n-fold iteration of the map is given by

$$g^n(x_0) = g(g(\cdots g(x_0)\cdots)). \tag{3.54}$$

Using the chain rule, we obtain

$$\left.\frac{dg^n(x)}{dx}\right|_{x_0} = \left.\frac{dg}{dx}\right|_{x_{n-1}} \left.\frac{dg}{dx}\right|_{x_{n-2}} \cdots \left.\frac{dg}{dx}\right|_{x_0}. \tag{3.55}$$

Substituting this result into the expression for the Lyapunov exponent and taking the limit $n \to \infty$, we obtain

$$\lambda = \lim_{n\to\infty} \frac{1}{n}\sum_{i=0}^{n-1} \ln\left|\left.\frac{dg}{dx}\right|_{x_i}\right| \tag{3.56}$$

The inverse of the Lyapunov exponent, λ^{-1}, defines the *Lyapunov time*, which characterises the timescale over which the dynamics of the system remain predictable. Once the evolution time exceeds the Lyapunov time, small uncertainties in the initial conditions grow exponentially, and the system effectively becomes chaotic and unpredictable [29].

Chapter 4

Review on Random Matrix Theory

Up until now, we have not defined chaos really means for a quantum system in general. Chaos on the quantum level may be introduced without apriori relation to any classical correspondence. In the 1950s, Wigner proposed that the energy level spacings of heavy, complex nuclei could be modeled by the eigenvalues of large random matrices. This was because the interactions were too complex for a deterministic description. One of the remarkable quantum chaotic properties is that the distribution of the eigenvalues displays universality. Wigner's idea was popularized by Micheal Berry, who coined the phrase *quantum chaology* in late 1970s. He showed the spectral statistics of partly regular and partly chaotic can be understood as the superposition of spectra from different universality classes, each spectrum being associated with a different chaotic or regular region in classical phase space. Also the properties of the quantum mechanical spectrum are intimately related to the temporal evolution [5]. This is a consequence of the spectral theorem, which states that the time-evolution operator can always be expanded in the energy eigen basis of the Hamiltonian. Hence, irregular and complex dynamics go hand in hand with the quantum chaotic properties of the spectra. This section gives a brief introduction to the theory of random matrices of finite size, modeling real physical systems with discrete spectra.

4.1 Level Statistics

We start with calculating the eigenvalues of an arbitrary 2×2 hermitian matrix $H = H^\dagger$

$$\begin{pmatrix} H_{11} & H_{12} \\ H_{12}^* & H_{22} \end{pmatrix} \tag{4.1}$$

The eigenvalues are easily computed

$$E_\pm = \frac{1}{2}(H_{11} + H_{22}) \pm \frac{1}{2}\sqrt{(H_{11} - H_{22})^2 + 4|H_{12}|^2} \equiv \frac{1}{2}(H_{11} + H_{22}) \pm \sqrt{D}.$$

We can now distinguish the following possible cases:

- **No interaction between the levels i.e.** $H_{12} = 0$**:** In these cases, the eigenvalues are simply

$$E_+ = H_{11}, \qquad E_- = H_{22}.$$

Both eigenvalues can be forced into a crossing by a single real parameter, say an appropriate parameter λ (the crossing parameter) which enters the element H_{22}, such that $H_{11} - H_{22}(\lambda) = 0$. Here, λ is the external control parameter of the Hamiltonian (e.g. magnetic field, coupling constant, deformation strength).

- **More general case:** $H_{12} \neq 0$, and we have a determinant

$$D = \frac{1}{4}(H_{11} - H_{22})^2 + \mathrm{Re}(H_{12})^2 + \mathrm{Im}(H_{12})^2.$$

For real matrices, $\mathrm{Im}(H_{12}) = 0$, implying that we need to change two matrix elements simultaneously to obtain a level crossing, i.e., a degeneracy of the two eigenvalues. This can be formalized as

$$\frac{1}{4}\big(H_{11} - H_{22}(\lambda_1)\big)^2 + H_{12}(\lambda_2)^2 = 0$$

or equivalently,

$$H_{11} - H_{22}(\lambda_1) = \pm 2i\, H_{12}(\lambda_2),$$

for an appropriate pair of real parameters (λ_1, λ_2). If $\mathrm{Im}(H_{12}) \neq 0$, we can easily see that three independent real parameters are, in general, necessary to enforce a level crossing.

For classically regular system, levels are labeled by their respective quantum numbers. However it is not the case for non-integrable and chaotic systems, where symmetries may allow to separate a few degrees of freedom. However, we still lack a full set of quantum numbers to all states in Hilbert space. Therefore, to study the eigenvalue spectra of the system, we probe the fluctuations of the level distances, which tells us whether the two levels cross each other, resulting in degeneracy or level repulsion due to the real parameter λ. Such systems can be modeled by matrices with essentially random entries. The random elements describe random couplings between the various degrees of freedom. This idea goes back to Wigner and a simplified picture of Bohr who thought of the scattering process between a hadron and a heavy nucleus as a classical billiard-ball-like game. Now it is the theory of random matrices which brings both aspects together in the question of how good the spectra of physical systems reflect the statistics of random matrix ensembles [16].

4.2 Density of States and Unfolding of Spectra

When we study the energy eigenvalue spectra of a quantum system, we are interested in the density of the energy eigenvalues. This gives us an idea on the sparseness of the energy levels, which is not constant over the energy range. It is because the classical density of states changes with energy. In addition, the geometry or potential of the system affects global trends e.g how dense the energy spectrum is globally at E. In the case of quantum chaos, we are interested in the statistics of local eigenvalue fluctuations and not in global trends which are system specific. Local fluctuations of energy tells use how the neighboring levels interact statistically. Our goal here is to remove the smooth background variation of the level density so that only the local fluctuation survives, giving us the universal signatures of chaotic

or regular dynamics. For doing so, we split the total spectrum into independent eigenvalue subspaces each corresponding to a single symmetry of the system. We will consider a single symmetry class for our analysis because the levels belonging to different symmetry classes are uncorrelated statistically. So we first reduce the full spectrum to one subspace. Then we renormalize (rescale) the eigenenergies inside that subspace so that their mean density becomes constant. This is known as unfolding of the spectra. So after unfolding, the mean energy spacing of the system becomes 1.

4.3 Nearest-Neighbour Statistics for Integrable Systems

We start with the assumption that the energy levels after unfolding is given by a set of order numbers

$$-\infty < x_1 < x_2 < x_3 < .... < x_N < +\infty.$$

If the numbers x_i are independent random variables e.g. their positions are uncorrelated, then the probability of finding a particular level does not depend on where the preceding energy level was. This situation is mathematically identical to a Poisson process on the real line (a random sequence of "events" with constant average rate). Now, let $g(s)ds$ be the probability of finding a level between $[x+s, x+s+ds]$. $P(s)ds$ is the probability that the distance between two consecutive energy levels (after unfolding) lies between s and $s+ds$. We have two cases,

- The cumulative probability that the level spacing is less than or equal to s,

$$\int_0^s P(s')ds' = \text{Prob(spacing} \leq s)$$

- The cumulative probability that the level spacing is greater than s,

$$\text{Prob(spacing} > s) = \int_\infty^s P(s')ds' = 1 - \int_0^s P(s')ds'$$

Therefore,

$$P(s)ds = g(s)ds \times \int_s^\infty P(s')ds' \tag{4.2}$$

The solution is given by,

$$P(s) = g(s)e^{-\int_0^s ds' g(s')} \tag{4.3}$$

Assuming a uniform distribution of random numbers with $g(s) = 1$, the conditions of normalization and average level spacing one

$$\int_0^\infty dsP(s) = 1 \text{ and } \int_0^\infty ds \times s \times P(s) = 1 \tag{4.4}$$

$$P(s) = e^{-s}$$

Here, for the integrable system, the most likely case is $s = 0$, which implies a level crossing. In the limit of large energies (semiclassical limit), the statistical properties of the quantum spectra of classically integrable systems correspond to the prediction for randomly distributed energy levels [16].

4.3.1 Berry–Tabor Conjecture

Generally, for classically integrable nonlinear systems, i.e.

$$\det\left(\frac{\partial^2 H}{\partial I_i \partial I_j}\right) \neq 0, \tag{4.5}$$

with respect to the action variables I_i, and with at least two independent degrees of freedom, Berry and Tabor convincingly argued in favour of the following conjecture [3]:

Berry–Tabor Conjecture

In the limit of large energies (semiclassical limit), the statistical properties of the quantum spectra of classically integrable systems correspond to the prediction for randomly distributed energy levels.

In order to discuss Berry's conjecture, we need to introduce the Wigner function $W(\mathbf{x},\mathbf{p})$, which is defined as the Wigner–Weyl transform of the density matrix $\hat{\rho}$. For pure state, we have $\hat{\rho} = |\psi\rangle\langle\psi|$ [17]

$$W(\mathbf{x},\mathbf{p}) = \frac{1}{(2\pi\hbar)^{3N}}\int d^{3N}\xi \psi^*\Big(\mathbf{x}+\frac{\xi}{2}\Big)\Big(\mathbf{x}-\frac{\xi}{2}\Big)\exp\Big[-i\frac{\mathbf{p}\,\xi}{\hbar}\Big] \tag{4.6}$$

where x, p are the coordinates and momenta of $N-$particles spanning a $6N-$ dimensional phase space. For a mixed state, one replaces the product [13]

$$\left(\mathbf{x}+\frac{\xi}{2}\right)\left(\mathbf{x}-\frac{\xi}{2}\right) \;\rightarrow\; \left\langle \mathbf{x}+\frac{\xi}{2}\middle|\hat{\rho}\middle|\mathbf{x}-\frac{\xi}{2}\right\rangle = \hat{\rho}\Big(\mathbf{x}+\frac{\xi}{2},\mathbf{x}-\frac{\xi}{2}\Big) \tag{4.7}$$

Similarly, the Wigner function can be defined by integrating over momentum,

$$W(\mathbf{x},\mathbf{p}) = \frac{1}{(2\pi\hbar)^{3N}}\int d^{3N}\eta\; \phi^*\Big(\mathbf{p}+\frac{\eta}{2}\Big)\,\phi\Big(\mathbf{p}-\frac{\eta}{2}\Big)\exp\left[\frac{i}{\hbar}\mathbf{x}\eta\right], \tag{4.8}$$

where $\phi(\mathbf{p})$ is the Fourier transform of $\psi(\mathbf{x})$. From either of the two representations, it immediately follows that

$$\int d^{3N}p\, W(\mathbf{x},\mathbf{p}) = |\psi(\mathbf{x})|^2, \qquad \int d^{3N}x\, W(\mathbf{x},\mathbf{p}) = |\phi(\mathbf{p})|^2. \tag{4.9}$$

The Wigner function is uniquely defined for any wave function (or density matrix) and plays the role of a quasi-probability distribution in phase space. In particular, it allows one to compute the expectation value of any observable $\hat{O}$ as a standard average:

$$\langle\hat{O}\rangle = \int d^{3N}x\, d^{3N}p\, O_W(\mathbf{x},\mathbf{p})\, W(\mathbf{x},\mathbf{p}), \tag{4.10}$$

where $O_W(\mathbf{x},\mathbf{p})$ is the Weyl symbol of the operator $\hat{O}$,

$$O_W(\mathbf{x},\mathbf{p}) = \frac{1}{(2\pi\hbar)^{3N}}\int d^{3N}\xi\; \left\langle \mathbf{x}-\frac{\xi}{2}\middle|\hat{O}\middle|\mathbf{x}+\frac{\xi}{2}\right\rangle \exp\left[-\frac{i}{\hbar}\mathbf{p}\xi\right]. \tag{4.11}$$

Berry's conjecture postulates that, in the semiclassical limit of a quantum system whose classical counterpart is chaotic, the Wigner function of energy eigenstates (averaged over a vanishingly small phase space region) reduces to the microcanonical distribution. More precisely, define

$$W(\mathbf{X},\mathbf{P}) = \int_{\Delta\Omega_1} \frac{dx_1\, dp_1}{2\pi\hbar} \cdots \int_{\Delta\Omega_N} \frac{dx_N\, dp_N}{2\pi\hbar}\, W(\mathbf{x},\mathbf{p}). \tag{4.12}$$

where $\Delta\Omega_j$ is a small phase-space volume centered around the point $\mathbf{X},\mathbf{P}$. This volume is chosen such that, as $\hbar \to 0$, $\Delta\Omega_j \to 0$ and at the same time $\hbar/\Delta\Omega_j \to 0$. Berry's conjecture then states that, as $\hbar \to 0$,

$$\overline{W}(\mathbf{X},\mathbf{P}) = \frac{1}{\displaystyle\int d^{3N}X\, d^{3N}P\, \delta[E - H(\mathbf{X},\mathbf{P})]}\, \delta[E - H(\mathbf{X},\mathbf{P})]\,, \tag{4.13}$$

where $H(\mathbf{X},\mathbf{P})$ is the classical Hamiltonian describing the system, and $\delta[\cdots]$ is a one-dimensional Dirac delta function. In Berry's words, "$\psi(\mathbf{x})$ is a Gaussian random function of $\mathbf{x}$ whose spectrum at $\mathbf{x}$ is simply the local average of the Wigner function $\overline{W}(\mathbf{x},\mathbf{p})$." Berry also considered quantum systems whose classical counterpart is integrable. He conjectured that the structure of the energy eigenstates of such systems is very different [4], [13]. For example, in the case of quantum kicked rotor, which is an integrable system, the energy level spacing forms a poisson distribution. Anderson localization give eigenstates which have exponentially small overlap in real (or momentum) space, and hence essentially independently distributed energy levels which do not "feel each" other. This implies regular behaviour and Poisson distributed level spacings, despite the classical chaoticity of the kicked rotor [16].

4.4 Nearest–Neighbour Statistics for Non-integrable Systems

To model what happens locally near a crossing of two levels in integrable system, we take a 2×2 effective Hamiltonian depending on crossing parameter λ,

$$\begin{pmatrix} E_1(\lambda) & 0 \\ 0 & E_2(\lambda) \end{pmatrix}. \tag{4.14}$$

For some λ_c, $E_1(\lambda_c) = E_2(\lambda_c)$ which implies a level crossing. For non-integrable system, we do not get a level crossing. Instead, the levels experience repulsion which is modeled by a coupling V.

$$H = \begin{pmatrix} E_0 - \Delta & V \\ V^* & E_0 + \Delta \end{pmatrix}, \qquad E_\pm = E_0 \pm \sqrt{\Delta^2 + |V|^2}. \tag{4.15}$$

Here, Δ is a parameter which depends on λ; $\Delta \to 0$ implies that two levels are the closest. The gap between two eigenvalues is given by $\Delta E = E_+ - E_- = 2\sqrt{\Delta^2 + |V|^2}$ [16]. This implies that the minimum gap between two levels is $2|V|$. We estimate the probability for small energy level spacing e.g. $\Delta E \to 0$, by

$$P(\Delta E) \sim \int dV_R \int dV_I \int d\Delta\; P(V_R, V_I, \Delta)\, \delta(\Delta E - D).$$

Assuming $P(V_R, V_I, \Delta) \sim$ constant > 0 For $V_R.V_I \to 0$ Then the three-dimensional volume integral over (V_R, V_I, Δ) can be computed as

$$P(\Delta E) \sim 4\pi \int dV\, V^2\, \delta(\Delta E - V) \propto \Delta E^2. \tag{4.16}$$

For a real matrix with just two independent parameters (V, Δ), both real, we obtain in a similar manner:

$$P(\Delta E) \sim \int dV \int d\Delta\, P(V, \Delta)\, \delta(\Delta E - D) \sim 2\pi \int dV\, V\, \delta(\Delta E - V) \propto \Delta E, \tag{4.17}$$

for small $\Delta \to 0$ to allow for the approximation $D \approx |V|$ in the argument of the δ-function. Based on experiments, it was found that the excitation spectra of heavy nuclei correspond quite well to the predictions made for certain ensembles of random matrices. Different symmetry conditions lead to different predictions for level spacings, depending on whether the Hamiltonian is real or complex. A real Hamiltonian corresponds to the Gaussian orthogonal ensemble (GOE), which describes time-reversal invariant systems with integer spin, while a complex Hamiltonian corresponds to the Gaussian unitary ensemble (GUE), associated with systems where time-reversal symmetry is broken. The level statistics of systems with a special time reversal invariance – like systems with half-integer spin particles – coincides with Gaussian symplectic ensemble (GSE).

$$P(s) = \begin{cases} e^{-s}, & \text{integrable,} \\ \dfrac{\pi}{2}\, s\, e^{-\frac{\pi s^2}{4}}, & \text{GOE,} \\ \dfrac{32}{\pi^2}\, s^2\, e^{-\frac{4s^2}{\pi}}, & \text{GUE,} \\ \dfrac{2^{18}}{36\pi^3}\, s^4\, e^{-\frac{64 s^2}{9\pi}}, & \text{GSE.} \end{cases}$$

s is dimensionless such that all spectra can be directly compared without another scaling factor.

4.4.1 Bohigas–Giannoni–Schmit Conjecture

The Bohigas–Giannoni–Schmit (BGS) conjecture establishes a fundamental connection between classical chaos and quantum spectral statistics.

BGS Conjecture

The eigenvalues of a quantum system, whose classical analogue is fully chaotic, obey the same universal statistics of level spacings as predicted for the eigenvalues of Gaussian random matrices.

This conjecture provides a quantum signature of classical chaos: instead of Poisson level statistics (which characterize integrable systems), chaotic systems exhibit level repulsion described by Random Matrix Theory (RMT). RMT was originally

introduced by Wigner in the context of nuclear spectra. Dyson later developed a systematic classification of random matrix ensembles based on symmetry considerations. Thus, according to the BGS conjecture, the presence of classical chaos implies universal Wigner–Dyson level statistics, with the precise form determined solely by the underlying symmetries of the quantum system [16].

4.5 Gaussian Ensembles of Random Matrices

As discussed, the idea of random matrix models in context of modeling many body systems to probe the level statistics of heavy nuclei. The goal was to assume as little as possible about the detailed structure of the system and consider its symmetries only. We thus build a statistical ensemble of matrices with reasonable constraints on their entries. The conditions are the following:

- **Statistical Invariance:** The matrix entries are statistically uncorrelated random numbers. That means the distribution of a whole matrix factorizes into its independent parts:
$$P(H) = \prod_{i,j} p_{ij}(H_{ij}). \tag{4.18}$$

- **Basis invariance:** The physical predictions are independent of the choice of basis. Physical predictions must not depend on the choice of basis. Therefore, the distribution must remain invariant under symmetry-preserving transformations of the Hamiltonian.

These requirements lead to three universality classes, classified by their time-reversal symmetries. We note that T is the anti unitary time reversal operator. T only commutes with the Hamiltonian if the system is invariant under time reversal. This operator can be used to determine the statistical properties of the eigenvalue spectrum, which is given by the symmetry class of random matrix ensemble.

- **Gaussian Orthogonal Ensemble (GOE):** For time-reversal invariant systems with $T^2 = 1$, the Hamiltonian can be taken real and symmetric. The probability distribution is invariant under orthogonal transformations,
$$P(H) = P(OHO^T), \quad O \in O(N). \tag{4.19}$$

- **Gaussian Unitary Ensemble (GUE):** When time-reversal symmetry is broken, the Hamiltonian is complex Hermitian. The distribution is invariant under unitary transformations,
$$P(H) = P(UHU^\dagger), \quad U \in U(N). \tag{4.20}$$

- **Gaussian Symplectic Ensemble (GSE):** For systems with time-reversal symmetry but $T^2 = -1$ (e.g. half-integer spin systems), Kramers degeneracy arises. The distribution is invariant under symplectic transformations,
$$P(H) = P(SHS^\dagger). \tag{4.21}$$

By imposing statistical and basis invariance of the systems, we find that the statistical distributions take Gaussian form, which is given by,

$$P(H) = C \exp\left(-A \operatorname{tr}(H^2)\right), \tag{4.22}$$

where A and C are positive constants determined by normalization. For example, in the GOE case,

$$\operatorname{tr}(H^2) = \sum_{i,j} H_{ij}^2, \tag{4.23}$$

This implies that the joint distribution factorizes into Gaussian distributions for each independent matrix element. Similar expressions hold for GUE and GSE, with appropriate treatment of real and imaginary parts.

Although it is difficult to compute the exact spectral statistics for large random matrices, Wigner surmises provides a remarkably accurate approximation to that. For the Gaussian orthogonal ensemble (GOE), this yields

$$P(s) = \frac{\pi}{2} s \exp\left(-\frac{\pi}{4} s^2\right), \tag{4.24}$$

which exhibits level repulsion, $P(s) \to 0$ as $s \to 0$. Analogous expressions hold for the GUE and GSE, with stronger level repulsion. These universal distributions provide a direct signature of quantum chaos and form the basis for comparing spectral statistics of physical systems with random matrix predictions.

So far we have discussed just one property of the predictions for the universal random-matrix ensembles, the level spacing distributions. The level spacing distributions only characterise local correlations in the spectrum, dealing with the nearest-neighbour distances of levels. However, random matrix theory offers more sophisticated tools to probe high order spectral correlation which accounts for global correlations. Two methods of inspecting global correlations are spectral rigidity and number variance.

Chapter 5

Out of Time Order Correlators in Quantum Mechanics

Over the years, numerous tools have been developed in order to probe chaos in quantum system. Out of time order correlators (OTOC) has recently emerged as an useful tool for testing chaotic dynamics in a quantum systems. OTOC has enabled researchers to probe the evolution of Heisenberg operators at different times and thus extend quantum chaos research beyond the limited scope of time independent, one body systems [27]. Black-holes were shown to exhibit the early exponential time-growth of the OTOC expected in classically chaotic systems. Such a behavior enabled to place black-holes in the class of fast scramblers, where the information is rapidly spread. Moreover, Stanford and Maldacena [18] conjectured the existence of an upper bound to the growth-rate of the OTOC, essentially given by the temperature of the system. Why are we particularly interested in OTOC for understanding quantum chaos? In his paper, Hashimoto et al. [19] showed that out-of-time order correlators are a better measure of quantum chaos than energy level statistics for a system of coupled harmonic oscillators. So, instead of using level statistics to test whether our system of interest is quantum chaotic, we will extract quantum Lyapunov exponent. In this section, we will introduce the concepts of out-of-time order correlators in quantum mechanics. In particular, we will derive a semi classical approximation of OTOC and a quantum analogue of 'Lyapunov exponent'– which will be a useful measure of chaos in quantum systems. In addition, we will brief discuss the causal structure of operators associated with OTOC and how OTOC are used to described scrambling of quantum information in a system.

5.1 Definition

The out-of-time-order correlator (OTOC) is a time-dependent function defined by an averaged double commutator as

$$C_{VW}(t) = \left\langle [\hat{W}_t, \hat{V}]^\dagger [\hat{W}_t, \hat{V}] \right\rangle . \tag{5.1}$$

Here,

- $\hat{V}$ and $\hat{W}$ are operators in a Hilbert space $\mathcal{H}$.

- The subscript t denotes the time evolution of an operator $\hat{O}$ in the Heisenberg picture:
$$\hat{O}_t = \hat{U}_t^\dagger \hat{O} \hat{U}_t, \quad \text{with} \quad \hat{U}_t = e^{-i\hat{H}t/\hbar}. \tag{5.2}$$
- $\langle \cdot \rangle = \mathrm{Tr}\{\hat{\rho} \cdot\}$ represents the thermal average in the canonical ensemble.
- The density matrix is given by
$$\hat{\rho} = Z^{-1} e^{-\beta \hat{H}}, \tag{5.3}$$
where Z is the partition function and
$$\beta = (k_B T)^{-1},$$
with T the temperature and k_B the Boltzmann constant.

The definition above holds for arbitrary operators. However, in many physical applications one considers Hermitian operators $\hat{V}$ and $\hat{W}$, for which the OTOC becomes
$$C_{VW}^{(H)}(t) = -\left\langle [\hat{W}_t, \hat{V}]^2 \right\rangle. \tag{5.4}$$
Expanding the general definition, the OTOC can be written as
$$C_{VW}(t) = D_{VW}(t) + I_{VW}(t) - 2\,\mathrm{Re}\left\{F_{VW}(t)\right\}. \tag{5.5}$$
The different contributions are given by:
$$D_{VW}(t) = \left\langle \hat{V}^\dagger (\hat{W}^\dagger \hat{W})_t \hat{V} \right\rangle \tag{5.6}$$
$$I_{VW}(t) = \left\langle \hat{W}_t^\dagger \hat{V}^\dagger \hat{V} \hat{W}_t \right\rangle \tag{5.7}$$
$$F_{VW}(t) = \left\langle \hat{W}_t^\dagger \hat{V}^\dagger \hat{W}_t \hat{V} \right\rangle \tag{5.8}$$
In the unitary case,
$$D_{\hat{V}\hat{W}}(t) = I_{\hat{V}\hat{W}}(t) = 1, \tag{5.9}$$
and then
$$C_{\hat{V}\hat{V}}^{\mathrm{uni}}(t) = 2\left(1 - \mathrm{Re}\{F_{\hat{V}\hat{V}}(t)\}\right). \tag{5.10}$$
The three-point functions $D_{VW}(t)$ and $I_{VW}(t)$, and the four-point function $F_{VW}(t)$, are time-correlators of different complexity. While $D_{VW}(t)$ involves only two evolution operators in its definition, $I_{VW}(t)$ and $F_{VW}(t)$ depend on four evolution operators. The simplest correlator is thus $D_{VW}(t)$, which can be expressed as a time-ordered product. The function $F_{VW}(t)$ is a genuine out-of-time-order correlator, as it involves operators that are not time-ordered in the conventional sense. Due to this non-standard ordering, it is expected to exhibit a non-trivial time dependence. For this reason, $F_{VW}(t)$ is often referred to as the OTOC. For notational simplicity, we will drop the subscripts and referred it as the four point correlation function. The growth of the OTOC is associated with the spread of quantum information, a process commonly referred to as information scrambling.

5.1.1 Microcanonical and Thermal OTOC

Let us consider a quantum system described by a time-independent Hamiltonian

$$\hat{H} = H(\hat{x}_1, \ldots, \hat{x}_N, \hat{p}_1, \ldots, \hat{p}_N), \tag{5.11}$$

in the Heisenberg picture. In the following, we focus on a single degree of freedom and denote $\hat{x} \equiv \hat{x}_1$ and $\hat{p} \equiv \hat{p}_1$. The time-evolved position operator is given by

$$\hat{x}(t) = e^{i\hat{H}t}\hat{x}e^{-i\hat{H}t}. \tag{5.12}$$

The out-of-time-order correlator (OTOC) of interest is defined as

$$C_T(t) = \left\langle [\hat{x}(t), \hat{p}]^2 \right\rangle_T, \tag{5.13}$$

where $\langle\cdot\rangle_T$ denotes the thermal average at inverse temperature $\beta = 1/T$:

$$\langle \hat{O} \rangle_T = \frac{1}{Z(T)} \mathrm{Tr}\left(e^{-\beta\hat{H}}\hat{O}\right), \quad Z(T) = \mathrm{Tr}\left(e^{-\beta\hat{H}}\right). \tag{5.14}$$

Assuming discrete energy eigenvalues, the thermal OTOC can be expressed in the energy eigenbasis as

$$C_T(t) = \frac{1}{Z(T)} \sum_n e^{-\beta E_n} c_n(t), \tag{5.15}$$

where

$$c_n(t) = \langle n|[\hat{x}(t), \hat{p}]^2|n\rangle, \tag{5.16}$$

and $\hat{H}|n\rangle = E_n|n\rangle$. We refer to $C_T(t)$ as the thermal OTOC and $c_n(t)$ as the microcanonical OTOC. This impplies that once we compute the microcanonical OTOC, we can obtain the thermal OTOC by taking their thermal average.
As a concrete example, consider a one-dimensional harmonic oscillator,

$$\hat{H} = \frac{\hat{p}^2}{2} + 2\hat{x}^2. \tag{5.17}$$

In this case, the Heisenberg equations of motion can be solved exactly, yielding

$$\hat{x}(t) = \hat{x}\cos t + \frac{\hat{p}}{2}\sin t, \tag{5.18}$$

$$\hat{p}(t) = \hat{p}\cos t - 2\hat{x}\sin t. \tag{5.19}$$

Using these expressions and the canonical commutation relation $[\hat{x}, \hat{p}] = i$, one obtains

$$c_n(t) = \cos^2 t, \quad C_T(t) = \cos^2 t. \tag{5.20}$$

A higher-dimensional harmonic oscillator yields the same result, since the different degrees of freedom are decoupled [19]. Notice that this result in indepenent of temperature T and energy level n.

Let us rewrite the microcanonical OTOC using matrix elements of $\hat{x}$ and $\hat{p}$ for numerical calculations. Using the completeness relation

$$I = \sum_m |m\rangle\langle m|, \tag{5.21}$$

we can express the microcanonical OTOC as

$$c_n(t) = \sum_m b_{nm}(t)\, b^*_{nm}(t), \quad b_{nm}(t) \equiv -i\langle n|[\hat{x}(t), \hat{p}]|m\rangle. \tag{5.22}$$

Note that $b_{nm}(t)$ satisfies $b_{nm}(t) = b^*_{mn}(t)$. Substituting $\hat{x}(t) = e^{i\hat{H}t}\hat{x}e^{-i\hat{H}t}$ and inserting the completeness relation again, we obtain

$$b_{nm}(t) = -i\sum_k \left(e^{iE_{nk}t}x_{nk}p_{km} - e^{iE_{km}t}p_{nk}x_{km}\right), \tag{5.23}$$

where

$$E_{nm} = E_n - E_m, \quad x_{nm} = \langle n|\hat{x}|m\rangle, \quad p_{nm} = \langle n|\hat{p}|m\rangle. \tag{5.24}$$

In this expression, matrix elements of $\hat{p}$ appear, which are not ideal for numerical computations since they involve derivatives of wavefunctions. For a natural Hamiltonian of the form

$$\hat{H} = \sum_{i=1}^{N} \hat{p}_i^2 + U(x_1, \ldots, x_N), \tag{5.25}$$

we can instead express p_{nm} in terms of x_{nm}. Using the commutation relation

$$[\hat{H}, \hat{x}] = -2i\hat{p}, \tag{5.26}$$

and taking matrix elements, we obtain

$$p_{nm} = \frac{i}{2}E_{nm}x_{nm}. \tag{5.27}$$

Substituting this into the expression for $b_{nm}(t)$, we arrive at

$$b_{nm}(t) = \frac{1}{2}\sum_k x_{nk}x_{km}\left(E_{km}e^{iE_{nk}t} - E_{nk}e^{iE_{km}t}\right). \tag{5.28}$$

Therefore, once the matrix elements of $\hat{x}$ and the energy spectrum E_n are known, the OTOC can be computed using the above expressions.

5.1.2 Numerical Implementation of the OTOC

In this work, the out-of-time-order correlator (OTOC) is computed numerically for a system of coupled quantum harmonic oscillators with a non-linear coupling. The implementation is carried out in a truncated Fock basis, which provides a convenient representation for bosonic degrees of freedom. It makes the code faster by invoking linear algebra libraries of different programming languages. Primarily, we have used Julia and Python.

We begin by constructing the Hilbert space as a tensor product of individual oscillator Fock spaces. Each basis state is labeled by occupation numbers,

$$|n_1, n_2, n_3\rangle, \tag{5.29}$$

where n_i denotes the excitation number of the i-th oscillator. Next, we impose a cut-off on the maximum number occupation number to keep the size of the Hilbert space

finite. We then define the ladder operators for each oscillators and thus construct position and momentum operators,

$$\hat{x}_i \propto \hat{a}_i + \hat{a}_i^\dagger, \qquad \hat{p}_i \propto -i(\hat{a}_i - \hat{a}_i^\dagger). \tag{5.30}$$

The Hamiltonian of our interest consists of a harmonic part and a nonlinear interaction term. The harmonic contribution is diagonal in the Fock basis and given by

$$\hat{H}_0 = \sum_i \left(n_i + \frac{1}{2} \right), \tag{5.31}$$

while the interaction is constructed from products of position operators, leading to terms of the form

$$\hat{H}_{\text{int}} \sim g_0 \, \hat{x}_i^2 \hat{x}_j^2. \tag{5.32}$$

We then add all terms to get the fill Hamiltonian operator. The Hamiltonian is then diagonalized numerically to obtain its eigenvalues E_n and eigenvectors $|n\rangle$. Using this eigenbasis, operators are transformed accordingly, allowing efficient computation of their time evolution. We implement time-dependent position operator in the heisenberg picture using the spectral decomposition of hamiltonian, which reduces the time evolution to phase factors of the form $e^{i(E_n - E_m)t}$. The OTOC is computed from the commutator

$$[\hat{x}(t), \hat{p}], \tag{5.33}$$

and its expectation value in energy eigenstates,

$$c_n(t) = \langle n | [\hat{x}(t), \hat{p}]^2 | n \rangle. \tag{5.34}$$

This quantity corresponds to the microcanonical OTOC. Thermal average can be

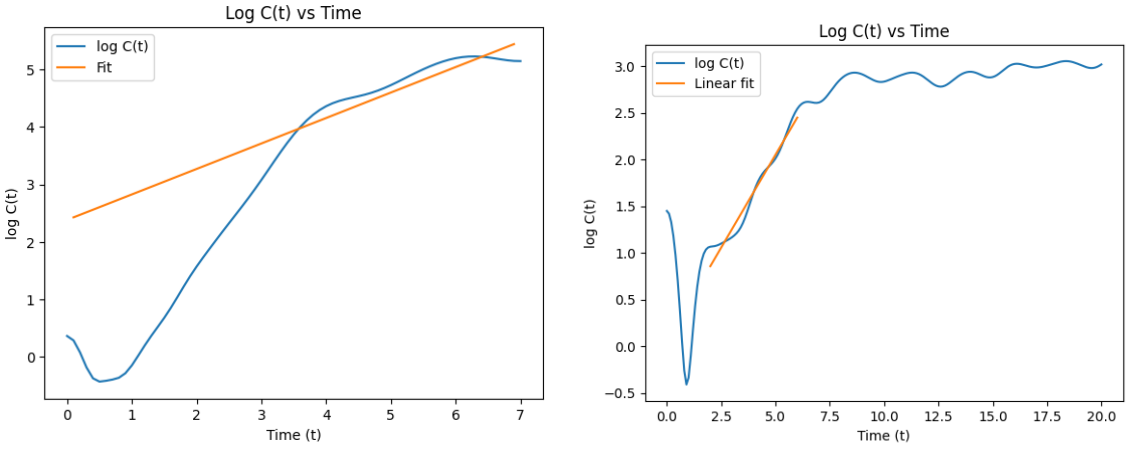

Figure 5.1: Time evolution of thermal OTOC for two (left) and three couple harmonic oscillator in log scale. The straight line illustrates the exponential growth of OTOC

obtained by weighting these contributions with Boltzmann factors. This numerical approach is equivalent to the matrix-element formulation of the OTOC, but is more suitable for implementation in interacting many-body systems, where operators are naturally represented as matrices in a truncated Hilbert space.

5.2 Physical Interpretation of OTOC

The growth of the OTOC is associated with the spread of quantum information, a process commonly referred to as information scrambling. Such a spreading can be quantified in operator space by choosing $\hat{W}$ and $\hat{V}$ as operators that act locally on spatially separated regions. In this case, they initially commute, i.e., $[\hat{W}, \hat{V}] = 0$. The Baker–Campbell–Hausdorff expansion of the time-evolved operator $\hat{W}_t$ leads to a series of nested commutators,

$$\hat{W}_t = \sum_{k=0}^{\infty} \frac{(it)^k}{k!} \underbrace{[\hat{H}, [\hat{H}, \ldots, [\hat{H}, \hat{W}] \ldots]]}_{k \text{ times}}. \tag{5.35}$$

If the Hamiltonian contains local n-body interactions (for instance, $n = 2$ in the case of nearest-neighbour coupling in a spin chain), it follows from the above expansion that the support of the operator $\hat{W}_t$ grows with time. In particular, each successive commutator with $\hat{H}$ increases the spatial extent of $\hat{W}_t$, causing it to act on an increasingly larger region of the system which can be thought of the increasing number of sited activated within a lattice system. In the diagram, it has been illustrated as the propagation cone. As time progresses, the operator $\hat{W}_t$ spreads

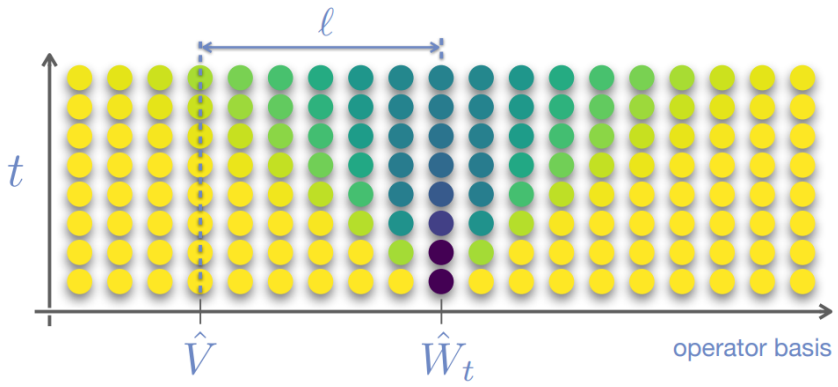

Figure 5.2: Sketch illustrating the spreading of an operator $\hat{W}$, initially localized at the central site of a one-dimensional system (e.g., a spin chain), under Heisenberg time evolution [27].

over an increasing number of sites in the operator basis. A second operator $\hat{V}$, located at a distance l from the center, is initially unaffected (yellow region), but becomes influenced at later times once it enters the propagation cone of $\hat{W}_t$ (green region). This behavior reflects the growth of operator and support the emergence of a light-cone-like structure associated with information spreading. Essentially, we are measuring the growth of one operator through its interaction with the light-cone of another operator. The time evolution of the operators are determined by $\hat{H}$, the sites associated with the operator $\hat{V}$ is also involved. Such an effect can be probed through the non-vanishing commutator between $\hat{V}$ and $\hat{W}_t$, and therefore by the OTOC.

The early-time behavior of scrambling is expected to depend on the combination $t - \ell/v_B$, which typically exhibits an exponential growth. In particular, $C_{VW}(t)$

remains very small when $t \ll \ell/v_B$, indicating that $\hat{V}$ lies outside the propagation cone of $\hat{W}_t$. The so-called butterfly velocity v_B determines the slope of this propagation cone (see Fig. (5.2)) and characterizes the speed at which quantum information spreads through the system. Furthermore, the sequence of operators $\hat{U}_t$ and $\hat{U}_t^\dagger$ appearing in the definition of the OTOC, $C_{VW}(t)$, and in the out-of-time-order function, $F_{VW}(t)$, can be interpreted as an alternation of forward and backward time evolution. This structure is reminiscent of the Loschmidt echo. The Loschmidt echo measures how identical the state is to the state once time-evolved by a Hamiltonian H' and then time-evolved backward in time by a slightly different Hamiltonian H.

5.3 Semi-Classical limit of the OTOC

To probe specific characteristics of the behavior of OTOC as a function of time and its universal features, we take the semi classical limit to $\hbar \to 0$. Given the well known relation between the commutator of two operators and the Poisson brackets of the corresponding classical symbols (considered as phase-space functions),

$$\lim_{\hbar\to 0} \frac{1}{i\hbar}[\hat{W}, \hat{V}] \to \{W, V\} \tag{5.36}$$

while making the choice $\hat{W} = \hat{X}$ and $\hat{V} = \hat{P}_X$, the quasiclassical limit of the commutator $[\hat{X}_t, \hat{P}_X]$ can be expressed as

$$[\hat{X}_t, \hat{P}_X] \to \ i\hbar\{X(t), P_X(0)\} = i\hbar \frac{\partial X(t)}{\partial X(0)} \tag{5.37}$$

If the classical dynamics is fully chaotic, the exponential sensitivity with respect to the initial condition translates into

$$\frac{\partial X(t)}{\partial X(0)} \sim \exp(\lambda t), \tag{5.38}$$

where λ is the Lyapunov exponent. Therefore, the quasi-classical limit of the OTOC is given by

$$C^{\mathrm{qc}}_{P_X X}(t) \sim \hbar^2 \exp(2\lambda t) \tag{5.39}$$

Here, λ is called the quantum Lyapunov exponent. This relationship is particularly interesting, since it establishes the signature of the Lyapunov exponent, which is a purely classical quantity, in the OTOC, which is a quantum object. This is a new measure of chaos in quantum system and has been shown to be a better measure than level statistics since we are required to calculate a significantly lower of number of eigenstates to see in chaos using OTOC [19]. Thus, the OTOC for the harmonic oscillator exhibits oscillatory behavior and does not display exponential growth as given in (5.20). This is consistent with the fact that the system is integrable and non-chaotic, as we found previously in discussion on the thermal and microcanonical OTOC for simple harmonic oscillators.

To study our system of interest, we start by writing down its Hamiltonian,

$$\hat{H} = \Big(\frac{\hat{p}_x^2}{2} + \frac{\omega_x^2}{2}\hat{x}^2\Big) + \Big(\frac{\hat{p}_y^2}{2} + \frac{\omega_y^2}{2}\hat{y}^2\Big) + g_0\,\hat{x}^2\hat{y}^2. \tag{5.40}$$

This result is a very simple model of two harmonic oscillators with nonlinear coupling. Generalizing for $N-$ oscillators, we have,

$$\hat{H} = \sum_{i=1}^{N} \left(\frac{\hat{p}_i^2}{2} + \frac{\omega_i^2}{2} \hat{x}_i^2 \right) + g_0 \sum_{i<j} \hat{x}_i^2 \hat{x}_j^2. \tag{5.41}$$

Ignoring the mass terms and prefactors, we have the energy

$$E = p_x^2 + p_y^2 + g_0 x^2 y^2. \tag{5.42}$$

This system allows the following scaling transformation:

$$(x, y) \to (\lambda x, \lambda y), \qquad E \to \lambda^4 E, \qquad t \to \lambda^{-1} t. \tag{5.43}$$

So, we conclude that

$$\lambda_{\rm cl} \propto E^{1/4}, \qquad \lambda_{\rm cl} \propto T^{1/4} \tag{5.44}$$

For this system, the thermal OTOC increases exponentially. In addition, we can make numerical fitting of data of our thermal OTOC for $T \geq 3$ and in the time domain $2 \leq t \leq 6$ by an exponential function,

$$C_T(t) \approx a(T)\, e^{2\lambda_q(T) t}, \tag{5.45}$$

where $\lambda_q(T)$ is the temperature-dependent quantum Lyapunov exponent. We then extract $\lambda_q(T)$ for different values of the temperature, namely

$$T = 3,\ 3.5,\ 4,\ 4.5,\ 5 \tag{5.46}$$

and analyze its dependence on T. It is important to note that the classical CHO system is subject to a phase transition from the regular to the chaotic phase, when going from lower to higher energy scales. For two coupled harmonic oscillators, we have a classical phase transition at $T = 3$. Therefore, we expect that the thermal OTOC grows exponential when $T \geq 3$.

For systems of three coupled harmonic oscillators, the expression for energy is given by,

$$E = p_x^2 + p_y^2 + p_z^2 + g_0 x^2 y^2 z^2. \tag{5.47}$$

The energy remains invariant under the following scale transformation

$$(x, y) \to (\alpha x, \alpha y), \qquad E \to \alpha^6 E, \qquad t \to \alpha^{-2} t. \tag{5.48}$$

Since, the Lyapunov exponent has the dimension of inverse of time, we conclude that

$$\lambda_{cl} \propto \alpha^2\, \lambda_{cl}$$

So, we conclude that

$$\lambda_{\rm cl} \propto E^{1/3}, \qquad \lambda_{\rm cl} \propto T^{1/3}. \tag{5.49}$$

For this system, we considered the following values of the temperature, starting from the possible phase transition point of the system at $T = 1.8$

$$T = 1.8,\ 2,\ 2.5,\ 3,\ 3.5,\ 4,\ 4.5,\ 5,\ 5.5. \tag{5.50}$$

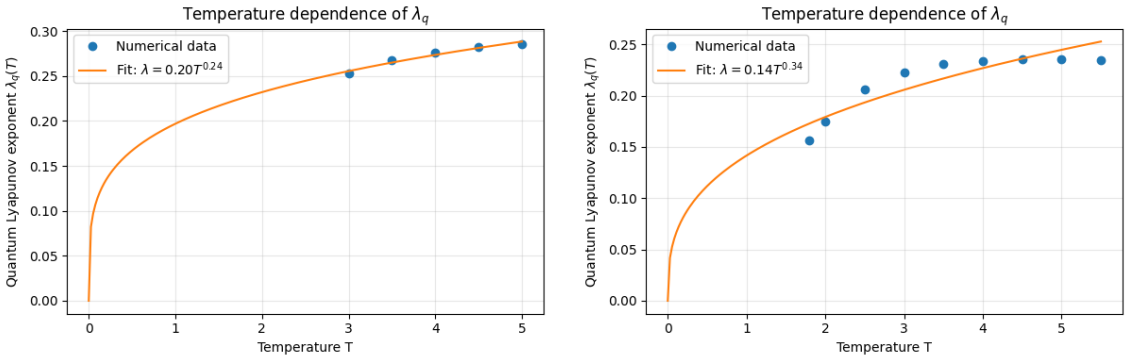

Figure 5.3: Temperature dependence of quantum Lyapunov exponents for two (left) and three (right) coupled harmonic oscillators. In addition, the value of quantum Lyapunov exponent is positive for both systems: λ_L is 0.221 for two oscillators and 0.455 for three oscillators.

We see that both of the curve fitting agree very well with the classical expectations. Due to the following two observations about the exponents, we claim that the thermal OTOCs of the CHO systems grow exponentially.

1. The order of magnitude of classical and quantum lyapunov exponent is the same. The OTOC $C_T(t)$ is defined as the quantum analogue of classical poisson bracket given by $\{x(t), p\}^2 \sim e^{2\lambda_{\rm cl}t}$. Therefore, we can expect a similar behavior for the quantum OTOC,

$$C_T(t) \sim e^{2\lambda_{\rm cl}t}, \tag{5.51}$$

as long as the quantum dynamics closely follows the classical evolution, i.e., up to the Ehrenfest time. Note that after Ehrenfest time, the system becomes fully quantum so the semi classical approximation fails. Therefore, it is natural to expect that the quantum Lyapunov exponent λ_q is of the same order as the classical Lyapunov exponent $\lambda_{\rm cl}$.

2. The temperature dependence of the quantum Lyapunov exponent λ_q is found to be similar to the energy dependence of the classical Lyapunov exponent $\lambda_{\rm cl}$. Motivated by this observation, we postulate a power-law dependence of the form

$$\lambda_q(T) = b\,T^c, \tag{5.52}$$

where b and c are fitting parameters. We fit our numerical results using this functional form. The chosen ansatz satisfies $\lambda_q(T = 0) = 0$, consistent with the expectation that no exponential growth occurs at zero temperature. From the fit, we obtain

$$\lambda_q(T) \propto T^c, \qquad c \approx 0.24,\, 0.33 \tag{5.53}$$

For two and three coupled harmonic oscillators, respectively. At sufficiently high energies, the classical Lyapunov exponent exhibits the scaling behavior for systems of two and three coupled harmonic oscillators with non-linear coupling, we have

$$\lambda_{\rm cl} \propto E^{1/4}, \qquad \lambda_{\rm cl} \propto E^{1/3}, \tag{5.54}$$

Since the typical energy at finite temperature scales as $E \sim T$, one expects the quantum Lyapunov exponent to follow

$$\lambda_q(T) \propto T^{1/4}, \qquad \lambda_q(T) \propto T^{1/3} \tag{5.55}$$

The temperature dependence of quantum lyapunov exponent is extremely remarkable. Although we are dealing with a system of few degrees of freedom and the Ehrenfest time is supposed to be very short, we can still find a region where the classical exponential growth of OTOC can be detected in thermal OTOC. From this we can identify where classical behavior of thermal OTOC e.g. the region within which thermal OTOC is energy dependent and thus calculate the Ehrenfest time.

5.4 Time windows

We saw that the semi classical limit of the OTOC suggests the emergence of classical properties in quantum systems. However, this holds only for very specific systems and within very specific time frames. Many previous studies on the time evolution of various systems have shown that the OTOC can generally be classified into three different time-windows.

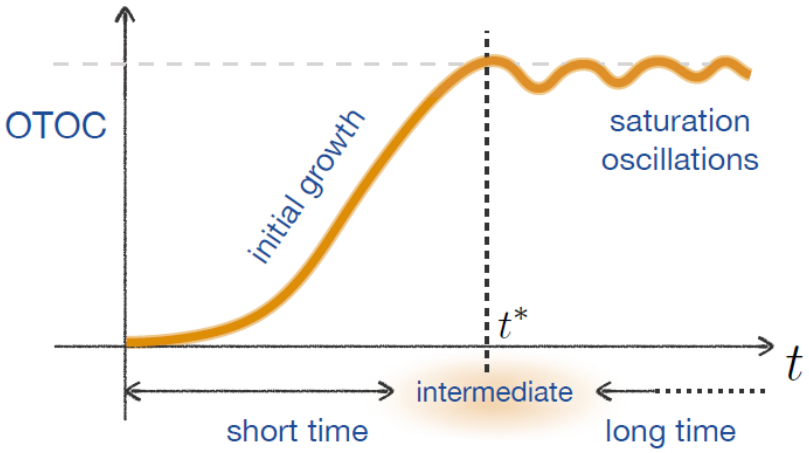

Figure 5.4: Schematic picture for the time evolution of the OTOC. The initial growth is expected to be exponential if the system is chaotic. It can take any other form depending on the dynamics of the system. After the scrambling time t^* the OTOC saturates, showing oscillations around a constant value. In the chaotic case the oscillations are strongly suppressed and the OTOC approaches an approximately constant value. Illustration has been adopted from [27]

Short times

The short-time window signals the start of the process where the influence of the time-dependent Heisenberg operator expands, driven by the dynamics of the Hamiltonian. Using the BCH formula, at the beginning, the OTOC is predicted to increase following a power law. Following this initial stage, the OTOC will continue

to increase steadily for a brief period before reaching scrambling time t^*. Previously, we have calculated the quantum Lyapunov exponent to calculate the growth of OTOC for systems with a low degrees of freedom. This behavior emerges after a much faster growth during an extremely short time window [31].

Intermediate times

At around the scrambling time, t^*, the initial growth of the operator stops and thus the OTOC becomes relatively stable. In this time window, the OTOC value remains almost constant with minor fluctuations. This time interval is commonly referred to as "intermediate times" and is particularly significant for highly chaotic systems, as it represents the duration between t^* and complete relaxation.

In addition, the scrambling time t^* marks the point at which information about the initial state becomes widely spread throughout the available space. Information scrambling can be roughly approximated to be the process through which the width of the wavefunction takes the same value as the size of the system. Beyond semi classical regime, scrambling refers to the delocalization of quantum information in Hilbert space rather than simple spatial spreading. For a single particle system with a bounded space and classical chaotic dynamics, this time corresponds to the Ehrenfest time t_E. The Ehrenfest time is defined as the time it takes for a narrow, coherent wave-packet to spread over whole system. It is given by

$$t_E = \lambda^{-1} \ln\left(\frac{a}{\hbar}\right), \tag{5.56}$$

where the constant a is determined by the system size and the initial wave-packet size [25].

Long times

For strongly chaotic systems, the OTOC becomes constant after the scrambling time. During this time, the dynamics is influenced by the asymptotic behavior of the OTOC. The long-time behaviour of the OTOC can provide accurate measures of quantum chaos, and analyzing its oscillations can quantify the shift from regular to chaotic dynamics. For non-chaotic systems, it is expected that OTOCs at long times will exhibit strong oscillations, whereas for strongly chaotic systems these oscillations are expected to be suppressed.

Chapter 6

Eigenstate Thermalisation Hypothesis

In thermodynamics and statistical mechanics, we typically study certain dynamical properties of many-body systems. These properties include the thermal equilibrium state of the system and the values of observables in thermal equilibrium, which depend only on the nature of the system and conserved quantities such as energy. The fluctuations of measured values of operators about their equilibrium values are also examined. Recent developments in statistical mechanics investigate to what extent these properties can be understood as consequences of quantum chaos, provided certain constraints and statistical properties are imposed on the energy eigenvalues and eigenstates. In particular, the non equilibrium nature of thermalisation makes it a suitable testbed of quantum chaos. Since there is no direct quantum analogue to classical ergodic hypothesis, thermalization in quantum sense remains a puzzling question. In his paper, Sredicki [8] showed that a bounded, isolated quantum system of many particles in a specific initial state will approach thermal equilibrium if the energy eigenfunctions which are superposed to form that state obey Berry's conjecture, where the process of approach to thermal equilibrium state is called thermalization [3]. Berry's conjecture is expected to hold only if the corresponding classical system is chaotic, and essentially states that the energy eigenfunctions behave as if they were gaussian random variables. The matrix elements of typical observables have these certain properties hold for a canonically quantized system whose classical phase space is fully chaotic at the energies of interest, and they are likely to hold at least approximately for a broader array of systems. This discussion illustrates how the structure of the eigenstates of a system obeying ETH influences the structure of operators when expressed in the energy eigenbasis, which is essentially what Wigner thought about the operator elements of quantum chaotic systems. In particular, the Eigenstate Thermalization Hypothesis (ETH) tells us how an isolated quantum many-body system thermalizes without any external heat bath.

6.1 Eigenstate thermalisation

Sredincki starts off with predicting the outcome of measuring the momentum of one specific atom in a gas of N hard spheres at some time t, after starting the entire system in a known quantum state. Let us now put our gas of N hard spheres into

some initial state specified by the momentum-space wave function:

$$\tilde{\psi}(\mathbf{P},0) = \Sigma_\alpha C_\alpha \tilde{\psi}(\mathbf{P}) \tag{6.1}$$

Here, α is the label of eigenfunctions. The initial wave function will evolve in time according to the Schrodinger equation:

$$\tilde{\psi}(\mathbf{P},t) = \Sigma_\alpha C_\alpha e^{-iU_\alpha t/h} \tilde{\psi}(\mathbf{P}). \tag{6.2}$$

Now the system is repeatedly prepared in the same initial state (specified by the C_α's), and the momentum of one atom is repeatedly measured after the same elapsed time t. The theoretical prediction for the fraction of atoms with momentum in a range d^3p around $\mathbf{p}$ is $f_{\rm QM}(\mathbf{p},t)d^3p$, where

$$\begin{aligned} f_{\rm QM}(\mathbf{p}_1,t) &= \int d^3p_2 \ldots d^3p_N \left|\widetilde{\psi}(\mathbf{P},t)\right|^2 \\ &= \sum_{\alpha\beta} C^*_\alpha C_\beta e^{i(U_\alpha - U_\beta)t/\hbar} \int d^3p_2 \ldots d^3p_N \, \widetilde{\psi}^*_\alpha(\mathbf{P}) \widetilde{\psi}_\beta(\mathbf{P}) \\ &= \sum_{\alpha\beta} C^*_\alpha C_\beta e^{i(U_\alpha - U_\beta)t/\hbar} \Phi_{\alpha\beta}(\mathbf{p}_1). \end{aligned} \tag{6.3}$$

Here,

$$\Phi_{\alpha\beta}(\mathbf{p_1}) = \int d^3p_1 .... d^3p_3 \tilde{\psi^*}_\alpha(\mathbf{p_1}) \tilde{\psi}_\beta(\mathbf{p_1}). \tag{6.4}$$

Berry's conjecture for the hard-sphere gas implies the following two-point correlation function in momentum space [7]:

$$\left\langle \widetilde{\psi}^*_\alpha(\mathbf{P}) \widetilde{\psi}_\beta(\mathbf{P}') \right\rangle_{\rm EE} = \delta_{\alpha\beta} \mathcal{N}^2_\alpha \hbar^{3N} \delta(\mathbf{P}^2 - 2mU_\alpha) \, \delta^{3N}_D(\mathbf{P} - \mathbf{P}'),$$

which obeys the normalization condition

$$\int d^3p_1 \Phi_{\alpha\beta}(\mathbf{p_1}) = \delta_{\alpha\beta}$$

To find $\langle \Phi_{\alpha\alpha}(\mathbf{p}_1) \rangle_{\rm EE}$, we set $\alpha = \beta$ and $\mathbf{P} = \mathbf{P}'$, and integrate over the momenta of particles 2 to N:

$$\langle \Phi_{\alpha\alpha}(\mathbf{p}_1) \rangle_{\rm EE} = \int d^3p_2 \ldots d^3p_N \left\langle |\widetilde{\psi}_\alpha(\mathbf{P})|^2 \right\rangle_{\rm EE}.$$

Substituting the correlation function:

$$\langle \Phi_{\alpha\alpha}(\mathbf{p}_1) \rangle_{\rm EE} = \int d^3p_2 \ldots d^3p_N \mathcal{N}^2_\alpha \hbar^{3N} \delta(\mathbf{P}^2 - 2mU_\alpha) \, \delta^{3N}_D(0).$$

The function $\delta^{3N}_D(0)$ is approximated by its value at the origin for a large box

$$\delta^{3N}_D(0) = \hbar^{-3N} \int_D d^{3N}X e^{i\mathbf{0}\cdot\mathbf{X}/\hbar} = \hbar^{-3N} \times \text{Volume} = \hbar^{-3N} L^{3N}.$$

Substituting this cancels the $\hbar^{3N}$ factor:

$$\langle \Phi_{\alpha\alpha}(\mathbf{p}_1) \rangle_{\rm EE} = \mathcal{N}^2_\alpha L^{3N} \int d^3p_2 \ldots d^3p_N \delta(\mathbf{P}^2 - 2mU_\alpha). \tag{6.5}$$

Determining the Normalization Constant $\mathcal{N}_\alpha$

The normalization condition for $\Phi_{\alpha\alpha}(\mathbf{p}_1)$ is:

$$\int d^3p_1 \Phi_{\alpha\alpha}(\mathbf{p}_1) = 1.$$

We enforce that the average of this integral in the EE is also 1:

$$\left\langle \int d^3p_1 \Phi_{\alpha\alpha}(\mathbf{p}_1) \right\rangle_{\text{EE}} = 1 \quad \Rightarrow \quad \int d^3p_1 \left\langle \Phi_{\alpha\alpha}(\mathbf{p}_1) \right\rangle_{\text{EE}} = 1.$$

Substituting equation (6.5):

$$\int d^3p_1 \left[\mathcal{N}_\alpha^2 L^{3N} \int d^3p_2 \dots d^3p_N \delta(\mathbf{P}^2 - 2mU_\alpha) \right] = 1.$$

Note that $\int d^3p_1 \int d^3p_2 \dots d^3p_N = \int d^{3N}\mathbf{P}$, so:

$$\mathcal{N}_\alpha^2 L^{3N} \int d^{3N}\mathbf{P} \delta(\mathbf{P}^2 - 2mU_\alpha) = 1.$$

Let us define the function $I_D(x)$ as the surface area of a sphere of radius $\sqrt{x}$ in D-dimensional momentum space:

$$I_D(x) \equiv \int d^D\mathbf{P} \delta(\mathbf{P}^2 - x) = \frac{(\pi x)^{D/2}}{\Gamma(D/2)x}.$$

Applying this to equation (6.5) with $D = 3N$ and $x = 2mU_\alpha$:

$$\int d^{3N}\mathbf{P} \delta(\mathbf{P}^2 - 2mU_\alpha) = I_{3N}(2mU_\alpha).$$

Thus, normalization becomes:

$$\mathcal{N}_\alpha^2 L^{3N} I_{3N}(2mU_\alpha) = 1 \quad \Rightarrow \quad \mathcal{N}_\alpha^{-2} = L^{3N} I_{3N}(2mU_\alpha)$$

Computing the integral

Substitute the normalization constant back into the starting equation (6.5). Note that $\mathcal{N}_\alpha^2 = 1/(L^{3N} I_{3N}(2mU_\alpha))$:

$$\langle \Phi_{\alpha\alpha}(\mathbf{p}_1) \rangle_{\text{EE}} = \frac{1}{L^{3N} I_{3N}(2mU_\alpha)} \cdot L^{3N} \int d^3p_2 \dots d^3p_N \delta(\mathbf{P}^2 - 2mU_\alpha).$$

The L^{3N} factors cancel:

$$\langle \Phi_{\alpha\alpha}(\mathbf{p}_1) \rangle_{\text{EE}} = \frac{1}{I_{3N}(2mU_\alpha)} \int d^3p_2 \dots d^3p_N \delta(\mathbf{P}^2 - 2mU_\alpha). \tag{6.6}$$

The integral $\int d^3p_2 \dots d^3p_N \delta(\mathbf{P}^2 - 2mU_\alpha)$ is over all momenta for particles 2 to N, with the constraint $\mathbf{p}_1^2 + \mathbf{p}_2^2 + \dots + \mathbf{p}_N^2 = 2mU_\alpha$.
Define $\mathbf{Q} = (\mathbf{p}_2, \dots, \mathbf{p}_N)$, a vector in $(3N-3)$-dimensional space. The constraint becomes:

$$\mathbf{Q}^2 = 2mU_\alpha - \mathbf{p}_1^2.$$

Therefore, the integral is the surface area of a sphere in $(3N-3)$-dimensional space with radius $\sqrt{2mU_\alpha - \mathbf{p}_1^2}$:

$$\int d^3p_2 \dots d^3p_N \delta(\mathbf{P}^2 - 2mU_\alpha) = \int d^{3N-3}\delta(\mathbf{Q}^2 - (2mU_\alpha - \mathbf{p}_1^2)) = I_{3N-3}(2mU_\alpha - \mathbf{p}_1^2). \tag{6.7}$$

Final Result

Substituting (6.7) into (6.5) yields the core result:

$$\langle \Phi_{\alpha\alpha}(\mathbf{p}_1)\rangle_{\mathrm{EE}} = \frac{I_{3N-3}(2mU_\alpha - \mathbf{p}_1^2)}{I_{3N}(2mU_\alpha)} = \frac{\Gamma(3N/2)}{\Gamma((3N-3))/2}\left(\frac{1}{2\pi m U_\alpha}\right)^{3/2}\left(1-\frac{\mathbf{p_1}}{2mU_\alpha}\right)^{(3N-5)/2}.$$

Now, setting $U_\alpha = \frac{3}{2}NKT_\alpha$ and taking the N very large, we get

$$\langle \Phi_{\alpha\alpha}(\mathbf{p}_1)\rangle_{\mathrm{EE}} = (2\pi mkT_\alpha)^{-3/2} e^{-\mathbf{p_1^2}/2mkT_\alpha}. \tag{6.8}$$

This is precisely the Maxwell-Boltzmann Distribution $f_{\mathrm{MB}}(\mathbf{p}_1, T_\alpha)$. That means if we calculate the average single-particle momentum distribution $\langle \Phi_{\alpha\alpha}(\mathbf{p_1})\rangle_{\mathrm{EE}}$ for an eigenstate within this random eigenstate ensemble, you obtain the microcanonical distribution, which becomes the Maxwell-Boltzmann (MB) distribution in the thermodynamic limit ($N \to \infty$) [7]. This distribution can be Maxwell–Boltzmann, Bose–Einstein, or Fermi–Dirac, depending on whether the energy eigenfunctions are nonsymmetric, completely symmetric, or completely antisymmetric functions of the N particle positions. This shows us that individual quantum energy eigenstates already encode thermodynamic properties. It is important to note that to prepare a system in a state with a perfectly definite energy U_α (i.e., a energy eigenstate), we must measure its energy with perfect precision. The energy uncertainty ΔE must be zero. The time-energy uncertainty principle states that such a perfect measurement requires an infinite amount of time. More precisely, to resolve two energy levels separated by a gap δ, you need a measurement time on the order of $\tau \sim \hbar/\delta$ – known as the Heisenberg time. Although it is unphysical to work with a single energy eigenstate, it is an instructive exercise since a generic, physically preparable initial state (e.g., all atoms in one corner) is not an energy eigenstate. Instead, it is a superposition of many energy eigenstates! [7]

Calculating the flucation of of the single-particle momentum distribution

In this section, we prove that the fluctuations of the single-particle momentum distribution $\Phi_{\alpha\alpha}(\mathbf{p_1})$ around its thermal value are exponentially small in the number of particles N. This means that for a typical eigenstate, $\Phi_{\alpha\alpha}(\mathbf{p_1}) \approx f_{\mathrm{MB}}(\mathbf{p_1}, T\alpha)$ is an excellent approximation. To approximate this, We need to quantify how much $\Phi_{\alpha\beta}(\mathbf{p}_1)$ varies from one random eigenstate to another. The standard measure for this is the variance.

$$[\Delta\Phi_{\alpha\beta}(\mathbf{p}_1)]^2 \simeq \left\langle |\Phi_{\alpha\beta}(\mathbf{p}_1)|^2\right\rangle_{\mathrm{EE}} - \left|\langle \Phi_{\alpha\beta}(\mathbf{p}_1)\rangle_{\mathrm{EE}}\right|^2 \tag{6.9}$$

From the definition (3.6):

$$\Phi_{\alpha\beta}(\mathbf{p}_1) \equiv \int d^3p_2 \ldots d^3p_N\, \widetilde{\psi}^*_\alpha(\mathbf{P})\widetilde{\psi}_\beta(\mathbf{P})$$

Therefore, the square of the absolute value this function is given by:

$$|\Phi_{\alpha\beta}(\mathbf{p}_1)|^2 = \left(\int d^3p_2 \ldots d^3p_N\, \widetilde{\psi}^*_\alpha(\mathbf{P})\widetilde{\psi}_\beta(\mathbf{P})\right)\left(\int d^3p'_2 \ldots d^3p'_N\, \widetilde{\psi}^*_\alpha(\mathbf{P}')\widetilde{\psi}_\beta(\mathbf{P}')\right)^*$$

$$= \iint d^3p_2 \dots d^3p_N \, d^3p'_2 \dots d^3p'_N \, \widetilde{\psi}^*_\alpha(\mathbf{P})\widetilde{\psi}_\beta(\mathbf{P})\widetilde{\psi}_\alpha(\mathbf{P}')\widetilde{\psi}^*_\beta(\mathbf{P}'),$$

where $\mathbf{P} = (\mathbf{p}_1, \mathbf{p}_2, \dots, \mathbf{p}_N)$ and $\mathbf{P}' = (\mathbf{p}_1, \mathbf{p}'_2, \dots, \mathbf{p}'_N)$. Now we take the eigenstate ensemble average:

$$\left\langle |\Phi_{\alpha\beta}(\mathbf{p}_1)|^2 \right\rangle_{\text{EE}} = \iint d^3p_2 \dots d^3p_N \, d^3p'_2 \dots d^3p'_N \, \left\langle \widetilde{\psi}^*_\alpha(\mathbf{P})\widetilde{\psi}_\beta(\mathbf{P})\widetilde{\psi}_\alpha(\mathbf{P}')\widetilde{\psi}^*_\beta(\mathbf{P}') \right\rangle_{\text{EE}}$$

We recall that Berry's conjecture asserts that the eigenstate ensemble is gaussian, so that all multipoint correlation functions are given in terms of the two-point correlation function known as the Wick's theorem e.g.,:

$$\left\langle \widetilde{\psi}^*_\alpha(\mathbf{P})\widetilde{\psi}_\beta(\mathbf{P})\widetilde{\psi}_\alpha(\mathbf{P}')\widetilde{\psi}^*_\beta(\mathbf{P}') \right\rangle_{\text{EE}} = \left\langle \widetilde{\psi}^*_\alpha(\mathbf{P})\widetilde{\psi}_\beta(\mathbf{P}) \right\rangle_{\text{EE}} \left\langle \widetilde{\psi}_\alpha(\mathbf{P}')\widetilde{\psi}^*_\beta(\mathbf{P}') \right\rangle_{\text{EE}}$$

$$+ \left\langle \widetilde{\psi}^*_\alpha(\mathbf{P})\widetilde{\psi}_\alpha(\mathbf{P}') \right\rangle_{\text{EE}} \left\langle \widetilde{\psi}_\beta(\mathbf{P})\widetilde{\psi}^*_\beta(\mathbf{P}') \right\rangle_{\text{EE}} + \left\langle \widetilde{\psi}^*_\alpha(\mathbf{P})\widetilde{\psi}^*_\beta(\mathbf{P}') \right\rangle_{\text{EE}} \left\langle \widetilde{\psi}_\beta(\mathbf{P})\widetilde{\psi}_\alpha(\mathbf{P}') \right\rangle_{\text{EE}}$$

From the two-point correlation function (Eq. 2.9):

$$\left\langle \widetilde{\psi}^*_\alpha(\mathbf{P})\widetilde{\psi}_\beta(\mathbf{P}') \right\rangle_{\text{EE}} = \delta_{\alpha\beta} \, \mathcal{N}^2_\alpha \, h^{3N} \delta(\mathbf{P}^2 - 2mU_\alpha) \, \delta^{3N}_D(\mathbf{P} - \mathbf{P}')$$

This implies that cross terms like $\left\langle \widetilde{\psi}^*_\alpha(\mathbf{P})\widetilde{\psi}_\beta(\mathbf{P}) \right\rangle_{\text{EE}}$ vanish for $\alpha \neq \beta$. For the diagonal case ($\alpha = \beta$) we are interested in, the first and third terms vanish, leaving only the second term:

$$\left\langle \widetilde{\psi}^*_\alpha(\mathbf{P})\widetilde{\psi}_\beta(\mathbf{P})\widetilde{\psi}_\alpha(\mathbf{P}')\widetilde{\psi}^*_\beta(\mathbf{P}') \right\rangle_{\text{EE}} = \left\langle \widetilde{\psi}^*_\alpha(\mathbf{P})\widetilde{\psi}_\alpha(\mathbf{P}') \right\rangle_{\text{EE}} \left\langle \widetilde{\psi}_\beta(\mathbf{P})\widetilde{\psi}^*_\beta(\mathbf{P}') \right\rangle_{\text{EE}}$$

Substituting the explicit form, we have:

$$= \left[\mathcal{N}^2_\alpha \, h^{3N} \delta(\mathbf{P}^2 - 2mU_\alpha) \, \delta^{3N}_D(\mathbf{P} - \mathbf{P}') \right] \left[\mathcal{N}^2_\beta \, h^{3N} \delta(\mathbf{P}^2 - 2mU_\beta) \, \delta^{3N}_D(\mathbf{P} - \mathbf{P}') \right]$$

$$= \mathcal{N}^2_\alpha \mathcal{N}^2_\beta \, h^{6N} \delta(\mathbf{P}^2 - 2mU_\alpha) \, \delta(\mathbf{P}^2 - 2mU_\beta) \, \left[\delta^{3N}_D(\mathbf{P} - \mathbf{P}') \right]^2 .$$

Now using the substitution rule:

$$\left[\delta^{3N}_D(\mathbf{P} - \mathbf{P}') \right]^2 \to (L/h)^{3N} \delta^{3N}_D(\mathbf{P} - \mathbf{P}').$$

Thus, we have:

$$\left\langle |\Phi_{\alpha\beta}(\mathbf{p}_1)|^2 \right\rangle_{\text{EE}} = \mathcal{N}^2_\alpha \mathcal{N}^2_\beta \, h^{6N} (L/h)^{3N} \iint d^3p_2 \dots d^3p_N \, d^3p'_2 \dots d^3p'_N$$

$$\delta(\mathbf{P}^2 - 2mU_\alpha) \, \delta(\mathbf{P}^2 - 2mU_\beta) \, \delta^{3N}_D(\mathbf{P} - \mathbf{P}').$$

The Final Result

The second term in the fluctuation, $\left| \langle \Phi_{\alpha\beta}(\mathbf{p}_1) \rangle_{\text{EE}} \right|^2$, is of order $\langle \Phi_{\alpha\alpha} \rangle \langle \Phi_{\beta\beta} \rangle$ and is negligible compared to the first term for the purpose of this calculation. Therefore, the fluctuation is dominated by the first term:

$$[\Delta\Phi_{\alpha\beta}(\mathbf{p}_1)]^2 \simeq \mathcal{N}^2_\alpha \mathcal{N}^2_\beta \, L^{3N} h^{3N} \iint d^3p_2 \dots d^3p_N \, d^3p'_2 \dots d^3p'_N$$

$$\delta(\mathbf{P}^2 - 2mU_\alpha)\,\delta(\mathbf{P}'^2 - 2mU_\beta)\,\delta_D^{3N}(\mathbf{P} - \mathbf{P}').$$

Replacing $\delta_D^{3N}(\mathbf{P} - \mathbf{P}')$ by its maximum value $(L/h)^{3N}$ everywhere, we get the following approximation,

$$[\Delta\Phi_{\alpha\beta}(\mathbf{p}_1)]^2 \left\langle \Phi_{\alpha\alpha}(\mathbf{p}_1)\right\rangle_{\mathrm{EE}} \left\langle \Phi_{\beta\alpha}(\mathbf{p}_1)\right\rangle_{\mathrm{EE}}.$$

For the seek of a better approximation to $[\Delta\Phi_{\alpha\beta}(\mathbf{p}_1)]^2$, We approximate $\delta_D^{3N}(\mathbf{P}-\mathbf{P}')$ with a gaussian:

$$\delta_D^{3N}(\mathbf{P} - \mathbf{P}') \simeq (L/h)^{3/2} \exp[-(\mathbf{P} - \mathbf{P}')^2 L^2/4\pi\hbar^2].$$

This is a natural choice. The exact function is sharply peaked at $\mathbf{P} = \mathbf{P}'$ and decays away from it. A Gaussian is the simplest function that captures this behavior with the correct width and normalization. Also this function is significant only when $|\mathbf{P} - \mathbf{P}'|\hbar/L$, which is an incredibly small momentum difference for a macroscopic box (L is large)

$$\begin{aligned}[\Delta\Phi_{\alpha\alpha}(\mathbf{p}_1)]^2 = \mathcal{N}_\alpha^4 (L\hbar)^{3N}(L/h)^{3N} \int d^3p_2 \ldots d^3p_N d^3p_2' \ldots d^3p_N' \\ \times \delta(\mathbf{P}^2 - 2mU_\alpha)\delta(\mathbf{P}'^2 - 2mU_\alpha) \exp\left[-(\mathbf{P} - \mathbf{P}')^2 L^2/(4\pi\hbar^2)\right].\end{aligned} \tag{6.10}$$

In low density ($Na^3 \ll L^3$), setting $\alpha = \beta$ and taking the large N limit,

$$\Delta\Phi_{\alpha\alpha}(\mathbf{p_1}) = \mathcal{O}(1) N^{1/2} e^{-3N/4} (L/\lambda_\alpha)^{-(3N-6)/2} e^{\mathbf{p_1}^2/4\,m\,k\,T_\alpha} f_{MB}(\mathbf{p_1}, T_\alpha). \tag{6.11}$$

Since we have $\lambda_\alpha \ll L$, we see that the fluctuations in $\Phi_{\alpha\alpha}(\mathbf{p_1})$ about $f_{MB}(\mathbf{p_1}, t)$ are negligibly small for large N. That is to say, an energy eigenstate which satisfies Berry's conjecture predicts a thermal distribution for the momentum of a single constituent particle. We will refer to this remarkable phenomenon as eigenstate thermalization.

6.2 Observables in ETH

In his paper [8], Srednicki proposed an alternative approach to ETH involving an ansatz of the hermitian operators corresponding to an observable of interests. We start off by making two assumption about the system:

1. If any two sums of equal numbers of energy eigenvalues are equal,

$$E_{\alpha_1} + \cdots + E_{\alpha_n} = E_{\beta_1} + \cdots + E_{\beta_n}, \tag{6.12}$$

then $\{\beta_1, \ldots, \beta_n\}$ is a permutation of $\{\alpha_1, \ldots, \alpha_n\}$; that is, the corresponding eigenstates are the same for both sides. In particular, $E_\alpha = E_\beta$ implies that $|\alpha\rangle = |\beta\rangle$, so that all the energy eigenvalues are nondegenerate. This assumption is expected to hold in general for a quantized chaotic system in which all unitary symmetries have been removed by changing the potential well such as by putting the system in an irregularly shaped box.

2. Our second assumption is the crucial one. Let A be a Hermitian operator corresponding to an observable of interest that is a smooth, $\hbar$-independent function of the classical coordinates and momenta. We assume that the matrix elements of A in the energy eigenstate basis take the form [7], [20]

$$A_{\alpha\beta} = \mathcal{A}(E)\,\delta_{\alpha\beta} + e^{-S(E)/2}\,f(E,\omega)\,R_{\alpha\beta}. \tag{6.13}$$

First, for notational convenience we define

$$E \equiv \frac{1}{2}(E_\alpha + E_\beta), \qquad \omega \equiv E_\alpha - E_\beta \tag{6.14}$$

$S(E)$ is the thermodynamic entropy at energy E, given by

$$e^{S(E)} \equiv \sum_\alpha \delta_\epsilon(E - E_\alpha), \tag{6.15}$$

where the delta function ensures the monotonicity of $S(E)$. Also, $\mathcal{A}(E)$ and $f(E,\omega)$ are smooth function of energy. In addition, we assume $f(E,\omega)$ is a real and even function of ω with $R^*_{\alpha\beta} = R_{\alpha\beta}$, which guarantees that A is a hermitian operator. The function $\mathcal{A}(E)$ is related canonical ensemble avergae $\langle A\rangle_T$ by the following expression

$$\mathcal{A}(E) = \langle A\rangle_T + \mathcal{O}(N^{-1}) + \mathcal{O}(e^{-S/2}) \tag{6.16}$$

The last two terms are negligible for systems with large degrees of freedom. The energy bandwidth W of $A_{\alpha\beta}$ is given by, [8]

$$W = \frac{\int_{-\infty}^{\infty} d\omega\,|f(\omega,E)|^2}{|f(0,E)|^2} \tag{6.17}$$

Deutsch [20] discussed two key assumptions for ETH which explains why a isolated quantum chaotic system thermalises. His idea was to seperate the behaviour of diagonal and off diagonal elements of the local operators (operators acting only on a few degrees of freedom) acting on such system in the context of ETH ansatz.

Conjecture 1

This conjecture describes the diagonal elements of the ETH ansatz which are equivalent to the expectation values.

$$O_{ii} = \langle \hat{O}\rangle_{micro,E} + \Delta_i \tag{6.18}$$

where Δ_i has zero mean and Δ_i^2 has a magnitude of order

$$\langle \hat{O}^2\rangle_{\text{micro},E_i}\, e^{-S(E)} \;\propto\; \langle \hat{O}^2\rangle_{\text{micro},E_i}\, e^{-\text{const}\cdot N}.$$

The sole fact that O_{ii} varies very little among neighboring eigenstates implies that it must be equal to the microcanonical result, because $\langle O_{ii}\rangle$, averaged over a small energy window, must give the microcanonical average. Thus, the ETH is really a statement about the small size of fluctuations of expectation values between eigenstates. It says that the microcanonical average for non-integrable systems, for most purposes, does not need to be taken at all, and a single eigenstate can be used. However, when specified the size of the Δ_i, Δ_i is exponentially small in N. But when the

Hilbert space itself is exponentially large, and we have not specified the distribution of the Δ_i. It is therefore possible that an exponentially small fraction of eigenstates do not obey the ETH and have expectation values that differ significantly from the microcanonical ensemble. This scenario is referred to as the *weak ETH*.

In the figures (6.3) and (6.1), we have illustarted the diagonal and off diagonal elements of x_1^2 operators of a system of low ($n = 2, 3$) degrees of freedom. Previously, we have showed that these two systems are quantum chaotic by numerically calculating their quantum lyapunov exponents. To understand the thermalization of these operators, we now check their consistency with ETH ansatz. The relative fluctuation of the diagonal elements of x_1^2 operator for the case of two and three coupled harmonic oscillators (with a non-linear coupling) are ~ 0.21 and ~ 0.37, respectively. The relative fluctuation appears to be higher for three oscillators because we have used different scale for the energy in the $x-$ axis. Since the relative fluctuation is small, we can conclude that the variation from microcanonical average of the diagonal elements of the ETH ansatz is also small. Therefore, the systems demonstrate weak ETH.

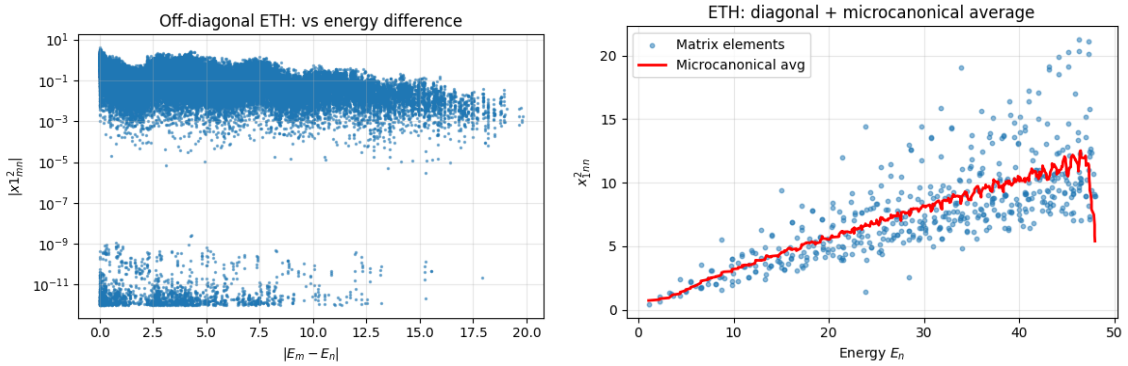

Figure 6.1: Diagonal and off diagonal elements of x_1^2 operator of system of two coupled harmonic oscillators with non-linear coupling

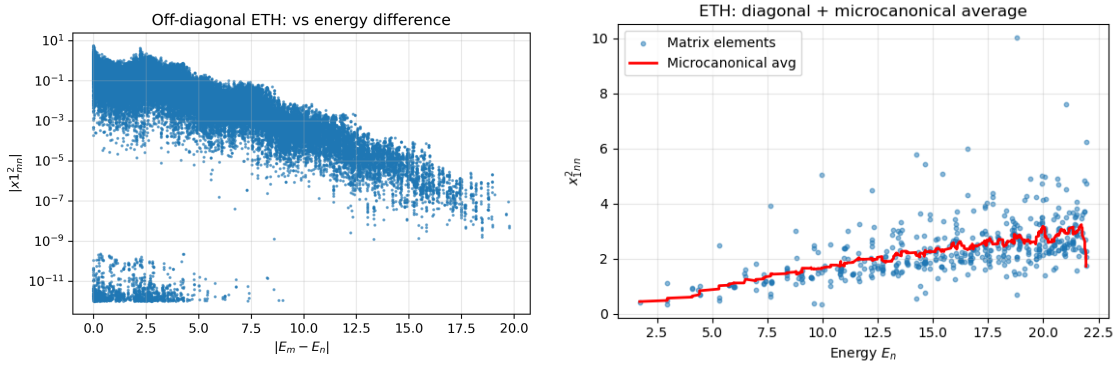

Figure 6.2: Diagonal and off diagonal elements of x_1^2 operator of system of three coupled harmonic oscillators with non-linear coupling

On the other hand, if one asserts that O_{ii} is always very close to the microcanonical value for *all* i, then this corresponds to the *strong ETH* [20]. In other words, suppose that we have an isolated system, which we partition into two subsystems:

a system of interest A and the remainder B, which can be regarded as a bath for A. We consider initializing the system out of equilibrium in an arbitrary product state of A and B. If all such initial states lead to thermalization of subsystem A, then this requires that the ETH holds. Moreover, it requires that the ETH holds in the *strong* sense, namely that all energy eigenstates are thermal. If this were not the case, there would exist certain initial product states whose time evolution would not lead to thermalization.

Conjecture 2:

This conjecture descirbes the behaviour of off diagonal elements of ETH matrix ansatz and thus provides to additional understanding of the dynamics of correlation functions and how those operators approach thermal equilibrium. For $i \neq j$, we have $O_{ij} = \Delta_{ij}$, where Δ_{ij} appears stochastic and follows the same distribution as (6.18). These elements are therefore extremely small. Because the statistics of this quantity should vary smoothly as a function of E_i and E_j, we can attempt to quantify this for a single system by performing averages over nearby energy levels of i and j, denoted by $\langle \cdots \rangle_n$. We write,

$$\langle |O_{ij}|^2 \rangle = \langle \Delta_i \rangle^2 F(E_i, E_j) \tag{6.19}$$

with Δ_i the fluctuation in the O_{ii} described in (6.18). $F(E_i, E_j)$ is a function of order unity when $E_i = E_j$, and it goes to zero as $|E_i - E_j|$ becomes large. Defining

$$E_{ij} \equiv \frac{E_i + E_j}{2},$$

(6.19) can be written more symmetrically as

$$\langle |O_{ij}|^2 \rangle_n = \langle \hat{O}^2 \rangle_{\text{micro},\, E_{ij}}\, f(E_{ij}, E_i - E_j)\, e^{-S(E_{ij})/2} \tag{6.20}$$

where

$$f(E_{ij}, E_i - E_j) = F(E_i, E_j),$$

is a smooth function that goes to zero when $|E_i - E_j|$ becomes large. The O_{ij} cannot, in general, be zero. For example, if we consider an operator $\hat{A}$ such that $\hat{O} = \hat{A}^2$, then

$$\langle E_i | (\hat{A} - A_{ii})^2 | E_i \rangle = \sum_{j \neq i} |A_{ij}|^2 \tag{6.21}$$

The left-hand side is non-negative. The right-hand side contains the off-diagonal matrix elements. This implies that the off-diagonal matrix elements cannot all vanish; instead, they must be distributed in such a way that their collective contribution remains finite. Otherwise, the hypothesis would be violated. Now, we can interpret the plots for off-diagonal elements of ETH ansatz given in (6.3) and (6.1). We find that these elements create band-like structures since $f(\omega, E)$ is a smooth function. In addition, local operators only interact with states that have very small energy difference. Therefore, the energy fluctuation remains very small. Thus the contribute of the off diagonal ETH matrix elements contribute is finite. In addition, we see that in figure (6.1) and (6.3), the $\langle n | x_1^2 | m \rangle$ elements are vanishingly small when ω becomes large. This also reflects the consistency with ETH. In thermodynamic limit, we can expect full emergence of ETH behavior.

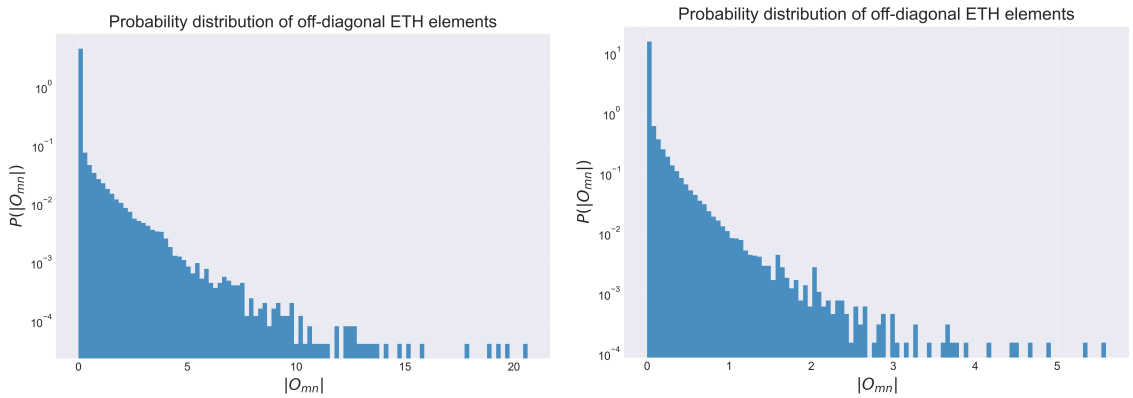

Figure 6.3: Probability distribution associated with off-diagonal elements of ETH anzats for a system of two CHO (left) and three CHO (right). These histograms show that the distribution of off-diagonal elements exhibit exponential decay rather than Gaussian-like matrix like behavior. This implies that these systems satisfy weak ETH.

An intuitive way of understanding the ETH, is to think of dividing the system into a smaller and larger region. Even for an energy eigenstate, we can then think of the larger region as acting as a thermal 'bath' for the smaller region. The ETH says that for the system in any energy eigenstate, measurements on only the smaller region are equivalent to a system at the appropriate equivalent temperature which is very similar to classical thermalisation. This aspect of classical thermalisation has a strong connection with ergodic hypothesis. However, we cannot have a ergodic hypothesis in quantum mechanics since the idea of phase space is meaningless in the Hilbert space construction. Therefore, ETH serves a similar purpose as ergodicity in quantum mechanics, in connecting microscopic dynamics to statistical mechanics [20].

6.3 ETH and Thermalisation

In this section, we study how thermalisation emerges in many-body quantum systems within the standard ETH framework. We begin by considering the long-time average of an observable $\hat{O}$. For an initial state evolving under unitary dynamics, the long-time average is given by

$$\langle \hat{O} \rangle = \lim_{t_0 \to \infty} \frac{1}{t_0} \int_0^{t_0} dt\, O(t) = \sum_m |C_m|^2 O_{mm} = \mathrm{Tr}\left[\hat{\rho}_{\mathrm{DE}}\, \hat{O}\right]. \tag{6.22}$$

This shows that, at long times, only the diagonal elements of the operator in the energy eigenbasis contribute. The corresponding density matrix is called the diagonal ensemble and is defined as

$$\hat{\rho}_{\mathrm{DE}} = \lim_{t_0 \to \infty} \frac{1}{t_0} \int_0^{t_0} \hat{\rho}(t)\, dt = \sum_m |C_m|^2 |m\rangle\langle m|. \tag{6.23}$$

This density matrix is diagonal because it contains no off-diagonal terms, meaning that there is no coherence between different energy eigenstates after long-time av-

eraging.

According to statistical mechanics, the expectation value of an observable in equilibrium is given by

$$O_{\mathrm{ME}} = \mathrm{Tr}\left[\hat{\rho}_{\mathrm{ME}}\,\hat{O}\right], \tag{6.24}$$

where $\hat{\rho}_{\mathrm{ME}}$ is the microcanonical ensemble density matrix. The key question is why the long-time average $\langle\hat{O}\rangle$ agrees with this thermal prediction. To understand this, we consider an initial state $|\psi\rangle = \sum_m C_m|m\rangle$ with a narrow energy distribution. The energy fluctuations of this state are given by

$$\delta E = \sqrt{\langle\psi|\hat{H}^2|\psi\rangle - \langle\psi|\hat{H}|\psi\rangle^2}. \tag{6.25}$$

If these fluctuations are small, then the coefficients $|C_m|^2$ are strongly peaked around the average energy $\langle E\rangle$. In this case, we can use the ETH assumption that the diagonal matrix elements are smooth functions of energy, i.e., $O_{mm} \approx O(E_m)$.
Since $O(E)$ is a smooth function, we can expand it around the average energy $\langle E\rangle$ as

$$O(E_m) \approx O(\langle E\rangle) + (E_m - \langle E\rangle)\left.\frac{dO}{dE}\right|_{\langle E\rangle} + \frac{1}{2}(E_m - \langle E\rangle)^2\left.\frac{d^2O}{dE^2}\right|_{\langle E\rangle}. \tag{6.26}$$

Substituting this expansion into the expression for the long-time average and using the fact that the first-order term vanishes, we obtain

$$\overline{O} \approx O(\langle E\rangle) + \frac{1}{2}(\delta E)^2 O''(\langle E\rangle). \tag{6.27}$$

Since the energy fluctuations δE are small (subextensive), the second term is negligible for large systems. Therefore,

$$\langle\hat{O}\rangle \approx O(\langle E\rangle). \tag{6.28}$$

On the other hand, in the microcanonical ensemble, the observable is also given by a smooth function of energy evaluated at $\langle E\rangle$, so that

$$O(\langle E\rangle) \approx O_{\mathrm{ME}}. \tag{6.29}$$

Thus, we arrive at the important result

$$\langle\hat{O}\rangle \approx O_{\mathrm{ME}}. \tag{6.30}$$

This shows that, for an initial state with a narrow energy distribution, the long-time expectation value of an observable agrees with the prediction of statistical mechanics. Remarkably, this result does not depend on the detailed form of the coefficients C_m, but only on the fact that they are concentrated within a small energy window.

This mechanism is fundamentally different from the usual equivalence of ensembles in statistical mechanics. Here, the system remains in a pure quantum state and evolves unitarily, yet the expectation values of observables behave as if the system were in thermal equilibrium. Therefore, within a narrow energy window, a non-equilibrium pure state effectively thermalises, even though the underlying quantum state itself remains non-thermal.

Chapter 7

Relating Eigenstate Thermalisation and Information Scrambling

In this section, we investigate a possible connection between dynamical quantum chaos and eigenstate thermalisation. The aim is to examine whether the exponential growth associated with dynamical quantum chaos, as predicted from the semiclassical behaviour of the four-point correlation function, can be inferred from the fine structure of energy eigenstates described by the Eigenstate Thermalization Hypothesis (ETH). The motivation for trying to see a possible connection is quite simple: the non equilibrium nature of quantum thermalization is often associated with quantum chaos. In particular, quantum chaos describes how the system evolve the available hilbert space. In their work, Murthy and Srednicki [24] showed that the well-known bound on the growth rate of the out-of-time-ordered four-point correlator in chaotic many-body quantum systems, originally derived in [18], follows directly from the general structure of operator matrix elements in systems that satisfy ETH. In that analysis, the authors employed a modified ETH ansatz based on the framework developed by Foini and Kurchan [23], which incorporates exponentially small correlations between different random variables appearing in the ansatz and is different Wick's theorem which assumes random variables are independent variables. Their treatment makes use of a single-operator representation of the OTOC. The inspiration of the problem statement of this paper comes from their work.

In this thesis we employ the standard ETH ansatz as formulated in [8] and consider the two-operator form of the OTOC as given in [19], [25]. This formulation allows us to examine more directly whether the dynamical manifestation of quantum chaos, characterised by the early-time exponential growth of the OTOC, can be captured solely from the statistical structure of operator matrix elements encoded in the standard ETH framework. In particular, the use of the two-operator form of the OTOC allows us to probe the causal structure of operator growth and information scrambling, providing additional insight into the relationship between dynamical chaos and the fine structure of energy eigenstates. We are particularly interested to find out whether the fine structure of the eigenstates and quantum observables of chaotic system predict quantum information scrambling.

7.1 Four-Point Correlation Function and ETH Analysis

We begin by defining the four-point correlation function in terms of position and momentum operators

$$F(t) = \langle\, x(t)\, p(0)\, x(t)\, p(0)\rangle_\beta, \tag{7.1}$$

where the thermal expectation value is defined as

$$\langle O\rangle_\beta = \frac{1}{Z}\mathrm{Tr}(e^{-\beta H}O), \qquad Z = \mathrm{Tr}(e^{-\beta H}). \tag{7.2}$$

Also,

$$C(t) = 2\left(1 - \mathrm{Re}\{F(t)\}\right). \tag{7.3}$$

To evaluate this correlator we expand it in the energy eigenbasis of the Hamiltonian. Let the Hamiltonian eigenstates satisfy

$$H|n\rangle = E_n|n\rangle, \tag{7.4}$$

with the completeness relation

$$I = \sum_n |n\rangle\langle n|. \tag{7.5}$$

Using this relation the correlator becomes

$$F(t) = \frac{1}{Z}\sum_\alpha e^{-\beta E_\alpha}\langle\alpha|x(t)\, p(0)\, x(t)\, p(0)|\alpha\rangle. \tag{7.6}$$

Next we insert identities between each pair of operators. This yields

$$F(t) = \frac{1}{Z}\sum_{a,b,c,d} e^{-\beta E_a}\langle a|x(t)|b\rangle\, \langle b|p(0)|c\rangle\, \langle c|x(t)|d\rangle\, \langle d|p(0)|a\rangle \tag{7.7}$$

Using the Heisenberg evolution of the momentum operator

$$x(t) = e^{iHt}\, x\, e^{-iHt}, \tag{7.8}$$

we obtain

$$\langle a|x(t)|b\rangle = e^{i(E_a - E_b)t}\, x_{ab}. \tag{7.9}$$

Substituting this expression into the correlator gives

$$F(t) = \frac{1}{Z}\sum_{a,b,c,d} e^{-\beta E_a} e^{i(E_a - E_b + E_c - E_d)t} x_{ab} p_{bc} x_{cd} p_{da}. \tag{7.10}$$

To analyse the structure of these matrix elements we now apply the Eigenstate Thermalization Hypothesis (ETH). According to ETH the matrix elements of an operator take the form

$$O_{mn} = O(\bar{E})\delta_{mn} + e^{-S(\bar{E})/2} f(\bar{E}, \omega) R_{mn}, \tag{7.11}$$

where

$$\bar{E} = \frac{E_m + E_n}{2}, \qquad \omega = E_m - E_n. \tag{7.12}$$

Here, R_{mn} is a random variable with zero mean and unit variance.

Applying the ETH ansatz to the operators p and x we obtain

$$p_{ab} = p(\bar{E}_{ab})\delta_{ab} \; + \; e^{-S(\bar{E}_{ab})/2} f_p(\bar{E}_{ab}, \omega_{ab}) R^{(p)}_{ab}, \tag{7.13}$$

$$x_{bc} = x(\bar{E}_{bc})\delta_{bc} \; + \; e^{-S(\bar{E}_{bc})/2} f_x(\bar{E}_{bc}, \omega_{bc}) R^{(x)}_{bc}, \tag{7.14}$$

$$p_{cd} = p(\bar{E}_{cd})\delta_{cd} \; + \; e^{-S(\bar{E}_{cd})/2} f_p(\bar{E}_{cd}, \omega_{cd}) R^{(p)}_{cd}, \tag{7.15}$$

$$x_{da} = x(\bar{E}_{da})\delta_{da} \; + \; e^{-S(\bar{E}_{da})/2} f_x(\bar{E}_{da}, \omega_{da}) R^{(x)}_{da}. \tag{7.16}$$

Substituting these expressions into the four-point function we find two contributions: one from purely diagonal terms of ETH and another contribution from off-diagonal terms of ETH. The fully diagonal terms are:

$$F \sim \frac{1}{Z} \sum_a \, e^{-\beta E_a} x_{aa} \, p_{aa} \, x_{aa} \, p_{aa} \tag{7.17}$$

Since this expression is constant, we conclude that the diagonal terms have $O(1)$ contribution to the time evolution of four point correlation function. We see that it does not involve any oscillatory terms and exponential suppression. So, we will only work with the off-diagonal terms to find interesting results. The off-diagonal terms have time dependent complex phase factors responsible for oscillation. Their contribution to four point correlation function is given by,

$$F(t) \sim \frac{1}{Z} \sum_{a,b,c,d} e^{-\beta E_a} e^{i(E_a - E_b + E_c - E_d)t} e^{-2S} f_p f_x f_p f_x R^{(p)}_{ab} R^{(x)}_{bc} R^{(p)}_{cd} R^{(x)}_{da}. \tag{7.18}$$

To evaluate the average over random variables we assume standard Gaussian statistics and use Wick's theorem

$$\langle R_{ab} R_{bc} R_{cd} R_{da} \rangle = \langle R_{ab} R_{bc} \rangle \langle R_{cd} R_{da} \rangle + \langle R_{ab} R_{cd} \rangle \langle R_{bc} R_{da} \rangle + \langle R_{ab} R_{da} \rangle \langle R_{bc} R_{cd} \rangle. \tag{7.19}$$

Using the contraction rule

$$\langle R_{ij} R_{kl} \rangle = \delta_{ik} \delta_{jl}, \tag{7.20}$$

we obtain non–zero contributions when

$$a = c, \qquad b = d. \tag{7.21}$$

Thus the four–index sum reduces to

$$F(t) \sim \frac{1}{Z} e^{-2S} \sum_{a,b} e^{-\beta E_a} e^{i 2 \omega_{ab} t} |f_p(\bar{E}, \omega)|^2 |f_x(\bar{E}, \omega)|^2. \tag{7.22}$$

For systems with many degrees of freedom the sums can be replaced by integrals over the density of states

$$\sum_a \to \int dE_a \rho(E_a). \tag{7.23}$$

At this stage, we no longer deal with individual energy eigenstates. Instead, we focus on the physical properties of the eigenstates within a small energy window $[E, E+\Delta E]$. This coarse-graining procedure is justified because chaotic eigenstates effectively "forget" their initial conditions, allowing their properties to be described statistically. Now we introduce the variables

$$\bar{E} = \frac{E_a + E_b}{2}, \qquad \omega = E_a - E_b. \tag{7.24}$$

This implies

$$E_a = \bar{E} + \frac{\omega}{2}, \qquad E_b = \bar{E} - \frac{\omega}{2}. \tag{7.25}$$

The density of states scales exponentially with entropy

$$\rho(E) \sim e^{S(E)}. \tag{7.26}$$

Therefore

$$\rho(\bar{E} + \omega/2)\rho(\bar{E} - \omega/2) = \exp\left[S(\bar{E} + \omega/2) + S(\bar{E} - \omega/2)\right]. \tag{7.27}$$

We now expand the entropy around $\bar{E}$

$$S(\bar{E} \pm \omega/2) = S(\bar{E}) \pm \frac{\omega}{2} S'(\bar{E}) + \frac{\omega^2}{8} S''(\bar{E}) + \cdots. \tag{7.28}$$

Adding the two expansions gives

$$S(\bar{E} + \omega/2) + S(\bar{E} - \omega/2) = 2S(\bar{E}) + \frac{\omega^2}{4} S''(\bar{E}). \tag{7.29}$$

Using the thermodynamic relation

$$S''(E) = -\frac{\beta^2}{C}, \tag{7.30}$$

we obtain

$$F(t) \sim \frac{1}{Z} \int d\bar{E} d\omega |f_p(\bar{E}, \omega)|^2 |f_x(\bar{E}, \omega)|^2 \exp\left[-\beta \bar{E} - \frac{\beta^2 \omega^2}{4C}\right] e^{i2\omega t}. \tag{7.31}$$

Defining the spectral function

$$G(\omega) = \int d\bar{E} |f_p(\bar{E}, \omega)|^2 |f_x(\bar{E}, \omega)|^2 e^{-\beta \bar{E}}, \tag{7.32}$$

The correlator can be written as

$$F(t) = \int_{-\infty}^{\infty} d\omega \, \tilde{G}(\omega) e^{i2\omega t}, \tag{7.33}$$

with

$$\tilde{G}(\omega) = G(\omega)e^{-\beta^2\omega^2/4C} \tag{7.34}$$

In the semiclassical regime the OTOC grows exponentially

$$F(t) \sim e^{2\lambda t}. \tag{7.35}$$

Since the exponential growth of the OTOC is valid only in the pre-scrambling regime, the integration is restricted to the interval

$$0 \leq t \leq t^*,$$

where t^* denotes the scrambling time. Beyond this timescale the growth saturates and the exponential approximation no longer holds. So, the fourier transform with appropiate limit becomes,

$$G(\omega) = \frac{e^{\beta^2\omega^2/4C}}{2\pi} \int_0^{t^*} dt\, e^{2\lambda t} e^{-2i\omega t}. \tag{7.36}$$

Evaluating the integral gives

$$G(\omega) = \frac{e^{\beta^2\omega^2/4C}}{4\pi} \frac{e^{2(\lambda - i\omega)t^*} - 1}{\lambda - i\omega} \tag{7.37}$$

Since $f(\bar{E}, \omega)$s are real and even function of ω, only the real part of $G(\omega)$ will be relevant for our calculation.

$$Re\, G(\omega) = \frac{e^{\beta^2\omega^2/4C}}{4\pi} \frac{\lambda A + \omega B}{\lambda^2 + \omega^2} \tag{7.38}$$

where,

$$A = e^{2\lambda t^*} \cos(2\omega t^*) - 1, \qquad B = e^{2\lambda t^*} \sin(2\omega t^*) \tag{7.39}$$

Here, we see that real part of $G(\omega)$ is a smooth function of energy level spacing. Therefore, we conclude that ETH anzats is consistent with information scrambling. Although ETH is directly related to thermalization in quantum chaotic systems, it provides a description of the operators and the structure of energy eigenstates. Thus we conclude that the gaussian randomness of eigenstates and operators aid to information scrambling quantum chaotic systems. It is important to note that our calculation does not guarantee information scrambling in quantum chaotic systems. It only shows that there is a coarse-grained picture of information scrambling which is captured in the ETH framework.

There is an alternative framework which developed by Foini and Kurchan [23]. Their ansatz is given by

$$\overline{R_{ab}R_{bc}R_{cd}R_{da}} = \delta_{ac} + \delta_{bd} + e^{-S(E)}\, g\big(E, \omega_{ab}, \omega_{bc}, \omega_{cd}\big). \tag{7.40}$$

Here the first two terms account for the fact that for $i = k$ or $j = l$, the left-hand side reduces to the product of the absolute squares of two R's, whose statistical average is unity. The final term accounts for exponentially small correlations between different R's. Such correlations arise from treating the inner product of energy eigenstates (within a small energy window) with eigenstates of A (within a small range

of its eigenvalues) as a pseudo-random unitary matrix [24]. This statistical correlation goes beyond standard Gaussian assumption as seen in [7], [8]. This anzats incorporate higher order correlates. This anzats is important for future directions of this thesis since recent work has shown that the initial exponential growth of the OTOCs for chaotic systems is in contradiction with the ETH assumptions implying the lack of correlation between matrix elements of local observables. Thus, the phenomenon of scrambling, or the short-time exponential growth, implies more structure than that required by ETH. They show that OTOC is sensitive to higher order correlation to the matrix elements of the ETH anzats that are not captured by the standard ETH anzats [22], [26], [27]. Higher order correlations modifies the short time behavior of OTOC. It has been observed that at long time the OTOC saturates. Here, OTOC demonstrates universal fluctuations and saturation behavior consistent with random matrix ensembles like the Gaussian Orthogonal Ensemble (GOE) [26]. While such correlations may modify the detailed prescription of short-time behavior of OTOC, particularly before the scrambling time, they do not alter the overall qualitative behavior obtained here.

Chapter 8

Conclusion

In this thesis, we choose to investigate quantum chaos in systems of two and three harmonic oscillators with nonlinear coupling to test whether such coupled harmonic systems satisfy the eigenstate thermalization hypothesis (ETH). First, we numerically compute the thermal OTOC for these systems and extract the temperature-dependent quantum Lyapunov exponent. The temperature dependence of the quantum Lyapunov exponent suggests that quantum chaos, like classical chaos, is closely related to thermalization. This approach is different from the traditional practice of analyzing dynamical properties of quantum systems, where level statistics are typically used to determine whether a system is integrable or non-integrable [17]. We use the quantum Lyapunov exponent for several reasons. First, for systems of the type considered here, it has been shown to provide a better and more direct measure of quantum chaos. Second, this approach is more intuitive, as classical chaos is characterized by the sensitive dependence on initial conditions, quantified by the Lyapunov exponent. In the quantum setting, this behavior is captured through the exponential growth of OTOCs. Finally, the Lyapunov exponent allows us to estimate the Ehrenfest time, beyond which quantum effects dominate, thereby providing a way to probe the onset of information scrambling in the system.

Next, we want to verify the consistency of the structure of observables in these systems within the framework of ETH. To this end, we numerically extract the diagonal and off-diagonal matrix elements of the operator x_1^2. We choose this operator because it is a local operator acting on a single degree of freedom, making it suitable for testing whether the system satisfies strong or weak ETH. We find that the relative fluctuation of the diagonal elements with respect to the microcanonical average is non-zero, although it remains small. Therefore, we conclude that these systems satisfy weak ETH.

Lastly, to verify whether standard ETH formulation can predict early time exponential growth characterized by the semiclassical Lyapunov exponent and thus guarantee information scrambling after the Ehrenfest time, we write down the ETH ansatz for $x(t)$ and $p(0)$ operators respectively. For the sake of notational simplicity, we have dropped the subscripts denoting that they are observables acting on single degrees of freedom. We assume that the $x(t)$ and $p(0)$ have different smooth spectral functions $f_x(\omega, E)$ and $f_p(\omega, E)$, encoding additional information regarding the structure of the operators, although ω and E is system specific. We replace

matrix elements of the Heisenberg operators in the four-point correlation function, e.g., the OTOC, with the evolved ETH ansatz. Restricting ourselves to the pre-scrambling regime and focusing on the real part of the smooth spectral function, we show that Gaussian randomness and the smooth spectral structure of observables and eigenstates in quantum chaotic systems play an important role in information scrambling. This aspect is particularly interesting for several reasons. As quantum information becomes scrambled, different parts of the system become nonlocally entangled. Consequently, when we consider a subsystem A and trace out the remainder of the system, the subsystem appears thermal, with the traced-out degrees of freedom effectively acting as a heat bath. We demonstrate that the structure of chaotic eigenstates and operators within the ETH framework can consistently account for signatures of information scrambling. Our calculation suggests that Gaussian randomness in operator matrix element and the smooth structure of the spectral functions is sufficient to produce the coarse-grained features of information scrambling in quantum chaotic systems. This establishes a clear connection between ETH and the coarse-grained signatures of information scrambling in quantum chaotic systems.

Bibliography

[1] H. Weyl, "Quantenmechanik und gruppentheorie," *Zeitschrift für Physik*, vol. 46, no. 1–2, pp. 1–46, 1927. DOI: 10.1007/BF02055756.

[2] J. E. Moyal, "Quantum mechanics as a statistical theory," *Mathematical Proceedings of the Cambridge Philosophical Society*, vol. 45, no. 1, pp. 99–124, 1949. DOI: 10.1017/S0305004100000487.

[3] M. V. Berry and M. Tabor, "Level clustering in the regular spectrum," *Proceedings of the Royal Society A*, vol. 356, no. 1686, pp. 375–394, 1977. DOI: 10.1098/rspa.1977.0140.

[4] L. D. Landau and E. M. Lifshitz, *Quantum Mechanics: Non-Relativistic Theory*, 3rd ed. Butterworth-Heinemann, 1981, vol. 3.

[5] M. V. Berry, "Quantum chaology," *Proceedings of the Royal Society of London A*, vol. 413, no. 1844, pp. 183–198, 1987. DOI: 10.1098/rspa.1987.0109.

[6] W. H. Zurek, "Decoherence and the transition from quantum to classical," *Physics Today*, vol. 44, no. 10, pp. 36–44, 1991. DOI: 10.1063/1.881293.

[7] M. Srednicki, "Chaos and quantum thermalization," *Physical Review E*, vol. 50, no. 2, pp. 888–901, 1994. DOI: 10.1103/PhysRevE.50.888. arXiv: cond-mat/9403051 [cond-mat].

[8] M. Srednicki, "The approach to thermal equilibrium in quantized chaotic systems," *Journal of Physics A: Mathematical and General*, vol. 32, no. 7, pp. 1163–1175, Jan. 1999, ISSN: 1361-6447. DOI: 10.1088/0305-4470/32/7/007. [Online]. Available: http://dx.doi.org/10.1088/0305-4470/32/7/007.

[9] J. B. Marion and S. T. Thornton, *Classical Dynamics of Particles and Systems*, 5th ed. Cengage Learning, 2003.

[10] W. H. Zurek, "Decoherence, einselection, and the quantum origins of the classical," *Reviews of Modern Physics*, vol. 75, no. 3, pp. 715–775, 2003. DOI: 10.1103/RevModPhys.75.715. arXiv: quant-ph/0105127 [quant-ph].

[11] J. P. Sethna, *Statistical Mechanics: Entropy, Order Parameters, and Complexity*. Oxford: Oxford University Press, 2006.

[12] S. J. Blundell and K. M. Blundell, *Concepts in Thermal Physics*, 2nd. Oxford: Oxford University Press, 2009.

[13] A. Polkovnikov, "Phase space representation of quantum dynamics," *Annals of Physics*, vol. 325, no. 8, pp. 1790–1852, 2010. DOI: 10.1016/j.aop.2010.02.006.

[14] D. Tong, *Lectures on kinetic theory*, http://www.damtp.cam.ac.uk/user/tong/kinetic.html, Lecture notes, University of Cambridge, 2012.

[15] D. Tong, *Statistical physics*, Lecture notes, University of Cambridge, 2012. [Online]. Available: http://www.damtp.cam.ac.uk/user/tong/statphys.html.

[16] S. Wimberger, *Nonlinear Dynamics and Quantum Chaos: An Introduction* (Graduate Texts in Physics). Cham: Springer, 2014.

[17] L. D'Alessio, Y. Kafri, A. Polkovnikov, and M. Rigol, "From quantum chaos and eigenstate thermalization to statistical mechanics and thermodynamics," *Advances in Physics*, vol. 65, no. 3, pp. 239–362, 2016. DOI: 10.1080/00018732.2016.1198134. arXiv: 1509.06411 [cond-mat.stat-mech].

[18] J. Maldacena, S. H. Shenker, and D. Stanford, "A bound on chaos," *Journal of High Energy Physics*, vol. 2016, no. 8, p. 106, 2016. DOI: 10.1007/JHEP08(2016)106. arXiv: 1503.01409 [hep-th].

[19] K. Hashimoto, K. Murata, and R. Yoshii, "Out-of-time-order correlators in quantum mechanics," *Journal of High Energy Physics*, vol. 2017, no. 10, p. 138, 2017. DOI: 10.1007/JHEP10(2017)138. arXiv: 1703.09435 [hep-th].

[20] J. M. Deutsch, "Eigenstate thermalization hypothesis," *Reports on Progress in Physics*, vol. 81, no. 8, p. 082 001, 2018. DOI: 10.1088/1361-6633/aac9f1.

[21] M. Schleier-Smith, "Quantum simulation: Probing information scrambling," *Nature Physics*, vol. 14, pp. 215–216, 2018. DOI: 10.1038/s41567-018-0054-3.

[22] A. Chan, A. De Luca, and J. T. Chalker, "Eigenstate correlations, thermalization, and the butterfly effect," *Physical Review Letters*, vol. 122, p. 220 601, 2019. DOI: 10.1103/PhysRevLett.122.220601.

[23] L. Foini and J. Kurchan, "The eigenstate thermalization hypothesis and out of time order correlators," *Physical Review E*, vol. 99, no. 4, p. 042 139, 2019. DOI: 10.1103/PhysRevE.99.042139. arXiv: 1803.10658 [cond-mat.stat-mech].

[24] C. Murthy and M. Srednicki, "Bounds on chaos from the eigenstate thermalization hypothesis," *Physical Review Letters*, vol. 123, no. 23, p. 230 606, 2019. DOI: 10.1103/PhysRevLett.123.230606. arXiv: 1906.03221 [cond-mat.stat-mech].

[25] T. Akutagawa, K. Hashimoto, T. Sasaki, and R. Watanabe, "Out-of-time-order correlator in coupled harmonic oscillators," *Journal of High Energy Physics*, vol. 2020, no. 8, p. 013, 2020. DOI: 10.1007/JHEP08(2020)013. arXiv: 2004.04381 [hep-th].

[26] M. Brenes, S. Pappalardi, M. T. Mitchison, J. Goold, and A. Silva, "Out-of-time-order correlations and the fine structure of eigenstate thermalization," *Physical Review E*, vol. 104, p. 034 120, 2021. DOI: 10.1103/PhysRevE.104.034120.

[27] I. Garcia-Mata, R. A. Jalabert, and D. A. Wisniacki, "Out-of-time-order correlators and quantum chaos," 2022, Dated: September 16, 2022. arXiv: 2209.07965.

[28] H. Nastase, *Quantum Mechanics*. Cambridge: Cambridge University Press, 2022.

[29] T. A. Ador and N. Farid, "Out-of-time-order correlators as a measure of quantum chaos for sinai, cardioid and diamond billiards," Undergraduate thesis, Bachelor of Science in Physics, BRAC University, Department of Mathematics and Natural Sciences, May 2023.

[30] J. Al-Khalili, *Lectures on quantum decoherence*, Department of Physics, University of Surrey, Jan. 2023.

[31] T. A. Ador, N. Farid, and T. Ali, "Out-of-time-order correlators and chaos in quantum billiards," 2024. DOI: https://doi.org/10.48550/arXiv.2408.04052. arXiv: 2408.04052.

Appendix A

Winger distribution

A.1 Wigner function for the ground and first excited states of a simple harmonic oscillator

```
(* Parameters *)
m = 1;
omega = 1;
hbar = 1;

(* Ground state Wigner function *)
W0[x_, p_] := (1/(Pi hbar)) Exp[-(m omega x^2)/hbar - (p^2)/(m omega hbar)]

(* 3D Plot *)
Plot3D[W0[x, p], {x, -3, 3}, {p, -3, 3},
 PlotRange -> All,
 PlotLabel -> "Wigner Function: Ground State (n=0)",
 AxesLabel -> {"x", "p", "W0(x,p)"},
 ColorFunction -> "ThermometerColors",
 Mesh -> None
]

(* Contour plot *)
ContourPlot[W0[x, p], {x, -3, 3}, {p, -3, 3},
 ColorFunction -> "AvocadoColors",
 PlotLabel -> "Wigner Function Contours (n=0)",
 FrameLabel -> {"x", "p"}
]

(* Parameters *)
m = 1;
omega = 1;
hbar = 1;

(* Hamiltonian in phase space *)
H[x_, p_] := p^2/(2 m) + (1/2) m omega^2 x^2

(* Wigner function for n = 1 *)
```

```
W1[x_, p_] := -(1/(Pi hbar)) (1 - (4 H[x, p])/(hbar omega)) *
  Exp[-(2 H[x, p])/(hbar omega)]

(* 3D plot *)
Plot3D[W1[x, p], {x, -3, 3}, {p, -3, 3},
 PlotRange -> All,
 AxesLabel -> {"x", "p", "W1(x,p)"},
 PlotPoints -> 70,
 Mesh -> None,
 ColorFunction -> "ThermometerColors",
 PlotLabel -> "Wigner Function: First Excited State (n=1)"
]

(* Contour plot *)
ContourPlot[W1[x, p], {x, -3, 3}, {p, -3, 3},
 ColorFunction -> "AvocadoColors",
 Contours -> 30,
 FrameLabel -> {"x", "p"},
 PlotLabel -> "Wigner Function Contours (n=1)"
]
```

A.2 Wigner Function of a Coherent State

```
(* Parameters *)
alpha1 = 1;    (* Re[alpha] *)
alpha2 = 0.5;  (* Im[alpha] *)

(* Wigner Function *)
W[x_, p_] := (1/Pi) Exp[-(x - Sqrt[2] alpha1)^2 - (p - Sqrt[2] alpha2)^2]

(* 3D Plot *)
Plot3D[W[x, p], {x, -4, 4}, {p, -4, 4},
 PlotRange -> All,
 AxesLabel -> {"x", "p", "W(x,p)"},
 ColorFunction -> "Rainbow",
 Mesh -> None,
 PlotLabel -> "Wigner Function of a Coherent State"
]

(* Contour Plot *)
ContourPlot[W[x, p], {x, -4, 4}, {p, -4, 4},
 Contours -> 20,
 ColorFunction -> "Viridis",
 FrameLabel -> {"x", "p"},
 PlotLabel -> "Wigner Function Contours (Coherent State)"
]
```

Appendix B

Eigenvalues, eigenvectors, and operators

In this section, we describe the numerical methods used for our simulation. As discussed in Section 5, our approach to computing the thermal OTOC differs from that of Hashimoto et al. [19]. Rather than directly constructing matrix elements of $\hat{x}$ and $\hat{p}$ in the energy eigenbasis, we work in a truncated Fock basis. Specifically, we construct the annihilation and creation operators $\hat{a}_i$ and $\hat{a}_i^\dagger$ for each mode i algebraically, using the standard bosonic relations

$$\hat{a}_i \left|n_i\right\rangle = \sqrt{n_i}\left|n_i - 1\right\rangle, \qquad \hat{a}_i^\dagger \left|n_i\right\rangle = \sqrt{n_i + 1}\left|n_i + 1\right\rangle, \tag{B.1}$$

using which the position and momentum operators

$$\hat{x}_i = \frac{\hat{a}_i + \hat{a}_i^\dagger}{\sqrt{2}}, \qquad \hat{p}_i = \frac{i\left(\hat{a}_i^\dagger - \hat{a}_i\right)}{\sqrt{2}}, \tag{B.2}$$

are built directly. The Hamiltonian with appropriate nonlinear quartic coupling is constructed in this same basis by applying the operator $\hat{x}_i^2 \hat{x}_j^2$ to each basis state and accumulating the resulting sparse matrix elements:

$$H = \sum_{i=1}^{n} \left(\hat{n}_i + \frac{1}{2}\right) + \lambda \sum_{i<j} \hat{x}_i^2\, \hat{x}_j^2, \tag{B.3}$$

where $\hat{n}_i = \hat{a}_i^\dagger \hat{a}_i$ is the number operator for mode i and $\lambda = 0.1$ is the coupling strength. The Fock basis is truncated by imposing a cutoff $N = 100$ on the total excitation number $\sum_i n_i$, yielding a Hilbert space of dimension

$$\dim \mathcal{H} = \binom{N+n}{n} = \binom{103}{3} = 176{,}851 \tag{B.4}$$

for $n = 3$ modes. The cutoff $N = 100$ is large enough that the low-lying eigenstates are well within the bulk of the truncated space. To ensure this, we check each eigenstate in order of increasing energy and keep only those whose weight on the top layer of the basis (states with $\sum_i n_i = N$) is less than $1/(N+1)$. All eigenstates from the first one that fails this check onwards are dropped, giving n_{eff} eigenstates that are free from boundary effects.

B.1 Solving energystates and energy eigenvalues of the Hamiltonian

```python
import numpy as np
from math import sqrt
from dataclasses import dataclass
from tqdm.auto import tqdm

import scipy.sparse as sp
import scipy.sparse.linalg as spla
import matplotlib.pyplot as plt
print('Packages loaded')
```

```python
# Parameters (matching the Julia script)
n = 2 # number of particles / modes in the Julia code
N = 150 # energy cutoff used to build basis
nev = 500
```

```python
    # Helper tuple utilities (Julia had 1-based indexing; Python uses 0-
        based)
def set_tuple(tup, i, val):
    tup = list(tup)
    tup[i] = val
    return tuple(tup) # immutatable order collection of elements = tuple

def add_tuple(tup, i, delta):
    return set_tuple(tup, i, tup[i] + delta)

def swap_tuple(i, j, tup):
    tup = list(tup)
    tup[i], tup[j] = tup[j], tup[i]
    return tuple(tup)

def get_basis(levels: int, particles: int):

    # creating a valid fock state (How many quanta are in each particle/
        mode)
    basis = [tuple([0]*(particles-1) + [levels])] # appends a single
        element list [level] so [0,0,0 .., level]

    def find_non_zero(base, start):
        for idx in range(start, len(base)):
            if base[idx] > 0:
                return idx
        return None

    def next_base(base):
        firstnonzero = find_non_zero(base, 0)
        if firstnonzero is None:
            raise RuntimeError('No non-zero entry found; basis generation
                bug.')
```

```
        if firstnonzero > 0:
            new = list(base)
            new[firstnonzero-1] = 1
            new[firstnonzero] = base[firstnonzero] - 1
            return tuple(new)

        # firstnonzero == 0
        secondnonzero = find_non_zero(base, 1)
        # firstnonzero == 0
        secondnonzero = find_non_zero(base, 1)
        if secondnonzero is None:
            raise RuntimeError(Expected a second non-zero entry, but didn't
                find one.')
        new = [0]*(secondnonzero-1) + [base[firstnonzero] + 1, base[
            secondnonzero] - 1] + list(base[secondnonzero+1:])
        new = (new + [0]*particles)[:particles]
        return tuple(new)
    while basis[-1][0] != levels:
        basis.append(next_base(basis[-1]))
    return basis
```

```
# Build full basis up to cutoff N (concatenation across levels 0..N)
# We built a basis whose elements are tuples that describe how different
# amounts of energy quanta are distributed among the modes, up to a
    maximum total energy N.
basis = []
for i in range(0, N+1): # N is the cut off
    basis.extend(get_basis(i, n))

d = len(basis)
# all operators made in this base are 1326 x 1326 dim matrices (reduced
    from inifinite dimensioanl matricies)
# each of this basis vector is called a fock state
print('basis made:', d)

# Dict: basis_state -> index
index = {basis[i]: i for i in range(d)}
```

```
# largestones projector onto states at/near cutoff energy (as in Julia)
# only keeping contribution from the highest energy states near cutoff
largestones = sp.dok_matrix((d, d), dtype=np.float64)

for i in range(d-1, -1, -1):
    if sum(basis[i]) < N:
        break
    largestones[i, i] = 1.0 # the projector has non-zero entries on total
        exictation is N. so this projects the wavefunction into the cutoff.
# so we can reduce its contribution
largestones = largestones.tocsr()
print('largestones projector built')
```

```
# Build sparse Hamiltonian H (Julia used spzeros(d,d) and in-place increments)
H = sp.dok_matrix((d, d), dtype=np.float64)

# Add harmonic terms: H[k,k] += sum(basis[k]) + 0.5*n
# hamiltonian is diagonal in number basis
for k in tqdm(range(d), desc='adding Harmonic Hamiltonians'):
    H[k, k] += sum(basis[k]) + 0.5*n

print('added Harmonic Hamiltonians')
```

```
@dataclass(frozen=True)
class Term:
    coef: float
    term: tuple # occupation tuple

def a(i: int, t: Term) -> Term:
    # annihilation-like operator on index i
    if t.term[i] < 0:
        return Term(0.0, t.term)
    newterm = add_tuple(t.term, i, -1) # reducing occuption number like annilators do
    return Term(t.coef * sqrt(t.term[i]), newterm)

def countnegatives(tup):
    # sum of absolute values of negative entries
    return sum(max(0, e) for e in tup) - sum(tup)

# a destroys one quantum and b creates one quantum
def b(i: int, t: Term) -> Term:
    # creation-like operator on index i, including Julia's special-case for negative entries
    if t.term[i] < 0 and countnegatives(t.term) == -t.term[i]:
        return Term(1.0, set_tuple(t.term, i, 0))
    newterm = add_tuple(t.term, i, 1)
    return Term(t.coef * sqrt(newterm[i]), newterm)

def num(i: int, t: Term) -> Term:
    return b(i, a(i, t))

def xx(i: int, t: Term):
    # Julia: [a(i,a(i,t)), b(i,b(i,t)), Term((1+(t.term[i]*2))*t.coef,t.term)]
    # additive contribution from all terms
    return [
        a(i, a(i, t)),
        b(i, b(i, t)),
        Term((1.0 + (t.term[i]*2.0)) * t.coef, t.term)
    ]

def xxxx(i: int, j: int, t: Term):
```

```
    # Julia: vcat([xx(j,term) for term in xx(i,t)]...)
    out = []
    for term in xx(i, t):
        out.extend(xx(j, term))
    return out
```

```
    # Add interaction terms (Julia nested loops + xxxx expansion)
interaction_strength = 0.1

for k in tqdm(range(d), desc='adding interaction Hamiltonians'):
    ket = basis[k]
    for i in range(n):
        for j in range(i+1, n):
            for t in xxxx(i, j, Term(1.0, ket)):
                idx = index.get(t.term, None)
                if idx is not None:
                    H[idx, k] += t.coef * interaction_strength

print('added all interaction Hamiltonians')

# Symmetrize: H = (H + H')/2
H = H.tocsr()
H = (H + H.T) * 0.5
```

```
# Sparse eigensolve (Julia: eigsolve(H, eigvals=nev, sigma=n/2, v0=
    normalize([1/i ...])))
# In SciPy: use eigsh for symmetric real matrices, with shift-invert via
    sigma.
k = min(nev, d-2) if d > 2 else 1
sigma = n/2 # shift as in Julia

v0 = np.array([1.0/(i+1) for i in range(d)], dtype=np.float64)
v0 = v0 / np.linalg.norm(v0)

print('Starting eigensolve (this can take a while for large d)...')
vals, vecs = spla.eigsh(H, k=k, sigma=sigma, v0=v0, which='LM')

# sort ascending
order = np.argsort(vals)
vals = vals[order]
vecs = vecs[:, order]

print('Eigensolved:', len(vals), 'eigenpairs')
```

```
# Reduce nev if eigenvectors have nontrivial weight on the cutoff-subspace
    (largestones)
nev_eff = len(vals)
for i in range(1, len(vals)):
    v = vecs[:, i]
    overlap = float(v.T @ (largestones @ v))
    if overlap > 1.0/(N+1):
```

```
        nev_eff = i
        break

vals = vals[:nev_eff]
vecs = vecs[:, :nev_eff]

print('Eigenvectors up to', {nev_eff}, ' do not have contributions from
    near cutoff energy')
```

B.2 Constructing Operators

```
# Build X and P operators (Julia used mode 1 only; that's index 0 in
    Python)
X = sp.dok_matrix((d, d), dtype=np.float64)
P = sp.dok_matrix((d, d), dtype=np.float64)

for k in tqdm(range(d), desc='creating x operator'):
    ket = basis[k]
    terms_x = [a(0, Term(1.0, ket)), b(0, Term(1.0, ket))]
    for t in terms_x:
        idx = index.get(t.term, None)
        if idx is not None:
            X[idx, k] += t.coef

for k in tqdm(range(d), desc='creating p operator'):
    ket = basis[k]
    terms_p = [a(0, Term(-1.0, ket)), b(0, Term(1.0, ket))]
    for t in terms_p:
        idx = index.get(t.term, None)
        if idx is not None:
            P[idx, k] += t.coef

X = X.tocsr()
P = P.tocsr()
print('x and p operators created')
```

B.3 Qualitative analysis of the operators

The following blocks of code numerically checks the validity of ETH for the observable $\hat{x}_1^2$, the squared position of the first mode. The first section constructs the sparse matrix representation of $\hat{x}_1 = (\hat{a}_1 + \hat{a}_1^\dagger)/\sqrt{2}$ in the truncated Fock basis. For each basis state, the code applies the annihilation term by reducing n_1 by one, with matrix element $\sqrt{n_1}/\sqrt{2}$ and the creation term by increasing n_1 by one, with matrix element $\sqrt{n_1+1}/\sqrt{2}$, provided the resulting state lies within the truncated basis in teh Hilbert space. The sparse matrix $\hat{x}_1$ is then squared to give $\hat{x}_1^2$, and projected into the energy eigenbasis via

$$O = V^\dagger \hat{x}_1^2 V, \tag{B.5}$$

where V is the matrix of eigenvectors. This gives the full matrix of $\hat{x}_1^2$ in the energy eigenbasis.

```
  import numpy as np

dim = len(basis)
x1 = np.zeros((dim, dim))

# fast lookup
basis_dict = {state: i for i, state in enumerate(basis)}

for i, (n1, n2) in enumerate(basis):

    # --- a1 term ---
    if n1 > 0:
        target = (n1 - 1, n2)
        j = basis_dict.get(target)
        if j is not None:
            x1[j, i] += np.sqrt(n1) / np.sqrt(2)

    # --- a1 dagger term ---
    target = (n1 + 1, n2)
    j = basis_dict.get(target)
    if j is not None:
        x1[j, i] += np.sqrt(n1 + 1) / np.sqrt(2)
```

```
x1_sq = x1 @ x1
O_energy = vecs.T.conj() @ x1_sq @ vecs
```

Next we extract the diagonal entries $O_{nn} = \langle n|\hat{x}_1^2|n\rangle$ by sorting energy eigenvalues. We then apply a moving average with a window of $n_{\text{eff}}/10$ states to obtain a smooth microcanonical estimate $\bar{O}(E)$. The ETH predicts that the diagonal elements should lie smoothly on this curve, with fluctuations that are small relative to the mean. To quantify this, the standard deviation of the residuals $O_{nn} - \bar{O}(E_n)$ is computed, and the relative fluctuation is given by the following formula.

$$\frac{\sigma}{\bar{O}} = \frac{\text{std}\big(O_{nn} - \bar{O}(E_n)\big)}{\langle\, |\bar{O}(E)|\,\rangle} \tag{B.6}$$

```
    # deviation from microcanonical average
deviation = diag - diag_smooth

std_dev = np.std(deviation)
print(f'Std deviation = {std_dev:.5f}')

mean_val = np.mean(np.abs(diag_smooth))
rel_fluct = std_dev / mean_val
print(f'Relative fluctuation = {rel_fluct:.5f}')
```

```
import numpy as np
import matplotlib.pyplot as plt
```

```
3
4  # --- Energy eigenvalues ---
5  E = vals
6
7  # --- Operator in energy basis ---
8  O = O_energy
9
10 # ============================================================
11 # Diagonal elements
12 # ============================================================
13 diag = np.real(np.diag(O))
14
15 # --- SORT ---
16 idx = np.argsort(E)
17 E = E[idx]
18 diag = diag[idx]
19
20 # ============================================================
21 # Microcanonical average (moving average)
22 # ============================================================
23 window = max(5, len(E)//20)
24 kernel = np.ones(window)/window
25
26 diag_smooth = np.convolve(diag, kernel, mode='same')
27
28 # ============================================================
29 #  Plot
30 # ============================================================
31 plt.figure(figsize=(6,4))
32
33 # raw data
34 plt.scatter(E, diag, s=10, alpha=0.5, label='Eigenstates')
35
36 # microcanonical average
37 plt.plot(E, diag_smooth, 'r', lw=2, label='Microcanonical avg')
38
39 plt.xlabel(r'Energy $E_n$')
40 plt.ylabel(r'$x_1^2{}_{nn}$')
41 plt.title('ETH: diagonal + microcanonical average')
42
43 plt.legend()
44 plt.grid(alpha=0.3)
45 plt.tight_layout()
46 plt.show()
```

We have produced two plots. The first shows the diagonal elements $\langle n|\hat{x}_1^2|n\rangle$ scattered against E_n with the microcanonical average overlaid, and the second shows the off-diagonal elements $|O_{mn}|$ on a log scale. Smooth diagonal behaviour and small off-diagonal elements together constitute numerical evidence that the system satisfies ETH.

```
1  # ============================================================
```

```
# Off-diagonal vs energy spacing
# ============================================================

# build energy difference matrix
E_i = E[:, None]
E_j = E[None, :]

delta_E = np.abs(E_i - E_j)

# mask to remove diagonal
mask = ~np.eye(len(E), dtype=bool)

x = delta_E[mask]
y = np.abs(O)[mask]

# remove very small numerical noise
valid = y > 1e-12
x = x[valid]
y = y[valid]

# ============================================================
# Plot off-diagonal elements
# ============================================================

plt.figure(figsize=(6,4))

plt.scatter(x, y, s=2, alpha=0.3)

plt.xlabel(r'$|E_m - E_n|$')
plt.ylabel(r'$|x1^2_{mn}|$')
plt.title('Off-diagonal ETH: vs energy difference')

plt.yscale('log')
plt.grid(alpha=0.3)
plt.tight_layout()
plt.show()
```

We have also plotted the probability distribution associated with the off diagonal elements of the ETH anzats.

```
    # ============================================================
# Energy matrices
# ============================================================

E_i = E.reshape(-1, 1)
E_j = E.reshape(1, -1)

# ============================================================
# Remove diagonal
# ============================================================

mask = ~np.eye(len(E), dtype=bool)
```

```
13
14  # ============================================================
15  # Magnitude of off-diagonal elements
16  # ============================================================
17
18  y = np.abs(O[mask])
19
20  # remove tiny numerical noise
21  y = y[y > 1e-16]
22
23  print(Number of off-diagonal elements =, len(y))
24
25  # ============================================================
26  # Probability distribution
27  # ============================================================
28
29  plt.figure(figsize=(7, 5), dpi=140)
30
31  plt.hist(
32      y,
33      bins=100,
34      density=True,
35      alpha=0.8
36  )
37
38  plt.xlabel(r'$|O_{mn}|$', fontsize=14)
39
40  plt.ylabel(r'$P(|O_{mn}|)$', fontsize=14)
41
42  plt.title(
43      'Probability distribution of off-diagonal ETH elements',
44      fontsize=15
45  )
46
47  plt.yscale('log')
48
49  plt.grid(True, alpha=0.3)
50
51  plt.tight_layout()
52
53  plt.savefig('ETH_probability_distribution_3osc.png',
54      dpi=400,
55      bbox_inches=tight
56  )
57  plt.show()
```

Appendix C

Out of time order correlator

C.1 Time evolution four point correlator

```
# OTOC evolution (matches Julia structure)
delt = 0.1
time = 7
times = np.arange(0, time + delt/2, delt)

# Project operators to eigenbasis
V = vecs # d x nev_eff
x = (V.T @ (X @ V)).astype(np.complex128)
p = (V.T @ (P @ V)).astype(np.complex128)

# Time-step unitary in eigenbasis
Udel = np.diag(np.exp(-1j * vals * delt))

# store diagonal of ( [x(t),p]^2 /4 ) as in Julia
comm0 = x @ p - p @ x
otoc_evolution = [np.diag((comm0 @ comm0) / 4.0).real]

for _ in tqdm(range(1, len(times)), desc='Calculating OTOCs'):
    x = Udel.conj().T @ x @ Udel
    commute = x @ p - p @ x
    OTOC = (commute @ commute) / 4.0
    otoc_evolution.append(np.diag(OTOC).real)

otoc_evolution = np.array(otoc_evolution) # (len(times), nev_eff)
print('OTOC evolution computed:', otoc_evolution.shape)
```

C.2 Log of OTOC

```
# choose a microcanonical window (adjust as needed)
Emin = int(0.2 * otoc_evolution.shape[1])
Emax = int(0.9 * otoc_evolution.shape[1])

Ct = np.mean(otoc_evolution[:, Emin:Emax], axis=1)
```

```
tmin = 2
tmax = 6

mask = (times > tmin) & (times < tmax)
```

```
import numpy as np
from scipy.optimize import curve_fit

# --- Ensure arrays are aligned ---
Ct = np.asarray(Ct)
times = np.asarray(times)

n = min(len(times), len(Ct))
times = times[:n]
Ct = Ct[:n]

# --- Define exponential model ---
def model(t, A, lambda_L):
    return A * np.exp(2 * lambda_L * t)

# --- Define fitting window ---
t_min = 0.0
t_max = times[-1] # or choose manually (e.g. 5 or 10)

mask = (times > t_min) & (times < t_max) & (Ct > 1e-12)

# --- Apply mask safely ---
t_fit = times[mask]
C_fit = Ct[mask]

# --- Initial guesses ---
A0 = C_fit[0]
lambda0 = 0.1

# --- Nonlinear fit ---
params, covariance = curve_fit(
    model,
    t_fit,
    C_fit,
    p0=[A0, lambda0],
    bounds=([0, 0], [np.inf, np.inf]) # keeps parameters physical
)

A_fit, lambda_L = params

# --- Goodness of fit ---
C_pred = model(t_fit, *params)
ss_res = np.sum((C_fit - C_pred)**2)
ss_tot = np.sum((C_fit - np.mean(C_fit))**2)
r2 = 1 - ss_res / ss_tot

```

```
# --- Output ---
print(f'Lyapunov exponent  = {lambda_L:.6f}')
print(f'Fit R = {r2:.6f}')
```

```
# --- Plot ---
plt.figure()

plt.plot(t_plot, logC, '-', label='log C(t)')

plt.plot(t_fit, np.log(C_pred), '-', label='Fit')

plt.xlabel('Time (t)')
plt.ylabel('log C(t)')
plt.title('Log C(t) vs Time')
plt.legend()

plt.show()
```

C.3 Temperature dependent quantum Lyapunov exponent

```
   import numpy as np
from scipy.optimize import curve_fit

def model(t, A, lambda_L):
    return A * np.exp(2 * lambda_L * t)

# --- EXACT temperatures from paper ---
temperatures = np.array([1.8, 2, 2.5, 3, 3.5, 4, 4.5, 5, 5.5])

# --- EXACT time window ---
tmin, tmax = 2.0, 6.0

lambda_q = []
T_used = []

for T in temperatures:
    beta = 1.0 / T

    weights = np.exp(-beta * vals[:nev_eff])
    Z = np.sum(weights)

    C_beta = (otoc_evolution @ weights) / Z

    # align arrays
    n = min(len(times), len(C_beta))
    t = times[:n]
    Ct = C_beta[:n]

```

```
    # apply STRICT window
    mask = (t >= tmin) & (t <= tmax) & (Ct > 1e-12)

    if np.sum(mask) < 5:
        continue

    t_fit = t[mask]
    C_fit = Ct[mask]

    # nonlinear fit
    params, _ = curve_fit(
        model,
        t_fit,
        C_fit,
        p0=[C_fit[0], 0.1],
        bounds=([0, 0], [np.inf, np.inf])
    )

    A_fit, lambda_L = params

    lambda_q.append(lambda_L)
    T_used.append(T)

lambda_q = np.array(lambda_q)
T_used = np.array(T_used)
```

```
    # log-log fit
logT = np.log(T_used)
logL = np.log(lambda_q)

b, loga = np.polyfit(logT, logL, 1)
a = np.exp(loga)

print(f'Final fit: lambda(T) = {a:.3f} T^{b:.3f}')
```

```
    import numpy as np
import matplotlib.pyplot as plt

# --- smooth curve starting from 0 ---
T_smooth = np.linspace(0, max(T_used), 200)
lambda_smooth = a * (T_smooth ** b)

# --- plot ---
plt.figure(figsize=(6, 4))

# data (includes T=0 point)
plt.plot(T_used, lambda_q, 'o', label='Numerical data')

# fit curve
plt.plot(T_smooth, lambda_smooth, '-',
         label=rf'Fit: $\lambda = {a:.2f} T^{{{b:.2f}}}$')
```

```
17
18 # labels
19 plt.xlabel('Temperature T')
20 plt.ylabel(r'Quantum Lyapunov exponent $\lambda_q(T)$')
21 plt.title(r'Temperature dependence of $\lambda_q$')
22
23 plt.legend()
24 plt.grid(alpha=0.3)
25
26 plt.tight_layout()
27 plt.show()
```